

**Characterization of the β 4GalNAc Transferases
and the β 4GalNAcTB Pilot Protein (GABPI) from
*Drosophila melanogaster***

Der Naturwissenschaftlichen Fakultät
der Gottfried Wilhelm Leibniz Universität Hannover
zur Erlangung des Grades

Doktorin der Naturwissenschaften
Dr. rer. nat.

genehmigte Dissertation

von
Dipl.-Biochem. Anita Stolz
geboren am 17. August 1979 in Essen

Hannover 2008

Referentin : Prof. Dr. Rita Gerardy-Schahn

Korreferent : Prof. Dr. Jürgen Alves

Tag der Promotion : Montag, den 03.03.08

ABSTRACT	1
ZUSAMMENFASSUNG	2
1 INTRODUCTION	4
1.1 Glycosylation.....	4
1.1.1 General overview.....	4
1.1.2 N-linked glycosylation	4
1.1.3 O-linked glycosylation	5
1.1.4 Glycosphingolipids.....	5
1.2 The secretory pathway – from the ER to the Golgi.....	6
1.2.1 General overview.....	6
1.2.2 Quality control system in the ER.....	8
1.2.3 Transport between ER and Golgi	10
1.3 Glycosyltransferases.....	10
1.3.1 The β 1,4-galactosaminyltransferase family	12
1.4 The DHHC protein family	14
1.5 Glycosylation in <i>Drosophila melanogaster</i>.....	15
1.6 Aim of this study.....	16
2 MATERIALS AND METHODS.....	17
2.1 Material	17
2.1.1 Chemicals	17
2.1.2 Standard buffer and media.....	19
2.1.3 Culture media and additives	20
2.1.4 Kits and further materials	20
2.1.5 Laboratory Equipment.....	21
2.1.5 Enzymes	22
2.1.6 Molecular weight markers.....	22
2.1.7 Antibodies.....	22
2.1.7.1 Primary Antibodies.....	22

2.1.7.2	Secondary Antibodies.....	23
2.1.8	Oligonucleotides.....	23
2.1.9	Plasmids.....	25
2.1.9.1	Plasmids with site-directed mutagenesis.....	27
2.1.10	Laboratory animals.....	28
2.1.11	Eukaryotic cell lines.....	28
2.1.12	Bacterial strains.....	29
2.2	Methods.....	30
2.2.1	Cell biological techniques.....	30
2.2.1.1	Transient transfection of HEK293 cells.....	30
2.2.1.2	Transient transfection of S2 cells.....	31
2.2.1.3	Generation of semi stable HEK293 cells.....	31
2.2.1.3	RNAi treatment of Drosophila Schneider cells.....	31
2.2.1.4	Immunocytochemistry.....	32
2.2.1.5	Immunofluorescence.....	32
2.2.2	Molecular biological techniques.....	33
2.2.2.1	Plasmid preparation.....	33
2.2.2.2	Polymerase chain reaction (PCR).....	33
2.2.2.3	Determination of DNA and RNA concentrations.....	35
2.2.2.4	Agarose gel electrophoresis of DNA.....	35
2.2.2.5	Isolation of DNA fragments from agarose gels.....	35
2.2.2.6	Restriction digest of DNA.....	35
2.2.2.7	Ligation of DNA.....	36
2.2.2.8	Precipitation of nucleic acids.....	36
2.2.2.9	Transformation of chemically competent <i>E.coli</i>	36
2.2.2.10	Transformation of electro competent <i>E.coli</i> YZ2000.....	36
2.2.2.11	Preparation of chemically competent <i>E.coli</i>	36
2.2.2.12	Preparation of <i>E.coli</i> DMSO-Stocks.....	37
2.2.2.13	Synthesis of dsRNA.....	37
2.2.2.14	Agarose gel electrophoresis of RNA.....	37
2.2.3	Biochemical techniques.....	38
2.2.3.1	Immunoprecipitation.....	38
2.2.3.2	Analyses of proteins from transfected HEK293 cells.....	38
2.2.3.3	Polyacrylamide gelelectrophoresis (SDS-PAGE).....	39

2.2.3.4	Western blot.....	39
2.2.3.5	Immunostaining of Western blots	39
2.2.3.6	Protein estimation	40
2.2.3.7	Golgi preparation.....	40
2.2.3.8	<i>In vitro</i> assay for β 4GalNAc transferases.....	40
2.2.3.9	Reverse-phase chromatography (<i>in vitro</i> assay).....	41
2.2.3.10	Glycosphingolipid preparation from HEK293 cells.....	41
2.2.3.11	Glycosphingolipid preparation from <i>D. melanogaster</i>	42
2.2.3.12	High-performance thin-layer chromatography (HPTLC).....	42
2.2.3.13	Immunostaining of HPTLC	42
2.2.3.14	Matrix assistance laser desorption (MALDI) mass spectrometry	43
3	RESULTS.....	44
3.1	Function of β4GalNAcTA and β4GalNAcTB <i>in vivo</i>	44
3.1.1	High-performance thin-layer chromatography analysis	44
3.1.2	Matrix-assisted laser-desorption/ionization time-of-flight mass spectrometry (MALDI-TOF-MS)	45
3.2	<i>In vitro</i> characterization of β4GalNAcTA and β4GalNAcTB	51
3.2.1	Cell surface staining	52
3.2.2	Glycolipid specificity of β 4GalNAcTA and β 4GalNAcTB.....	53
3.2.3	<i>In vitro</i> testing of β 4GalNAc transferases using Golgi vesicles	55
3.2.4	Physical interaction between β 4GalNAcTB and GABPI.....	57
3.3	Biosynthesis of lacdiNAc in β4GalNAcTA, β4GalNAcTB, or GABPI depleted <i>Drosophila</i> S2 cells.....	58
3.3.1	GSL structures in RNAi treated S2 cells.....	58
3.3.2	New glycosphingolipid structures in <i>Drosophila</i> S2 cells.....	61
3.4	Characterization of GABPI	63
3.4.1	Determination of the minimal functional unit.....	63
3.4.2	Transmembrane topology of GABPI.....	65
3.4.3	The loop regions of GABPI.....	70

3.4	The function of GABPI	72
3.4.1	Palmitoyltransferase activity of the DHHC family member GABPI	72
3.4.2	GABPI is required for Golgi targeting of β 4GalNAcTB, but not of β 4GalNAcTA.....	73
3.5	Interactions domains of β4GalNAcTB and GABPI	77
4	DISCUSSION.....	84
4.1	<i>In vivo</i> characterization of β4GalNAcTA and β4GalNAcTB	84
4.2	<i>In vitro</i> activity of β4GalNAcTA and β4GalNAcTB.....	86
4.2.1	Substrate specificity.....	86
4.2.2	The activation of β 4GalNAcTB by GABPI	87
4.2.3	The possibility of multi-enzyme complexes.....	88
4.3	Characteristics of GABPI	89
4.3.1	The loop regions of GABPI.....	90
4.4	Role of GABPI in subcellular localization.....	91
4.5	The stem region of β4GalNAcTB.....	93
4.7	Outlook	94
4.7.1	The three-dimensional structure of β 4GalNAcTA and β 4GalNAcTB	94
4.7.2	The function of GABPI- a working hypothesis.....	96
5	REFERENCES	98
6	ABBREVIATIONS	107
7	LEBENS LAUF	109
8	PUBLIKATIONS LISTE	110
9	ERKLÄRUNG ZUR DISSERTATION	113
10	DANKSAGUNG	114

Abstract

The biosynthesis of the lacdiNAc (GalNAc β ,4GlcNAc) epitope in the fruit fly *Drosophila melanogaster* is accomplished by two functionally active β 1,4 *N*-acetylgalactosaminyltransferases (β 4GalNAcTA and β 4GalNAcTB). Using a heterologous expression cloning system β 4GalNAcTB was shown to require a DHHC family protein for activity, while the second cloned GalNAc transferase (β 4GalNAcTA) was cofactor independent. In my study the goal was pursued to develop a differential picture of the catalytic functions of β 4GalNAcTA and β 4GalNAcTB. Particular attention was thereby given to the question how the DHHC family protein, called GABPI (for β 4GalNAcTB Pilot Protein), influences functionality. Detailed MALDI-TOF-MS analyses of *Drosophila* β 4GalNAcTA and β 4GalNAcTB mutants, which display relative mild phenotypes, confirmed that both transferases are involved in the biosynthesis of the lacdiNAc structure, which in the fly is a glycolipid specific modification. Moreover, it was also shown that β 4GalNAcTB is the major enzyme in the lacdiNAc epitope biosynthesis. In a double mutant lacking β 4GalNAcTA and TB, the trisaccharide product of egghead and brainiac (both essential glycosyltransferases in *Drosophila*), was the only glycosphingolipid structure, indicating that the trisaccharide is the minimally required structure for normal development in *Drosophila*. Glycolipid specificity for both transferases and the activity dependency of β 4GalNAcTB on the presence of GABPI was demonstrated in different *in vitro* assay systems. Further experiments pointed out that β 4GalNAcTB/GABPI complex formation and membrane integrity were essential requirements for functionality. In an RNAi based approach with *Drosophila* Schneider cells it was shown that lacdiNAc epitope formation was directly dependent on the expression of GABPI. GABPI could be characterized as a Golgi resident protein with six transmembrane domains. Functional analyses of GABPI truncation mutants demonstrated that only the four N-terminal transmembrane domains and the luminal loops contained in this fragment are necessary for the activation process. Functional analyses and subcellular localisation studies carried out for GABPI and β 4GalNAcTB in mammalian and insect cells indicated that β 4GalNAcTB in the absence of GABPI is neither able to attain functional folding nor correct subcellular destination. If expressed alone, β 4GalNAcTB remains in the ER as an inactive enzyme. In contrast, GABPI as well as β 4GalNAcTA are autonomous folding units and contain all the information for correct targeting to the Golgi apparatus. With the help of hybrid constructs generated between β 4GalNAcTA and -B, the catalytic domain and stem region of β 4GalNAcTB could be identified as important for complex formation with GABPI. In summary, the identification of GABPI as a pilot for folding, subcellular transport and activity of β 4GalNAcTB describes a novel way to generate specificity in the complex glycosylation pathway.

Keywords: Glycosyltransferases, β 4GalNAc transferases, *Drosophila melanogaster*

Zusammenfassung

Die Biosynthese der LacdiNAc (GalNAc β ,4GlcNAc) Struktur wird in der Fruchtfliege *Drosophila melanogaster* durch zwei funktionell aktive β 1,4 N-Acetylgalactosaminyltransferasen (β 4GalNAcTA und β 4GalNAcTB) katalysiert. Mit Hilfe eines heterologen Expressionsansatzes konnten vor Beginn dieser Arbeit beide Enzyme kloniert werden. In Folge dieses Klonierungsprozesses hatte sich gezeigt, dass für die Aktivität der β 4GalNAcTB in weiteres Protein benötigt wird, welches als Mitglied der DHHC Proteinfamilie identifiziert wurde. β 4GalNAcTA war dagegen ein unabhängig aktives Enzym. Mit meiner Arbeit sollten die Unterschiede in den katalytischen Funktionen der β 4GalNAc Transferasen herausgestellt und die Rolle des Kofaktors, des DHHC Proteins, welches im Verlauf dieser Arbeit als GABPI (β 4GalNAcTB Pilot Protein) bezeichnet wurde, untersucht werden. Im ersten Teil dieser Arbeit wurden die Glycanprofile von Fliegen mit genetischen Defekten in den β 4GalNAc Transferasen per MALDI-TOF-MS analysiert. Dabei zeigte sich, dass beide β 4GalNAc Transferasen an der Synthese von LacdiNAc Strukturen, die in der Fliege allein auf Glykolipiden zu finden sind, beteiligt sind. Hauptenzym bei der Biosynthese des LacdiNAc Epitops ist jedoch β 4GalNAcTB. In der Doppel-Mutante war kein LacdiNAc mehr detektierbar, entsprechend war die Trisaccharidstruktur, die den Akzeptor für die β 4GalNAc Transferasen darstellt deutlich angereichert. Dieses Trisaccharid, welches von den Glykosyltransferasen Egghead und Brainiac synthetisiert wird, ist für die Entwicklung von *Drosophila* essentiell. Die Phänotypen beider β 4GalNAcT-Einzelmutanten, ebenso wie der Phänotyp der Doppelmutante, sind dagegen mild. In verschiedenen *in vitro assay* Systemen konnte für beide β 4GalNAc Transferasen eine Substratspezifität für Glykolipide bestätigt werden. Die Aktivität der β 4GalNAcTB war dabei stets an die Anwesenheit des Kofaktors GABPI gebunden. Mit Hilfe von RNAi Studien in *Drosophila* Schneider Zellen wurde der direkte Einfluss von GABPI auf die LacdiNAc Biosynthese nachgewiesen und in weiteren Experimenten wurde gezeigt, dass sowohl die β 4GalNAcTB/GABPI Komplexbildung als auch die Stabilität dieses Komplexes im Golgi Apparat für die Aktivität von β 4GalNAcTB essentiell ist. GABPI stellt ein Golgi lokalisiertes 6-Transmembranprotein dar. Verkürzungsmutanten zeigten jedoch, dass nur das N-terminale Fragment, welches die ersten vier Domänen umfasst, für die Aktivierung benötigt wird, wobei die luminalen *loop* Regionen ebenfalls essentiell sind. Subzelluläre Lokalisationsstudien in Säugetier- und Insektenzellen zeigten, dass β 4GalNAcTB nach isolierter Expression als inaktives Enzym im ER verbleibt. Erst die Koexpression mit GABPI erlaubt den Transport in den Golgi. Aus den Transferasen A und B generierte Hybridkonstrukte zeigten schließlich, dass die katalytische Domäne und die Stammregion von β 4GalNAcTB an der Interaktion mit GABPI beteiligt sind. Die Charakterisierung von GABPI als Kofaktor für Proteinfaltung, subzelluläre Lokalisation und

Aktivität von β 4GalNAcTB zeigt einen neuen Mechanismus auf, über welchen Spezifität in komplexen Glykosylierungswegen hergestellt werden kann.

Schlagwörter: Glykosyltransferasen, β 4GalNAc-Transferasen, *Drosophila melanogaster*

1 Introduction

1.1 Glycosylation

1.1.1 General overview

Glycosylation as a modification of proteins and lipids plays an important role in various biological processes like cell-cell adhesion and signaling, development, pathogen–host interactions, and oncogenesis. The location of the complex glycosylation machinery is the secretory pathway, including endoplasmic reticulum (ER) and Golgi apparatus. Glycosylation proceeds while the glycosylation acceptors (proteins and lipids) are transported through the intracellular compartments, where enzymes involved in this process are vectorially organized. The prominent enzymes in glycoconjugate production are the glycosyltransferases, which catalyze the biosynthesis of disaccharides, oligosaccharides, and polysaccharides using activated monosaccharides as substrates (Coutinho et al., 2003). The spatial organisation of glycosyltransferases within ER and Golgi apparatus is fundamental for the regulation of glycoprotein and glycolipid biosynthesis. Understanding the mechanisms that install and survey the organization in these compartments is of paramount importance to enable strategies, with which cellular glycosylation pathways can, e.g. under pathophysiological circumstances, be modulated.

1.1.2 N-linked glycosylation

N-linked glycosylation is a co-translational modification, in which the carbohydrate moiety is bound to a protein via the nitrogen atom of asparagine (Asn) residues in the sequence context Asn-X-Ser/Thr, where X is any amino acid except proline. The *N*-glycosylation pathway starts in the ER with the transfer of a preformed oligosaccharide (14mer) onto the glycosylation sites directly when the nascent protein emerges from the ribosome into the lumen of the ER. The preformed oligosaccharide is membrane linked via dolichol-pyrophosphate (Abeijon and Hirschberg, 1992; Hirschberg and Snider, 1987). The enzyme that transfers the glycan to the protein is the oligosaccharyltransferase (OST), an hetero-oligomeric protein complex comprising seven or eight subunits (Kelleher and Gilmore, 2006). Complex processing steps in the *cis*-, *medial*-, and *trans*- Golgi cisternae lead to the characteristic *N*-linked glycan structures, specific for each cell type.

1.1.3 O-linked glycosylation

In general, a linkage in which a monosaccharide is attached to the hydroxyl group of an amino acid (serin, threonine, tyrosine, hydroxyprolin and hydroxylysin) is referred to as *O*-glycosidic bond. *O*-glycosylation, in contrast to *N*-glycosylation, is not restricted to clearly defined primary sequence motifs, and the glycan structure can be elongated by successive transfer of single monosaccharides resulting in oligosaccharides of various length with normally not more than two branches. Moreover, while the canonical *O*-glycan starts with GalNAc, this is not the only monosaccharide to prime a glycan chain. Alternatively, it can also be initiated by mannose, fucose, and glucose (for review see (Spiro, 2002)). Based on the chain initiating sugar, *O*-linked glycans are differentiated into subgroups. *O*-linked glycosylation is initiated in the ER for the O-mannose, fucose, and glucose, but the transfer of the most prominently added α -GalNAc seems to occur in the *cis*-Golgi.

1.1.4 Glycosphingolipids

Glycosphingolipids (GSLs) are molecules composed of a membrane bound sphingolipid or ceramide that is modified with an oligosaccharide chain. The minimal structural unit that defines a glycosphingolipid is a monosaccharide directly attached to a ceramide. GSLs are grouped into different series, which are defined by the third or the fourth sugar residue of the oligosaccharide structure. Vertebrate GSLs can be grouped into four main structural families: the ganglio-, globo-, isoglobo-, lacto-, and neolacto-series (Figure 1). In invertebrates different carbohydrate core structures could be identified: the arthro-, mollu-, schisto-, and spirometo-series (Lochnit G. et al., 2001) The GSL nomenclature follows the recommendations of the IUPAC-IUB Nomenclature Commission (1999).

The transfer of the first monosaccharide to the membrane anchor is catalyzed in the lumen or on the cytoplasmic site of the ER by highly specific glycosyltransferases, comprising the galactosylceramide synthase or the glucosylceramide synthase (Figure 1) (Holthuis et al., 2001). The monosaccharide-ceramide is translocated by an unknown mechanism to the Golgi lumen, where glycosyltransferases can catalyze the further elongation of the sugar chain by stepwise addition of nucleotide-sugars (Figure 1). Although all existing classifications of glycosphingolipids are based on variations in the core glycan structure, it is important to note that the ceramide moiety can also show substantial structural heterogeneity. The sphingosine base and the attached fatty acid chain can vary in length and degree of unsaturation and/or hydroxylation.

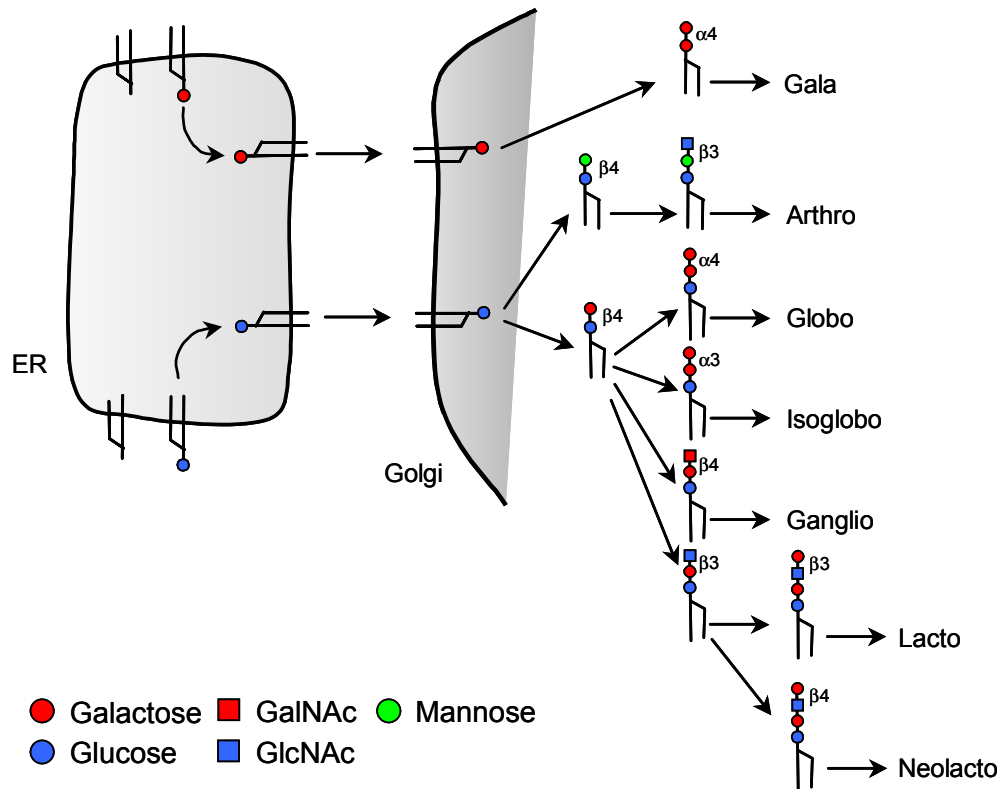


Figure 1: Pathways for the biosynthesis of the core structures of the glucosylceramides and galactosylceramides. Initiation takes place on the membranes of the ER or the Golgi. Further transfer of monosaccharides occurs in the Golgi. The types of possible outer chains and extensions are depicted. For simplicity only the arthro series of invertebrates is shown. Figure adapted and modified from Ajit Varki (Varki et al., 1999)

1.2 The secretory pathway – from the ER to the Golgi

1.2.1 General overview

The secretory pathway of eukaryotic cells describes the transport route by which proteins are delivered from the ER via the Golgi apparatus to the plasma membrane (Teasdale and Jackson, 1996). Even proteins that are resident in the lumen of the ER and Golgi, or that are sorted into lysosomes and other intracellular vesicular structures are transported and matured in this pathway. Proteins destined to enter the secretory pathway contain an N-terminally located signal peptide, which directs the peptides to the ribosomes on the surface of the ER and the proteins are synthesized into the lumen of this organelle.

The ER provides a quality control station. Only proteins that have folded correctly and have reached their mature, native state are allowed to leave the organelle. These proteins

are incorporated into small transport vesicles, which are decorated by COPII coat proteins that mediate vesicular transport from the ER to either the ER-Golgi intermediated compartment (ERGIC) (Appenzeller-Herzog and Hauri, 2006) or the Golgi complex (Bonifacino and Glick, 2004). During the transport through the Golgi apparatus, proteins but also the glycolipids, are subjected to a variety of posttranslational modifications of which glycosylation is the most prominent. Proteins destined for residence in the plasma membrane, in endosomes, or lysosomes are transported to these compartments in clathrin coated vesicles (Figure 2). Trafficking and sorting of proteins in the secretory pathway is a complex process. In general, vesicles bud from a “donor” compartment by specific processes that allow selective incorporation of cargo proteins into the forming vesicles. These vesicles are subsequently targeted to a specific “acceptor” compartment, where they fuse with the membrane and deliver cargo. The steps are tightly regulated and balanced so that the integrity and steady-state composition of the constituent organelle is maintained. For example, multiple mechanisms have been described for the retrieval of proteins from the Golgi to the ER, but only few signals that direct transport to the Golgi have been identified. The understanding of the Golgi complex as the organelle where complex glycans are formed and in which a multitude of proteins involved in the glycosylation machinery are localized, is fundamental towards understanding the regulation of glycoprotein and glycolipid biosynthesis.

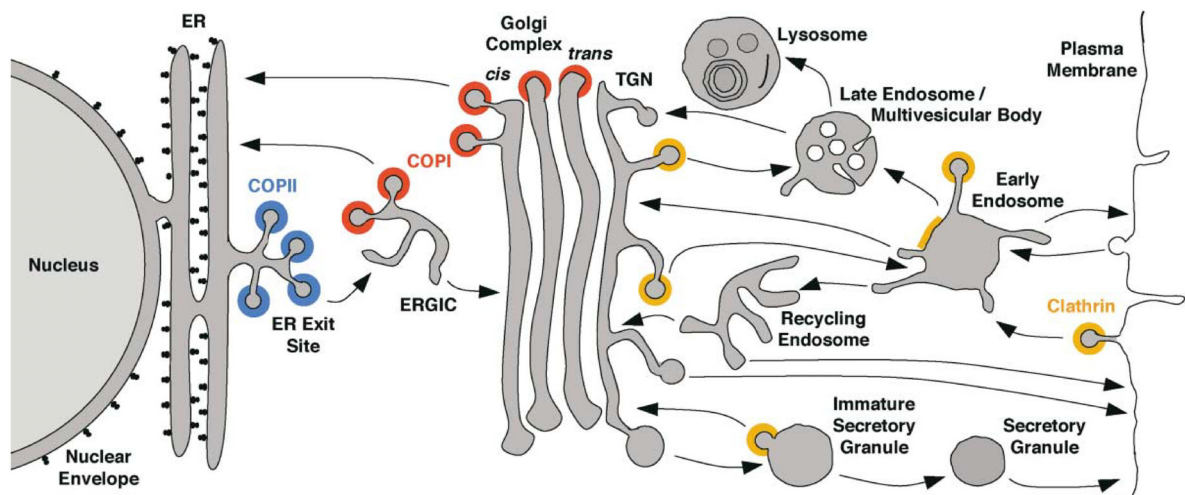


Figure 2: Intracellular transport pathways. The scheme shows the compartments of the secretory, lysosomal/vacuolar, and endocytotic pathways. The transports steps and their direction are indicated with arrows. The different vesicles coats (COPI (red), COPII (blue) and clathrin (orange)) are indicated by different colors. For simplicity other coat-like complexes are not shown (adapted from (Bonifacino and Glick, 2004)).

1.2.2 Quality control system in the ER

The ER is the location for “proof-reading” of newly synthesized proteins in the secretory pathway. This system is also known as quality control system. The function of quality control includes not only the folding processes, but also the regulation of degradation, a process called ER-associated degradation (ERAD). In contrast to the ER, the Golgi complex does not contain molecular chaperones and does not support protein folding.

In the ER, a protein has to fold correctly and reach the so called “native conformation” to be allowed to exit the ER and reach the final destination. The environment of the ER is optimized for protein folding and maturation. Specific ion concentrations, redox conditions, and the specialized set of enzymes facilitate post-translational modifications like disulphide-bond formation, signal-peptide cleavage, *N*-linked glycosylation and glycosylphosphatidylinositol (GPI)-anchor addition. A large set of chaperones exist, which are responsible for the folding process or for dispatching any improperly folded proteins for destruction. The ER resident chaperones belong to different families. The protein BiP (immunoglobulin heavy-chain binding protein (Haas and Wabl, 1983)) is a member of the Hsp70 family. BiP participates in many aspects of the quality control process by binding nascent proteins and assisting their folding. *In vitro* it was shown that BiP binds to heptapeptides with aliphatic amino acid chains. A second Hsp70 family member is the glucose-regulated protein (GRP) 170, but its function is still unknown (Easton et al., 2000). The Hsp40 family is represented with five (Erdj1-5) proteins, which has *in vitro* been shown to stimulate BiP ATPase activity (Qiu et al., 2006). GRP94 is a member of the Hsp90 family (Argon and Simen, 1999; Ni and Lee, 2007). Other factors involved in the quality control system are the peptidyl-prolyl isomerase (important for the catalysis of *cis/trans* isomerization of peptidyl-prolyl bonds) and the thiol-disulphide oxidoreductase (PDI) that catalyses the oxidation, isomerization, and reduction of disulphide bonds in the ER. All these factors are reviewed in (Ellgaard and Helenius, 2003). The exposure of hydrophobic regions, unpaired cystein residues or the tendency to aggregate are signal tags for chaperone proteins, which after binding cause retention of proteins in the ER (Amara et al., 1992; Aridor and Balch, 1999; Ellgaard and Helenius, 2003; Rutishauser and Spiess, 2002).

One of the best characterized mechanisms in the ER quality control system is the calnexin/calreticulin cycle (Figure 3). The lectins calnexin and calreticulin are homologous ER resident proteins that promote folding of glycoproteins and trap non-folded proteins in the organelle lumen until a native conformation has been reached. When a nascent protein

chain emerges from the translocation machinery in the lumen of the ER, the oligosaccharide precursor $\text{Glc}_3\text{Man}_9\text{GlcNAc}_2$ is transferred onto the nascent protein by the oligosaccharyltransferase. After the ER glucosidase I and II have removed two glucose residues, the structure $\text{Glc}_1\text{Man}_9\text{GlcNAc}_2$ is recognized by the calnexin/calreticulin system and retained until functional folding has been reached. A key enzyme in this process is the thiol-disulphide oxidoreductase ERp57, which catalyses the formation of disulphide bonds. If functional folding is sensed by the ER enzyme glucosidase II, the residual glucose residue is cleaved of the *N*-glycan and terminates the interaction with the calnexin/calreticulin system. Correctly folded proteins can then exit the ER, while proteins that have not attained correct folding are recognized by the UDP-glucose:glycoprotein glucosyltransferase, are reglucosylated and delivered to a new quality control cycle. Proteins still misfolded after several rounds are recognized by $\alpha 1,2$ -mannosidase I, which removes the mannose residues of the middle branch (Figure 3) and thus enables recognition of the glycoconjugate by the ER degradation-enhancing 1,2-mannosidase-like protein (EDEP), which finally targets misfolded proteins to the ER-associated degradation (ERAD) system (Williams, 2006).

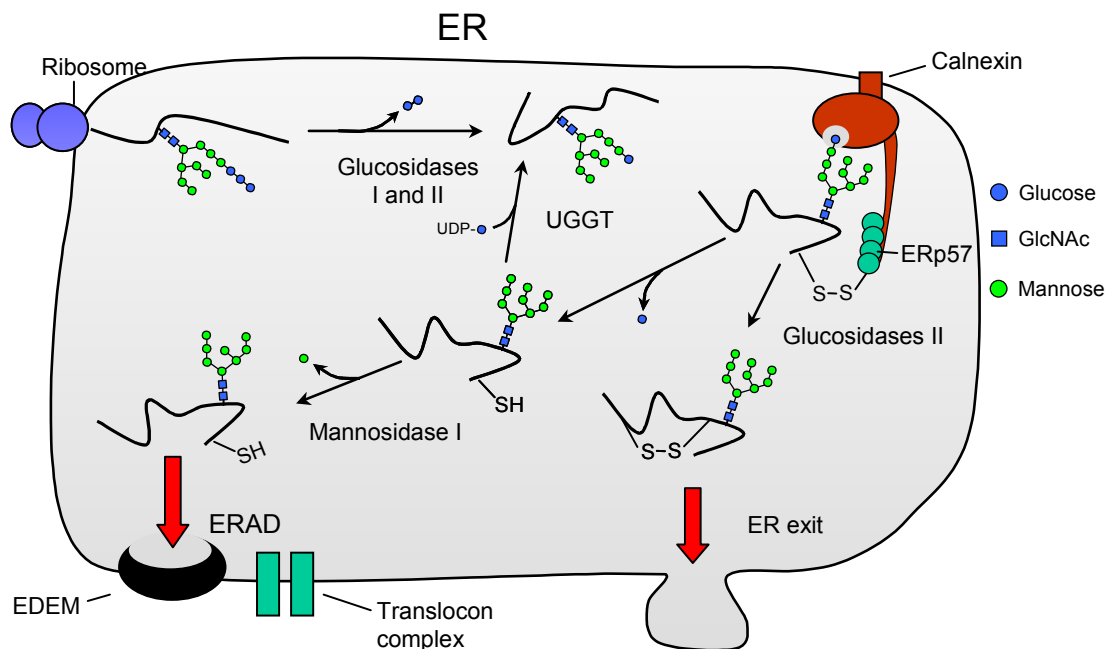


Figure 3: The calnexin/calreticulin pathway. Calnexin and calreticulin assist the folding of *N*-linked glycoproteins. For simplicity the proposed mechanism is shown only for calnexin. After transfer of the core oligosaccharide to the nascent polypeptide, glucosidases I and II remove the two terminal glucose residues. The remaining saccharide is recognized by calnexin. The chaperone associates with the thiol-disulphide

oxidoreductase ERp57, which forms disulphide bonds in the interacting glycoprotein. Cleavage of the remaining glucose by glucosidase II terminates the interaction with calnexin and the protein can exit the ER. Incorrectly folded proteins are re-glycosylated by the UDP-glucose:glycoprotein glucosyltransferase, allowing entry in a new chaperon assisted folding cycle. Proteins that withstand folding over several cycles are delivered to ER α 1,2- mannosidase I, which removes the mannose residues in the middle branch of the oligosaccharide and targets the protein to the ER-associated degradation (ERAD) (adapted and modified from (Williams, 2006)).

1.2.3 Transport between ER and Golgi

Transport between ER to Golgi represents a balanced system including forward and backward pathways. Generally, the transport is thought to be mediated by vesicular carriers. Formation of vesicles is thereby dependent on the assembly and binding of coat proteins (COPs) on the cytoplasmic face of the “donor” organelle membrane. Export of proteins from ER and transport to Golgi is mediated by COPII vesicles. COPII proteins recognize cargo proteins in the ER membrane and by physical rearrangements drive vesicle formation (Sato and Nakano, 2007). Proteins that have reached their native fold present export signals at the cytoplasmic site of the ER membrane, which directly or indirectly through transmembrane cargo adaptors and receptors interact with COPII coat subunits (Barlowe, 2003; Sato and Nakano, 2007). If proteins that are normally located in the ER are accidentally packed in vesicles and transported to the Golgi, a special retrograde transfer exist that shuttles proteins back to the ER. This pathway is also mediated by specific cytoplasmically located retrieval signals. The best known example is the KDEL sequence, but many other retrieval sequences have been described (Teasdale and Jackson, 1996). This retrograde transport from the Golgi to the ER is mediated by the coat protein COPI (Figure 2) (Antonny et al., 2005).

1.3 Glycosyltransferases

Glycosyltransferases catalyze the biosynthesis of glycans by using metabolically activated monosaccharides as substrates. Glycans can be formed with free sugars as acceptors (e.g. lactose), can be pure carbohydrate polymers, or glycan additions on proteins and lipids, which commonly are called glycoconjugates. Most glycosyltransferases involved in the biosynthesis of glycoconjugates are type II transmembrane proteins with a short N-terminal cytoplasmic tail, a transmembrane spanning region, and a luminal stem region that is followed by the large C-terminal catalytic domain (Paulson and Colley, 1989).

Glycosyltransferases catalyze the sequential transfer of monosaccharides and are specific for the donor substrate, the acceptor that is modified, and the glycosidic linkage that is catalysed. Unique domain structures for substrate recognition and nucleotide-sugar binding are located within the enzymatic molecule (Kapitonov and Yu, 1999). Nevertheless, the molecular basis on how glycosyltransferases discriminate between identically decorated intermediate products for use in subsequent steps is still poorly understood. An important observation is that acceptor specificity in many glycosyltransferases is not just a matter of recognition of one or a few specifically linked monosaccharides. It has been demonstrated that some protein glycosylating enzymes achieve additional selectivity by recognition of specific amino acid sequences in the acceptor structure (Okajima et al., 2005; Smith and Baenziger, 1988). For glycolipid biosynthesis it is suggested that a membrane bound activator protein is required to present glycolipid acceptors to the modifying glycosyltransferases (Ramakrishnan et al., 2002). Furthermore the organisation of glycosyltransferases in multi-enzyme complexes point towards additional organisation mechanisms that direct glycosylation events (Giraudo et al., 2001; Giraudo and Maccioni, 2003b; van Meer, 2001). Glycosyltransferases can also be switched in specificity *e.g.* by binding to factors that are not directly involved in the catalytic reaction, but trigger recognition of different substrates (Brew et al., 1968). The control of the vectorial organization of glycosyltransferases along the secretory pathway is crucial for their function. As a specific part of the quality control system in the ER, chaperones could be identified with high specificity for one client, *e.g.* the core 1 β 3-GalT, an enzyme involved in generation of the core 1 O-glycan (T-antigen). In the ER this transferase forms a complex with the chaperone named Cosmc, which is needed for folding and transport of the transferase to the Golgi (Ju and Cummings, 2002). In the sorting of glycosyltransferases not only the cytoplasmic tail but also the membrane spanning domain and the luminal oriented stem region can be involved. Moreover, the composition and thickness of compartmental membranes have been discussed to be part of the sorting machinery (Colley, 1997; Fenteany and Colley, 2005; Munro, 1995b; Munro, 1995a; Nilsson et al., 1991; Opat et al., 2001). Giraudo et al. identified the ER export motif [RK](X)[RK] at the N-terminus of Golgi resident glycosyltransferases (Giraudo and Maccioni, 2003a). Glycosyltransferases as well as other factors that are needed in particular places in the secretory pathway, but do not express targeting signals by themselves, can complex with other ER or Golgi resident factors and thus be hold in place. An example for this has been given in a previous study for the UDP-galactose transporter.

This protein, which lacks an ER retention or retrieval signal was shown to be retained in the ER via association with UDP-galactose:ceramide galactosyltransferase (Sprong et al., 2003). Glycosyltransferases that have reached their final destination form complexes with other in the pathway located factors. The formation of these complexes is believed to increase the efficiency and stability of Golgi localization and inhibits forward transport (Giraud et al., 2001; Giraud and Maccioni, 2003b; Jungmann and Munro, 1998).

1.3.1 The β 1,4-galactosaminyltransferase family

The name that is given to glycosyltransferases describes the stereochemistry of the reaction, the monosaccharide that is transferred and the recognized substrate. Comparison of sequences of different transferases pointed out that similarities exist in the primary nucleotide sequences. Based on these sequence similarities, different enzyme families were defined (Campbell et al., 1997; Coutinho et al., 2003). One example is the β 1,4-galactosyltransferase (β 4GalT) family. β 4GalTs catalyze the transfer of galactose from UDP-Gal to GlcNAc forming the Gal β 1-4GlcNAc structure, which is known as lacNAc and commonly found in outer chain moieties of *N*- and *O*-linked oligosaccharides and in lacto-series GSLs (Amado et al., 1999; Furukawa and Sato, 1999). The members of the β 4GalT gene family show high sequence homology in the catalytic domain. In this region, some characteristic short conserved sequence motifs were identified (FNRA, NVG, DVD and WGW(G/R)EDD(D/E)) (Amado et al., 1999). The crystal structure of the catalytic domain of the bovine β 4GalT in complex with UDP-Gal demonstrated that these conserved motifs are located in the binding pocket and are involved in UDP-Gal and substrate binding (Gastinel et al., 1999). Next to the described motifs there are four cysteine residues well conserved among the members of this family. By now, seven transferases of the β 4GalT family have been identified in mammals (β 4GalT1-7) (Amado et al., 1999; Furukawa and Sato, 1999). Six members of this family catalyze the transfer of Gal to acceptor substrates with terminal *N*-acetylglucosamine residues, and β 4GalT-7 has been shown to transfer galactose to xylose β 4-R (Almeida et al., 1999) and is involved in the biosynthesis of proteoglycan core structures. The primary function of β 4GalT-1 is the transfer of UDP-Gal to terminal GlcNAc residues, forming lacNAc as part of glycoconjugates. In mammals, β 4GalT-1 has been recruited for a second biosynthetic function, the tissue-specific production of the disaccharide lactose (Gal β ,4Glc), which takes place exclusively in the lactating mammary gland. The synthesis of lactose is

mediated by a protein heterodimer assembled from β 4GalT-1 and α -lactalbumin. This complex is termed lactose synthase (Ramakrishnan et al., 2001). The presence of α -lactalbumin also induces lactose synthase activity of β 4GalT-2, whereas β 4GalT-3 and β 4GalT-5 are largely insensitive to α -lactalbumin modulation (Sato et al., 1998; Schwientek et al., 1998). β 4GalT-3 and -4 catalyze the synthesis of lacNAc, whereby β 4GalT-4 seems to be mainly involved in formation of this structure on glycolipids (Amado et al., 1999; Schwientek et al., 1998). The transferases β 4GalT-5 and -6 have been shown to facilitate lacNAc synthesis on glycoproteins and additionally on glycolipids by galactosylation of Glc α 1-Cer. The latter activity of β 4GalT-5 is restricted to the membrane bound enzyme (Sato et al., 2000).

Next to the vertebrate members of the β 4GalT family, structurally related enzymes could be identified in invertebrates (Bakker et al., 1994; Kowar et al., 2002; Srivatsan et al., 1994; Vadaie et al., 2002; Vadaie and Jarvis, 2004; van, I et al., 1996). These transferases exhibit different substrate specificity and are able to transfer Gal, GlcNAc or GalNAc nucleotide sugars to terminal GlcNAc residues. In the *Drosophila melanogaster* genome, three members of the β 4GalT family exist (Haines and Irvine, 2005). One member is an ortholog of β 4GalT-7 and catalyses the transfer of xylose residues to polypeptides to initiate the formation of the glycosaminoglycan linker regions in *Drosophila* (Nakamura et al., 2002; Vadaie et al., 2002). The two other *Drosophila* β 4GalT family members have been shown to encode *N*-acetylgalactosaminyltransferases (GalNAcTs) that synthesise the GalNAc β 4GlcNAc unit, which is also known as lacdiNAc structure (Haines and Irvine, 2005; Sasaki et al., 2007a; Stolz et al., 2006) (Figure 4).

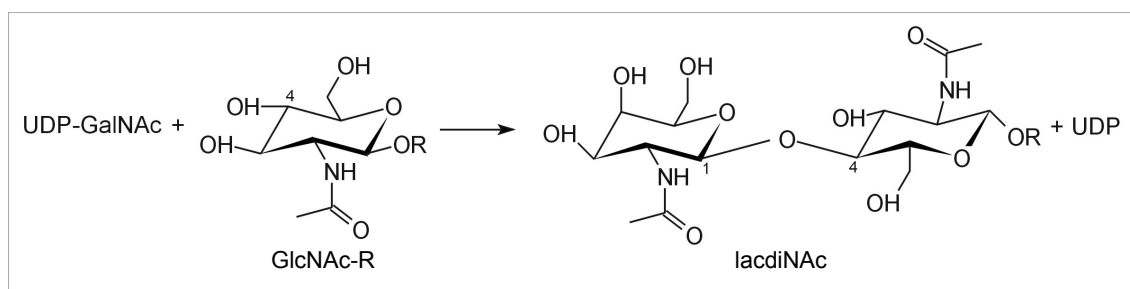


Figure 4: Reaction catalysed by *N*-acetylgalactosaminyltransferases (β 4GalNAcTs)

In *D. melanogaster* the lacdiNAc epitope is found on glycosphingolipids. The *Drosophila* β 4GalNAc transferases were cloned by Dr. Hans Bakker in the group of Prof. Rita Gerardy-Schahn by using an heterologous expression cloning system (Bakker et al., 1997). In this system, a cDNA library from *Drosophila melanogaster* was constructed and expressed in lacdiNAc-negative CHO cells. β 4GalNAc transferase activity, which resulted in the formation of the lacdiNAc epitope, was monitored with a monoclonal antibody (mAb). The mAb called 259-2A1 was originally raised against *Schistosoma mansoni* surface glycoconjugates, which are rich in lacdiNAc structures (van Remoortere et al., 2000). Using an elaborated sibling selection procedure, Dr. Bakker was able to demonstrate that lacdiNAc formation was depended on the coordinated activity of the products of two genes. One clone encoded a member of the β 4GalT family (β 4GalNAcTB; flybase CG14517) (Haines and Irvine, 2005; van Die et al., 1997), while the second (flybase CG17257) encoded a type III membrane protein. Based on primary sequence characteristics, this protein was identified as a member of a gene family referred to as DHHC proteins (Mitchell et al., 2006). Activity for the full length or soluble expressed β 4GalNAcTB was never detected in our laboratory as well as in others (Haines and Irvine, 2005), but in co-expression of β 4GalNAcTB with the type III membrane protein, lacdiNAc structures were synthesized. A second homologous enzyme β 4GalNAcTA (flybase CG8536) was identified by BLAST search and cloned by PCR. In contrast to β 4GalNAcTB, this enzyme exhibited autonomous activity after expression as full length or soluble enzyme (Haines and Irvine, 2005).

1.4 The DHHC protein family

DHHC proteins are multi-transmembrane proteins with a cysteine-rich domain (CRD) that presents a variant of the zinc finger domain (Putilina et al., 1999) and is further defined by the core Asp-His-His-Cys (DHHC) tetrapeptide sequence. This DHHC motif is required for the palmitoylation reaction catalyzed by the enzyme (for review see (Linder and Deschenes, 2007)). Palmitate is attached to a cystein residue in the cytoplasmic part of proteins normally close to the *N*-terminus of a protein through a reversible thioester linkage (S-palmitoylation). No signal sequence for palmitoylation has been identified yet (Linder and Deschenes, 2007). For catalytic reaction, the DHHC motif is required *in vitro* and *in vivo* and mutations in the amino acid sequence, especially replacement of the cystein residue, abolish protein acyltransferase (PAT) activity (Fernandez-Hernando et al.,

2006; Linder and Deschenes, 2004; Lobo et al., 2002a; Nadolski and Linder, 2007; Roth et al., 2002a). Palmitoylation has been implicated in the process of protein trafficking between organelles (Smotrys and Linder, 2004) and plays a key role in the targeting of proteins to nerve terminals including synapses (Huang and El Husseini, 2005).

Proteins containing a DHHC sequence and the cystein-rich domain are conserved throughout many species, but until now only a few are characterized in detail. The first DHHC proteins with PAT activity were identified in *Saccharomyces cerevisiae* (Lobo et al., 2002a; Roth et al., 2002a) and further biochemical studies confirmed PAT activity for three of the seven DHHC proteins in yeast (Linder and Deschenes, 2007). In mammals 23 different DHHC protein genes are identified (Dietrich and Ungermann, 2004; Mitchell et al., 2006) and investigations to characterize substrates, expression pattern and subcellular localization are in process (Fernandez-Hernando et al., 2006; Fukata et al., 2004; Fukata et al., 2006; Ohno et al., 2006). Although many different screening procedures were established and applied to many of the mammalian DHHC proteins, only six (DHHC 2, 3, 7, 8, 15, and 21) were shown to have PAT activity. The function of the other DHHC protein members is still not known.

1.5 Glycosylation in *Drosophila melanogaster*

The fruit fly *Drosophila melanogaster* is one of the predominant organisms for genetic analyses. In the field of glycobiology the fly has been used to characterize the essential functions for a number of glycoconjugates in developmental processes.

GSLs are important glycoconjugates during development in *Drosophila melanogaster*. The analyzed GSL structures in the fruit fly are characterized by a core structure with mannose linked to glucosylceramide that belong to the arthro-series (Seppo et al., 2000) and represent the common glycolipid series of arthropods and nematodes (Figure 1) (Sugita et al., 1982; Wiegandt, 1992). In *Drosophila*, acidic and zwitterionic GSLs are described. They specifically exhibit a high content of *N*-acetylhexosamine and the addition of phosphoethanolamine (PE) groups on GlcNAc residues. The initial GSL structure GalNAc β ,4(PE-6)GlcNAc β ,3Man β ,4Glc β Cer contains the lacdiNAc epitope (GalNAc β ,4GlcNAc). The longest described neutral glycolipid structure is an octaosylceramide (GalNAc β ,4(PE-6)GlcNAc β ,3Gal β ,3GalNAc α ,4GalNAc

β ,4(PE-6)GlcNAc β ,3Man β ,4Glc β Cer), designated as Nz8. The major acidic lipid, designated Az₂9, contains two PE groups and a glucuronic acid linked to a Gal-extended Nz₂8 oligosaccharide.

The biological function of glycolipids in *Drosophila* has been demonstrated by mutants lacking mannosyltransferase (*egghead*, *egh*) or GlcNAc transferase (*brainiac*, *brn*) (Schwientek et al., 2002a; Wandall et al., 2003; Müller et al., 2002; Wandall et al., 2005). These enzymes are responsible for the second and third step of GSL sugar elongation. Mutant flies have very similar lethal phenotypes and show defects in epithelial morphogenesis during oogenesis and embryogenesis (Goode et al., 1992; Goode et al., 1996). In contrast to this, mutants in the enzymes that are responsible for the transfer of the fourth sugar (β 4GalNAcTA and β 4GalNAcTB), show rather mild phenotypes. *Drosophila* mutants for *β 4GalNAcTA* display an abnormal locomotion phenotype, indicating a role for this enzyme in the neuromuscular system (Haines and Irvine, 2005; Haines and Stewart, 2007), whereas a small proportion of homozygous *β 4GalNAcTB* mutant flies exhibit abnormal oogenesis (Chen et al., 2007).

1.6 Aim of this study

Two functionally active *Drosophila* β 4GalNAcTs (β 4GalNAcTA and β 4GalNAcTB) were cloned in the laboratory of Prof. Gerady-Schahn and were demonstrated to behave very different in terms of functional activity. While β 4GalNAcTA was active after expression in different mammalian cell systems, activity for β 4GalNAcTB could only be installed if a second factor, belonging to the DHHC protein family, was co-expressed. The aim of this study was to analyze in detail the role played by the DHHC family protein in the activation of β 4GalNAcTB and to discriminate features that mediate the selective interaction between the type III membrane protein and β 4GalNAcTB. Moreover, because flies with single defects in the β 4GalNAcTs had been generated in the laboratory of K. Irvine, it was my goal to use these models to study the impact of each enzyme for lacdiNAc production *in vivo*. To reach this goal the comparative analysis of the GSL fractions isolated from wild type and mutant flies by mass spectrometry was planned.

2 Materials and Methods

2.1 Material

2.1.1 Chemicals

Acetic acid (100 %)	Merck
Acetone	Baker
Acrylamide 40% 4 K-Mix (37.5:1)	Serva
Adenosine-5'-triphosphate (ATP)	Sigma
Agarose	Serva
Ammonium chloride	Merck
Ammonium persulfate (APS)	Serva
6-Aza-2-thiothymine (ATT)	Sigma
BCA <i>Protein Assay Reagent</i>	Pierce
Beta-Mercaptoethanol	Sigma
Borate, sodium salt	Merck
Bromophenol Blue, sodium salt	Applichem
BSA (Fraktion V)	Applichem
BSA protein standard	Pierce
Chloroform	Baker
Digitonin	Sigma
Dimethylsulfoxide (DMSO)	Merck
Dipotassium hydrogen phosphate	Merck
Disodium hydrogen phosphate	Merck
Dithiothreitol (DTT)	Sigma
2,5-Dihydroxybenzoic acid (DHB)	Bruker
dNTPs (100 mM each)	Pharmacia
Dry milk	Applichem
EDTA, Disodium salt (Titriplex III)	Merck
Ethanol, absolute	Baker
Ethidium Bromide	USB Corporation
Fluorescent mounting medium	DakoCytomation
Formaldehyde	Sigma

Glycerol (99%)	KMF
Glycine	Sigma
Hexan	J.T. Baker
Hydrochloric acid (38%)	Baker
Hydrogen peroxide	Fluka
Imidazole	Fluka
Isopropanol (2-Propanol)	Merck
Magnesium chloride	Sigma
Manganese chloride	Merck
Methanol	Baker
MOPS	Applichem
Moviol	Baker
NonidetP-40 (NP-40)	Roche
Paraformaldehyde	Sigma
Phenylmethylsulfonyl fluorid (PMSF)	Sigma
Polyisobutylmethacrylat	Sigma
Ponceau S, sodium salt	Sigma
Potassium dihydrogen phosphate	Merck
Potassium chloride	Applichem
Proteaseinhibitor: Complete EDTA free	Roche
Roti-Blue Coomassie-stain (5x)	Roth
Saponin	Sigma
Sodium acetate	Merck
Sodium chloride	Merck
Sodium dihydrogen phosphate	Merck
Sodium dodecylsulfate (SDS)	Merck
Sodium hydroxide	Merck
Sucrose	Merck
TEMED (N,N,N',N'-Tetramethyl-ethylendiamin)	Serva
TRIS (Tris(hydroxymethyl)-aminomethan)	Merck
Tween-20	Fluka
Urea	GibcoBRL

2.1.2 Standard buffer and media

AP buffer	100 mM Tris-HCl pH 9.5 100 mM NaCl 5 mM MgCl ₂
DNA loading buffer	30 % Glycerol 60 mM EDTA pH 8,0 0,25 % (w/v) Orange G 1x TBE
2x Laemmli	200 mM Tris-HCl pH 6.8 30% (v/v) glycerol 3% (w/v) SDS 0.1% (w/v) bromophenol Blue 5% (v/v) 2-mercaptoethanol
PBS	10 mM sodium phosphate pH 7.4 150 mM NaCl
PBS/EDTA	10 mM sodium phosphate, pH 7.4 150 mM NaCl 2 mM EDTA
TAE	40 mM Tris-Acetate 2 mM EDTA pH 8.5
TBE	100 mM Tris-HCl, pH 8.0 100 mM Borate 2.5 mM EDTA
TBS	20 mM Tris-HCl, pH 7.4 150mM NaCl
2x Urea buffer	15 mM Tris/HCl pH 8,8 1 % SDS 10 % Glycerol 8,0 M Urea

2.1.3 Culture media and additives

Ampicillin, sodium salt	Serva
Carbenicillin, disodium salt	Fluka
DMEM/HAM's medium	Biochrom AG
Foetal calf serum (FCS)	Invitrogen
G 418 (50 mg/ml)	Calbiochem
TC100 Insect cell medium	Biochrom AG
Kanamycin	Sigma
Korsolex plus	Roche
LB-agar	Becton Dickinson
LB-medium	Becton Dickinson
Metafectene	Biontex
OptiMEM	GibcoBRL
Poly (L)-lysine	Sigma
Tryptan blue solution (0,4 %)	Sigma
Trypsin/EDTA	BiochromAG

2.1.4 Kits and further materials

Cell culture bottles and dishes	Sarstedt
Electroporation cuvettes	BioRad
Filter paper	Whatman
Glas capillaries	Macherey-Nagel
Glas tubes with Teflon cap	DIONEX
HPTLC-plates Nano-DURASIL-20 size 10 x 10 cm	Macherey-Nagel
MEGASCRIPT T7 transcription kit	Ambion
Microtiter plates 96-well polystyrol (U-bottom)	Greiner
PVDF-membrane	Waters
PCR-tubes (0,2 ml)	Biozym
Polypropylen tubes (14 ml, 50 ml)	Greiner
QIAGEN Plasmid Mini und Midi Kit	Qiagen
Qiaquick Gel Extraction Kit	Qiagen

Qiaquick PCR purification kit	Qiagen
Reaction tubes (0.5 ml, 1.5 ml)	Sarstedt
Reaction tubes safelock (1.5 ml, 2 ml)	Eppendorf
Sterile filters Millex GP (0,22 µM)	Milipore

2.1.5 Laboratory Equipment

AlphaImager	Alpha Innotech
Blotting chamber Fast-Blot B44	Biometra
Centrifuges :	
- Biofuge fresco	Heraeus
- Biofuge pico	Heraeus
- Multifuge 3 S-R	Heraeus
- Centrifuge 5415C	Eppendorf
- Coulter Avanti J-30I	Beckman
Rotors:	
- JA 25.50	Beckman
- JLA 10.500	Beckman
- JS-24.15	Beckman
Electroporator	BioRad
Electrophoresis chamber for agarose-gels	peqlab
Electrophoresis chamber for SDS-PAGE	BioMetra
ELISA-Reader: DigiScan	Asys Hitech
Heatingblock TB1	BioMetra
HeraSafe Hood	Heraeus
Incubators	Heraeus
Odyssey Infrared Imaging System	LI-COR Biosciences
Scales CP 224S (µg) / CP 3202 (g)	Sartorius
Sonifier 450	Branson
Spectrophotometer Ultrospec 2100 pro	Amersham Biosciences
Speedvac RVC 2-18	Christ
Standard Power Pack P25	Biometra
Thermocycler T1 and T Gradient	Biometra

Thermomixer compact	Eppendorf
ULTRAFLEX™ MALDI-TOF/TOF spectrometer	Bruker

2.1.5 Enzymes

<i>cloned Pfu</i> -DNA-Polymerase	Stratagene
Restriction enzymes	New England Biolabs
T4-DNA-Ligase	New England Biolabs
<i>Taq</i> -DNA-Polymerase	Sigma
Phusion™ High-Fidelity DNA Polymerase	Finnzymes

2.1.6 Molecular weight markers

‘1 kb DNA ladder’	Invitrogen
‘SDS-PAGE molecular weight standards high range’	BioRad
‘Prestained Protein Marker’	New England Biolabs

2.1.7 Antibodies

2.1.7.1 Primary Antibodies

mAb 259-2A1:	monoclonal antibody (mouse IgG1) directed against lacdiNAc supplied by Cornelis Hokke (van Remoortere et al., 2000)
anti-myc 9E10:	monoclonal antibody (mouse) directed against the myc- epitope EQKLISEEDL (in house production)
anti-Flag M5:	monoclonal antibody (mouse IgG1) directed against the FLAG-epitope DYKDDDDK (Sigma)
anti-HA 12CA5:	monoclonal antibody (mouse) directed against the HA- epitope YPYDVPDYA (in house production)
anti-HA 3F10	monoclonal antibody (rat) directed against the HA- epitope YPYDVPDYA (Roche)
anti-giantin	polyclonal antibody (antiserum rabbit) directed against the N-terminus of human giantin (Covance)
anti-calnexin	polyclonal antibody 575-593 (rabbit) against the ER protein calnexin (Acris)

anti-mannosidase II polyclonal antibody 575-593 (rabbit) against the Golgi protein mannosidase II (Acris)

2.1.7.2 Secondary Antibodies

Anti-mouse-IgG Cy3 conjugate	Sigma
Anti-rabbit-IgG Alexa 488 conjugate	Molecular Probes
Anti-rat-IgG-Cy3 conjugate	Chemicon
Anti-mouse-Ig AP conjugate	Dianova
Anti-mouse-Ig HRP conjugate	Dianova
Streptavidin AP conjugate	Caltag
Anti-mouse-IgG IRDye800 conjugate	LI-COR Biosciences
Anti-rat-IgG IRDye800 conjugate	LI-COR Biosciences

2.1.8 Oligonucleotides

All oligonucleotides were purchased from MWG.

Sequencing primers (5' → 3')

T7	TAATACGACTCACTATA
Sp6	GCATTTAGGTGACACTATAGAATAG
pcDNA3.1	CTCTGGCTAACTAGAGAAC
BGH-reverse	TAGAAGGCACAGTCGAGG

PCR amplification primers (5' → 3')

for dsRNA synthesis

AS3	GAATTAATACGACTCACTATAGGGAGACCGGCACCTCCAATTTTCTTTC
AS4	GAATTAATACGACTCACTATAGGGAGAGTCCATATCCCCACCTCGTCA
AS5	GAATTAATACGACTCACTATAGGGAGAATGTACCTCTTCACCAAGGCGA
AS6	GAATTAATACGACTCACTATAGGGAGAATAACCAATGTTTCATCATGGCA
AS7	GAATTAATACGACTCACTATAGGGAGATCAACTTTTCTGCCAACAATG
AS8	GAATTAATACGACTCACTATAGGGAGAACCACGCCGCCGAAAAGACC

for GABPI deletion constructs

AS16	AGTACTCGAGCGCGGAGGAGCCAAGCGA
AS17	AGTACTCGAGA ACTCAAAGACCGCCATAG
AS18	AGTACTCGAGCGGACCGCCACGCGGACA

AS28 AGTACTCGAGCAGGTTCTCTGCTGGAG
AS31 AGTACTCGAGTACTGGCTAAACTGCTGC
AS32 AGATTCTAGAGCAGCAGTTTAGCCAGTA
AS33 AGATTCTAGATGGATAACCAAGCGGTCG
HB36 AGTACTCGAGATGTTCTTGATGACAGCCGGCA
HB38 GTGATCTAGAGTAGTCACTTTAAGATGG
HB74 CAAGTCTAGACTTTAAGATGGCTCGCCAGT
HB85 AGATGACGTCCCCGATTACGCTTCGAGTGGCGAGGAGCA
HB86 AGATGACGTCATAAGGGTACTCGGCGATCCCAGGCAGCT

for internal HA-tag GABPI constructs

AS11 AGTAGACGTGGTATGGATAACCAAGCGGTCGCAC
AS12 AGATGACGTCCCCGATTACGAGGAGAACTACGCGTTAATG
AS13 AGATGACGTTCGTATGGATAAACCTGAAACTCAAATATG
AS14 AGATGACGTCCCCGATTACCGGACAACTTCTTTTTGAGC
AS15 AGATGACGTCATAAGGGTACCGCTTAGCCAGCTCCATGCC
AS57 AGATGACGTCCCCGACTACTGCAGTGAGGTGTTCTGAAG

for GABPI mutagenesis

AS37 TTTGAGTTTCAGGTTGCTCTGCTGGAGCTGGCT
AS38 AGCCAGCTCCAGCAGACGAACCTGGAAACTCAAA
AS39 CAGGTTCTCTGCTGGCGCTGGCTCCGGAGGAG
AS40 CTCCTCCGGAGCCAGCGCCAGCAGAGGAACCTG
AS41 CTGGAGCTGGCTCCGGCGGCGAACTACGCGTTAATG
AS42 CATTAACGCGTAGTTTCGCCCGGAGCCAGCTCCAG
AS43 CTGCTGGAGCTGGCTGCGGAGGAGAACTACGCG
AS44 CGCGTAGTTCTCCTCCGCAGCCAGCTCCAGCAG
AS45 CGACCGCTTGTTATGCAGTTCCTTTTGCCCGAC
AS46 GTCGGGCAAAGAAGAACTGCATAACCAAGCGGTCG
AS47 TATCCAGTTCCTTTGGCCGACGACTGCAGTGAG
AS48 CTCACTGCAGTCGTCGGCCAAAAGAAGAACTGGATA
AS49 CTTTTGCCCGACGACGCCAGTGAGGTGTTTCGAA
AS50 TTCGAACACCTCACTGGCGTCGTCGGGCAAAG
AS51 CCAGTTCCTTTGCCCGCCGCCTGCAGTGAGGTGTTTC
AS52 GAACACCTCACTGCAGGCGGCGGGCAAAGAAGAACTGG
AS53 TCGGTGAAGAGGCGCGCTCATCACAGCTACTGG
AS54 CCAGTAGCTGTGATGAGCGCGCCTCTTCACGCA
AS55 ACCTGCGTGAAGAGGCGCGCTGCTGCCGCCTACTGGCTAAACTGCTGC
AS56 GCAGCAGTTTAGCCAGTAGGCGGCAGCAGCGCGCCTCTTCACGCAGGT
AS58 TACATGATCATCATATTTGCGTTTCAGGTTCTCTGCTG

AS59	CAGCAGAGGAACCTGAAACGCAAATATGATGATCATGTA
AS60	ACCCTCACTTCCATTTGCGCTCCGTTTATGGTGGTGCGA
AS61	TCGCACCACCATAAACGGAGCGCAAATGGAAGTGAGGGT
AS62	CTCACTTCCATTTGCCATGCGTTTATGGTGGTGCGACCG
AS63	CGGTGCGACCACCATAAACGCATGGCAAATGGAAGTGAG
AS64	TGCGTGAAGAGGGCGCGATGCTCACAGCTACTGG
AS65	CCAGTAGCTGTGAGCATCGCGCCTCTTCACGCA
AS66	TGCGTGAAGAGGGCGCGATCATGCCAGCTACTGG
AS67	CCAGTAGCTGGCATGATCGCGCCTCTTCACGCA
AS77	CTGGAGCTGGCTCCGCAGCAGAACTACGCGTTAATG
AS78	CATTAACCGGTAGTTCTGCTGCGGAGCCAGCTCCAG
HB89	GAAGAGGCGCGATCATCACTGCTACTGGCTAAACTGCTG
HB90	CAGCAGTTTAGCCAGTAGCAGTGATGATCGCGCCTCTTC
HB91	GAAGAGGCGCGATCATCACGCCTACTGGCTAAACTGCTG
HB92	CAGCAGTTTAGCCAGTAGGCGTGATGATCGCGCCTCTTC

for β 4GalNAcTA/ β 4GalNAcTB hybrid constructs

HB70	GCAATGATCTCCGAGTAGGTGCAGTTGGCAAGGAGG
HB73	TCCGCCCTCCTTGCCAACTGCACCTACTCGGAGATCAT
HB77	GTGCTTAACTTTGTGGGCTTCCGTTTCGCATCGCACT
HB78	CGTAGTGCGATGCGAACCGGAAGCCCACAAAGTTAAG
HB79	TCCGCCCTCCTTGCCAACTGCACCTACTCGGAGATCAT
HB80	GCAATGATCTCCGAGTAGGTGCAGTTGGCAAGGAGG
HB134	AGCAGCGATGGAGCCGGAGGCTGCACCTACTCGGAGATCATT
HB135	AATGATCTCCGAGTAGGTGCAGCCTCCGGTCCATCGCTGCT
HB136	AGCAGCGATGGAGCCGGAGGCTGCACTGATCCCGATCCCCGT
HB137	ACGGGGATCGGGATCAGTGCAGCCTCCGGTCCATCGCTGCT

2.1.9 Plasmids

pcDNA3	Eukaryotic expression vector (Invitrogen)
pcDNA3Flag	Eukaryotic expression vector based on pcDNA3 bearing a Flag epitope (N-MBYKDDDDK-C) between the restriction sites <i>KpnI/BamHI</i> (synthesized by Anja Münster)
Flag-GalNAcTB	Eukaryotic expression vector based on pcDNA3 bearing Flag-tagged GalNAcTB (1507); PCR on cDNA library clone with primer HB033 and T7 cloned with <i>BamHI/XhoI</i> in pcDNA3Flag
Flag-GalNAcTA	Eukaryotic expression vector based on pcDNA3 bearing Flag-tagged GalNAcTA (1559); PCR on larval mRNA with primer HB54 and HB55 cloned with <i>EcoRI/XbaI</i> in pcDNA3Flag

myc-GABPI	Eukaryotic expression vector based on pcDNA3 bearing myc-tagged GABPI (1506); PCR on larval mRNA with primer HB36 and HB38 cloned with XhoI/XbaI in pcDNA3Myc2
myc-GABPI-HA	Eukaryotic expression vector based on pcDNA3 bearing N-terminal myc-tagged and C-terminal HA-tagged GABPI (1744); PCR on 1506 with primer HB74 and T7 cloned with HindIII/XbaI
myc- Δ 90 GABPI-HA	Eukaryotic expression vector based on pcDNA3 bearing N-terminal myc-tagged and C-terminal HA-tagged GABPI with N-terminal deletion (2338); PCR on 1506 with primer AS16 and HB74 cloned with XhoI/XbaI in myc-GABPI-HA
myc- Δ 117 GABPI-HA	Eukaryotic expression vector based on pcDNA3 bearing N-terminal myc-tagged and C-terminal HA-tagged GABPI with N-terminal deletion (2339); PCR on 1506 with primer AS17 and HB74 cloned with XhoI/XbaI in myc-GABPI-HA
myc- Δ 141 GABPI-HA	Eukaryotic expression vector based on pcDNA3 bearing N-terminal myc-tagged and C-terminal HA-tagged GABPI with N-terminal deletion (2340); PCR on 1506 with primer AS18 and HB74 cloned with XhoI/XbaI in myc-GABPI-HA
myc- Δ 167 GABPI-HA	Eukaryotic expression vector based on pcDNA3 bearing N-terminal myc-tagged and C-terminal HA-tagged GABPI with N-terminal deletion (2484); PCR on 1744 with primer AS28 and HB74 cloned with XhoI/XbaI in myc-GABPI-HA
myc- Δ 296 GABPI-HA	Eukaryotic expression vector based on pcDNA3 bearing N-terminal myc-tagged and C-terminal HA-tagged GABPI with N-terminal deletion (2487); PCR on 1744 with primer AS31 and HB74 cloned with XhoI/XbaI in myc-GABPI-HA
myc- Δ 141GABPI Δ 80-HA	Eukaryotic expression vector based on pcDNA3 bearing N-terminal myc-tagged and C-terminal HA-tagged GABPI with N- and C-terminal deletion (2491); PCR on 1744 with primer AS18 and HB33 cloned with XhoI/XbaI in myc-GABPI-HA
myc- Δ 141 GABPI Δ 124-HA	Eukaryotic expression vector based on pcDNA3 bearing N-terminal myc-tagged and C-terminal HA-tagged GABPI with N- and C-terminal deletion (2489); PCR on 1744 with primer AS18 and HB32 cloned with XhoI/XbaI in myc-GABPI-HA
myc-HA Δ 143-145 GABPI	Eukaryotic expression vector based on pcDNA3 bearing N-terminal myc-tagged and internal HA-tagged GABPI (2343); PCR on 1506 with primer AS14/HB38 and AS15/HB36 cloned with AatII/XbaI and AatII/XhoI in myc-GABPI
myc-HA Δ 170-176 GABPI	Eukaryotic expression vector based on pcDNA3 bearing N-terminal myc-tagged and internal HA-tagged GABPI (2342); PCR on 1506 with primer AS12/HB38 and AS13/HB36 cloned with AatII/XbaI and AatII/XhoI in myc-GABPI

myc-HA222 GABPI	Eukaryotic expression vector based on pcDNA3 bearing N-terminal myc-tagged and internal HA-tagged GABPI (1901); PCR on 1506 with primer HB85/HB38 and HB86/HB36 cloned with AatII/XbaI and AatII/XhoI in myc-GABPI
myc-HAΔ346-353 GABPI	Eukaryotic expression vector based on pcDNA3 bearing N-terminal myc-tagged and internal HA-tagged GABPI (2341); PCR on 1506 with primer AS57/HB38 and AS11/HB36 cloned with AatII/XbaI and AatII/XhoI in myc-GABPI
pBSK myc-GABPI	Eukaryotic expression vector based on pBlueScript vector bearing N-terminal myc-tagged GABPI (1928); 1506 cut XhoI/XbaI in pBSK vector
pIB/V5-His	Insect cell expression vector (1555)
pIB-His-myc-GABPI	Insect cell expression vector based on the pIB/V5 His bearing N-terminally myc-tagged GABPI (1597); cut with HindIII/XbaI from 1506 in insect cell vector 1555
pIB-His-Flag-β4GalNAcTA	Insect cell expression vector based on the pIB/V5 His bearing N-terminally Flag-tagged β4GalNAcTA (1599); cut with cut with HindIII/XbaI from 1559 in insect cell vector 1555
pIB-His-Flag-β4GalNAcTB	Insect cell expression vector based on the pIB/V5 His bearing N-terminally Flag-tagged β4GalNAcTB (1598); cut with cut with HindIII/XbaI from 1507 in insect cell vector 1555

2.1.9.1 Plasmids with site-directed mutagenesis

All plasmids generated by site-directed mutagenesis have a eukaryotic expression vector based on pcDNA3 bearing a point-mutated, N-terminally myc-tagged GABPI. PCRs were performed on pBSK myc-GABPI with primer as indicated. The PCR products were cut with XhoI/XbaI and cloned in 1506.

myc-E166A-DHHC	(2604); primer AS58/AS59
myc-P170A DHHC	(2563); primer AS37/AS38
myc-E173A-DHHC	(2564); primer AS39/AS40
myc-EE177/178AA-DHHC	(2565); primer AS41/AS42
myc-P176A-DHHC	(2566); primer AS43/AS44
myc-H335A-DHHC	(2605); primer AS60/AS61
myc-P336A-DHHC	(2606); primer AS62/AS63
myc-P346A-DHHC	(2567); primer AS45/AS46
myc-P350A-DHHC	(2568); primer AS47/AS48
myc-C353A-DHHC	(2569); primer AS49/AS50
myc-DD351/352AA-DHHC	(2570); primer AS51/AS52

myc-D293A-DHHC	(2571); primer AS53/AS54
myc-H294A-DHHC	(2607); primer AS64/AS65
myc-A295A-DHHC	(2608); primer AS66/AS67
myc-DHHC/AAAA	(2572); primer AS55/AS56
pBdrDHHC-S-C	(1921); primer HB89/HB90
pBdrDHHC-S-A	(1922); primer HB91/HB92

2.1.10 Laboratory animals

Drosophila melanogaster wild-type Wild-type strain Oregon R was kindly provided by Prof. Gerd Bicker, Tiermedizinische Hochschule Hannover.

Drosophila melanogaster $\beta 4GalNAcTA^{4.1}$ Single mutant flies of $\beta 4GalNAcTA$ (CG8536) were generated by P transposable element insertion in the 5' untranslated region. This strain as well as the following two were kindly provided by Nicola Haines, Department of Biology, University of Toronto, Canada.

Drosophila melanogaster $\beta 4GalNAcTB^{GT}$ Single mutant flies of $\beta 4GalNAcTB$ (CG14517) were generated by gene-targeted homologous recombination.

Drosophila melanogaster $\beta 4GalNAcTA^{4.1};\beta 4GalNAcTB^{GT}$ Double mutant flies of $\beta 4GalNAcTA$ and $\beta 4GalNAcTB$ were generated by crossing.

2.1.11 Eukaryotic cell lines

CHO K1 (C6) Chinese hamster ovary cell line, subclone of the fibroblast line CHO K1 (ATCC CRL 9618) produced by Dr. M. Eckhardt.

HEK293 Human embryonic kidney cells, original generated by transformation with sheared adenovirus 5' DNA.

S2 cells *Drosophila* S2 cells (Schneider cells) (Invitrogen)
The S2 cell line was derived from a primary culture of late stage (20-24 hours old) *Drosophila melanogaster* embryos.

2.1.12 Bacterial strains

E. coli XL-1 blue (Stratagene) Genotype: *recA1 endA1 gyr96 thi-1 hsdR17 supE44 relA1 lac* [F' *proAB lacI^fZΔM15 Tn10* (Tet^r)]

E. coli YZ 2000 (Gene Bridges) Genotype: *thr-1 leu-6 thi-1 lacY1 galK2 ara-14 xyl-5 mtl-1 proA2 his-4 argE3 str-31 tsx-33 supE44 recB21, recC22, sbcA23, rpsL31, tsx-33, supE44, his-328, mcrA, mcrBC, mrr, hsdMRS*

2.2 Methods

2.2.1 Cell biological techniques

CHO and HEK293 cells were cultured in a humidified incubator at 37°C and 5% CO₂. CHO cells were grown in α -MEM (GibcoBRL) and HEK293 cells in DMEM/HAM's (Biochrom AG) supplemented with 10% FCS. Every 3-4 days, confluent cell layers were detached from the cell culture flask with Trypsin/EDTA (GibcoBRL) and transferred to a new device at a concentration of 5×10^5 cells/75 cm² for CHO cells and 2×10^6 cells/75 cm² cells for HEK293 cells.

Drosophila Schneider cells were cultured in a humidified incubator at 27°C. The cells were grown in TC100 insect cell medium (Biochrom AG) supplemented with 10% FCS and 2mM Glut-L. Once a week, cell suspension cultures were transferred to a new device at a concentration of 5×10^5 cells/175 cm².

For long term storage in liquid nitrogen, cells were pelleted by centrifugation (5 min, 1000 x g, RT) and resuspended in culture medium containing 10 % FCS and 10 % DMSO at a concentration of 0.5×10^7 cells/ml. Aliquots of 1 ml were filled in cryo vials, stored overnight at -80°C and then transferred to liquid nitrogen.

To recover frozen cell pellets, the cells were thawed at room temperature (RT) and transferred into 10 ml α -MEM or DMEM/HAMs supplemented with 10% FCS. After centrifugation (5 min, 1000 x g, RT) the cell pellet was resuspended in culture medium (5 % FCS) and transferred to a culture flask.

2.2.1.1 Transient transfection of HEK293 cells

For the transient transfection of HEK293 cells in 75 cm² flasks, the cells were seeded at a concentration of 1.5×10^6 cells/75 cm² (of 1.2×10^5 cells/9.6 cm² well) and incubated for one day. For each flask (well), a transfection mixture was prepared by combining 7.5 μ g DNA in 750 μ l OptiMEM (1 μ g DNA with 100 μ l OptiMEM) with 45 μ l Metafectene[®] in 750 μ l OptiMEM (6 μ l Metafectene[®] in 100 μ l OptiMEM). For cotransfection of two different plasmids a DNA concentration of 3.75 μ g/plasmid was used. The mixture was incubated for 30 min at RT. Prior to the addition of the transfection mixture, 6 ml of fresh

medium was added to the cell layer. After 4 hours incubation at 37°C, 8 ml culture medium was added and the cells were analysed after 48 hours.

2.2.1.2 Transient transfection of S2 cells

For transient transfection, *Drosophila* Schneider cells were seeded in 6-well plates (9.6 cm²) at a concentration of 2×10^6 cells/well and incubated over night. For each well, a transfection mixture was prepared by combining 2 µg DNA in 100 µl OptiMEM with 8 µl Cellfectin in 92 µl OptiMEM. For cotransfection of two different plasmids a DNA concentration of 1 µg/plasmid was used. The mixture was incubated for 20 min at RT. Prior to the addition of the transfection mixture, 800 µl OptiMEM/well was added to the cell layer. After 4 hours of incubation at 27°C, 2 ml culture medium was added and the cells were analysed after 48 hours.

2.2.1.3 Generation of semi stable HEK293 cells

For the generation of a semi stable cells line, HEK293 cells were seeded in 6-well plates (9.6 cm²) at a concentration of 1.2×10^5 cells/ well and incubated for one day. The cells were transfected with the plasmid of interest as described in 2.2.1.1. One day after transfection the cells were resuspended and transfer in a 75 cm² flask. Two days later fresh medium containing the antibiotic G418 (neomycin) at a concentration of 800 µg/ml was added to the cells. The cells were grown in antibiotic containing medium until single colonies became visible. The single colonies were resuspended and incubated in the flasks until a dense cell layer was obtained. A part of the cells was prepared for long term storage in liquid nitrogen and the other part was seeded on glass cover slips for immunoprecipitation experiments or further transfection.

2.2.1.3 RNAi treatment of *Drosophila* Schneider cells

For RNAi knock-down experiments, 1×10^6 cells were plated per 6-well in serum-free medium and dsRNA was added directly to the media in a final concentration of 37 nM (15 µg) (Caplen et al., 2000). After 30 min at room temperature, 2 ml of Schneider's medium containing FCS were added and incubation was continued for 3 days at 27°C. For the immunocytochemical analysis of surface expressed lacdiNAc structures, the protocol described in 2.2.1.4 was used. To determine the subcellular localization of tagged proteins in dsRNA treated cells, the tagged enzymes were transiently transfected as described above (2.2.1.2) into cultures that were treated with dsRNA for 3 days. Immediately after

transfection, cells were washed with serum-free medium and RNAi treatment was repeated with a concentration of 18.5 nM dsRNA. Two days after transfection, indirect immunofluorescence staining (2.2.1.5) was used to visualize the tagged proteins, while markers for Golgi (dGrasp-GFP) (Kondylis et al., 2005) and ER (KDEL-GFP) (Okajima et al., 2005) were detected by direct fluorescence.

2.2.1.4 Immunocytochemistry

For immunocytochemistry, transiently transfected CHO, HEK293 or S2 cells (2.2.1.1), were washed once with 1 ml PBS and were fixed with 1 ml 1.5% glutaraldehyde in PBS for 10 min. The cell layer was washed twice with TBS and blocked in 2% milk powder/TBS for 30 min at RT. Cells were stained with mouse mAb 259-2A1 (1:350) in the same solution. This IgG3 antibody was originally raised against *Schistosoma mansoni* surface glycoconjugates (van Remoortere et al., 2000) and kindly provided from Cornelis Hokke from the Institute of Parasitology, Leiden Medical Center, The Netherlands. The first incubation was followed by HRP-conjugated goat-anti-mouse secondary antibody (1:4000). The cells were washed 3-4 times with 2 ml TBST (0.05% Tween) after each antibody incubation. Signal amplification was achieved by the incubation with a biotinyramid solution (Molecular Probes) in TBS for 10 min at RT, consisting of 0.1 M imidazole pH 7.6, 0.001% H₂O₂ and 1,7 mM biotinyramid (Speel et al., 2006). The cells were washed twice in TBST and incubated with Streptavidin AP (1:500).

For colour development, the substrate Fast-Red (Sigma) was dissolved in 0.1 M Tris/HCl pH 8.5 and 0.2 mg/ml Naphtol (Sigma) at a concentration of 1 mg/ml and incubated with the cells. The reaction was stopped by the addition of 1 ml water. Plates were analysed under a normal light microscope and red cells per plate were scored. The plates could be stored in 50% glycerol at 4°C for two years.

2.2.1.5 Immunofluorescence

Transiently transfected HEK293 or S2 cells (2.2.1.1/2.2.1.2) were grown on glass cover slides placed in 6 well plates. The cells were washed twice with PBS and fixed in 4% paraformaldehyde (PFA) for 30 min at RT. After three washing steps in PBS, additional binding sites were blocked with 0,1% BSA/PBS for 30 min at RT. To permeabilize the cells, 0.1% saponin was added to the blocking solution. For permeabilization with digitonin, before blocking the cells were incubated for 15 min at RT with the digitonin solution (5 µg/ml digitonin, 0.3 M Sucrose, 1 M KCl, 2.5 mM MgCl₂, 1 mM EDTA,

10 mM HEPES, pH 6.9). Afterwards cells were washed for three time with PBS and incubated with the blocking solution as described before. After blocking and permeabilization, samples were incubated with the primary antibodies diluted in 0.1% BSA in PBS for 1 hour at RT (mouse α -Flag M5 mAb 1:1000, mouse α -myc 9E10 mAb 1:1000, rat α -HA 3F10 mAb 1:500, rabbit α -mannosidase II antiserum 1:300, rabbit α -calnexin antiserum 1:500, rabbit α -giatin antiserum 1:1000). The cells were washed three times in 0.1% BSA in PBS and bound antibodies were detected with the corresponding secondary antibodies diluted in 0.1% BSA/PBS: α -mouse IgG Cy3 (1:500) and α -rabbit IgG Alexa488 (1:500); α -rat IgG Cy3 (1:500). After 1 hour at RT, the reactions were stopped by three washing steps in PBS. For cell nuclei staining with DAPI, the cells were incubated for 4 min at RT with the dye Hoechst 3228, followed by 20 times dipping in water. Slides were mounted in Fluorescent mounting medium and analyzed under a Zeiss fluorescence microscope.

2.2.2 Molecular biological techniques

2.2.2.1 Plasmid preparation

For analytical plasmid preparations, the ‘Qiaprep spin Miniprep Kit’ was used according to the manufacturers instructions.

For plasmid isolation in preparative scale the ‘Qiagen plasmid Kit Midi’ was used according to the manufacturers instructions.

2.2.2.2 Polymerase chain reaction (PCR)

To amplify DNA-fragments by PCR reaction, three different protocols were used, depending on the DNA-polymerase. Initial denaturation and the consecutive cycles of denaturation, annealing and elongation steps were optimized for each protocol. PCR reaction were either performed using the ‘GeneAmp System 2400’ (Perkin Elmer) or the ‘T1-Thermocycler’ (Biometra).

colony PCR

material of a single colony
 1x Thermopool buffer
 20 mM dNTPs
 0,5 μ M sense primer
 0,5 μ M antisense primer
 0,05 U/ μ l Taq Polymerase
 ad 12,5 μ l ddH₂O

program with 30 cycles

95 °C 3 min
 95 °C 30 sec
 58 °C 40 sec
 72 °C 90 sec
 72 °C 10 min
 4 °C ∞

Phusion PCR

10 ng template
 1 x HF Phusion buffer
 20 mM dNTPs
 0,5 μ M sense primer
 0,5 μ M antisense primer
 1 μ l DMSO (if necessary)
 0,02 U/ μ l Hot Start Phusion Polymerase
 ad 50 μ l ddH₂O

program with 30 cycles

98 °C 30 sec
 98 °C 10 sec
 60 °C 30 sec
 72 °C 30 sec
 72 °C 7 min
 4 °C ∞

mutagenesis PCR

50 ng template
 1 x Pfu buffer
 20 mM dNTPs
 1 μ M sense primer
 1 μ M antisense primer
 1 μ l Pfu Polymerase
 ad 50 μ l ddH₂O

program with 16 cycles for point mutation

95 °C 30 sec
 95 °C 30 sec
 55 °C 30 sec
 68 °C **calculated with**
 2 min/kb total template
 37 °C ∞

After site-directed mutagenesis PCR, 1 μ l DpnI restriction enzyme was added to the reaction mixture and incubated for 1 h at 37°C.

The samples were subjected to a PCR clean up reaction using the 'Qiaquick PCR purification kit'. The PCR reaction was mixed with 5 volumes of buffer PB and applied on

a Qiaquick column. After centrifugation for 1 min at 13000xg, the column was washed with 750 µl buffer PE and bound DNA fragments eluted in 50 µl TE.

2.2.2.3 Determination of DNA and RNA concentrations

DNA and RNA concentrations were determined photometrically and calculated from the absorbance measured at 260 nm: $c(\text{DNA}) = \text{absorbance}(260 \text{ nm}) \times 50 \mu\text{g/ml}$ and $c(\text{RNA}) = \text{absorbance}(260\text{nm}) \times 40 \mu\text{g/ml}$.

2.2.2.4 Agarose gel electrophoresis of DNA

DNA samples were diluted in 5 x GEBS and separated on horizontal agarose gels (0.6 to 1.5 % agarose in TBE buffer). To extract DNA fragments from agarose gels, ethidium bromide containing agarose gels in TAE buffer were used. Electrophoresis was performed at 5 V/cm in TBE buffer. The DNA was detected after staining in ethidium bromide (50 µg/ml) at 302 nm. For documentation the AlphaImager with the software AlphaEase FC Version 4.0 (Alpha Innotech) was used.

2.2.2.5 Isolation of DNA fragments from agarose gels

To isolate DNA fragments after restriction enzyme digest, DNA was separated on an agarose gel and the desired fragments were excised from the gel. For further DNA purification the 'Qiaquick PCR Purification Kit' (Qiagen) was used according to the manufacturers instructions. The gel slice was completely dissolved in 300 µl buffer QG per 100 mg gel at 50°C and applied to a Qiaquick column. The column was centrifuged (1 min, 13000xg) and the flow through discarded. After one washing step with 500 µl buffer PE, bound DNA was eluted in 50 µl EBC (10 mM Tris-Cl pH 8.5) or water.

2.2.2.6 Restriction digest of DNA

Restriction enzymes and reaction buffers were used according to the manufacturer's instructions (New England Biolabs). For preparative digests, 2 µg of DNA were incubated with 5 U of enzyme in a total volume of 50 µl with the added volume of enzyme less than 10%. The reaction was incubated over night at 37°C. For analytical digests, 1 µg of plasmid DNA was incubated for 2 hours at 37°C with 5 U of enzyme.

2.2.2.7 Ligation of DNA

30 ng of digested vector DNA and a 3 molar excess of the respective insert were incubated with 1 Weiss-U of T4-DNA-Ligase (NEB) in 20 μ l ligation buffer (50 mM Tris-HCl pH 7.8, 10 mM MgCl₂, 1 mM ATP, 10 mM DTT, 25 μ g/ml BSA). The ligation mix was incubated overnight at 16°C or for 1h at RT and transformed into competent *E.coli* cells.

2.2.2.8 Precipitation of nucleic acids

DNA was precipitated from aqueous solutions by the addition of 1/3 volume 7.5 M ammoniumacetate (pH 5) or 0.1 volume of 3 M sodium acetate (pH 5.2) and 2.5 volumes ethanol (100%) for 1-2 hours at -80°C or over night at -20°C. After centrifugation (13000 x g, 30 min, RT), the supernatant was decanted and the pellet washed with 500 μ l 70% ethanol. The sample was centrifuged for additional 10 min and the supernatant completely removed. The pellet was dried and dissolved in water or TE.

2.2.2.9 Transformation of chemically competent *E.coli*

50 μ l of competent *E.coli* were thawed on ice and 10 ng of plasmid DNA or 5 μ l of ligation mix (2.2.2.7) were added. The mix was left on ice for 30 min, subjected to a 45 sec heat shock at 42°C and incubated on ice for 2 min. 1 ml of LB-medium was added, the cell suspension was plated on selective LB-agar plates containing the appropriate antibiotics.

2.2.2.10 Transformation of electro competent *E.coli* YZ2000

40 μ l competent *E.coli* YZ2000 were thawed on ice and mixed with 5 μ l of precipitated, desalted ligation reaction in H₂O. The mixture was transferred into a cooled 0.1 cm cuvette and placed into a Bio-Rad electroporator. The sample was pulsed once with 1.25 kV, 200 Ω and 25 μ F. Immediately, 1 ml of sterile, 37°C warm SOC medium was added and the cell suspension transferred to a 15 ml culture tube. After 1 hour incubation at 37°C (200 rpm), the transformation was spread on selective LB-agar plates containing the appropriate antibiotic.

2.2.2.11 Preparation of chemically competent *E.coli*

Chemically competent cells were prepared according to a protocol published by Molthoff *et al.*, (1990). *E.coli* were grown on LB agar plates containing the appropriate antibiotic. One colony was inoculated in 2 ml SOB and incubated over night at 37°C. 200 ml SOB medium were inoculated with 1 ml of the starter culture and incubated for 1-2 days

(200 rpm) at 18°C until an OD_{600nm} of 0.6 was reached. The culture was centrifuged at 2000 x g for 10 min at 4°C. The supernatant was removed and the pellet resuspended in 1/3 of the original volume cooled TB (250 mM KCl, 10 mM Hepes, free acid, 15 mM CaCl₂, 55 mM MgCl₂). The solution was centrifuged as before and the pellet resuspended in 1/12 of the original volume TB. DMSO was added to a final concentration of 7% and the cells divided into 100 µl batches. The batches were immediately flash frozen in liquid nitrogen and stored at -80°C.

2.2.2.12 Preparation of *E.coli* DMSO-Stocks

For long time storage, 930 µl of an *E.coli* over night culture was mixed with 70 µl DMSO (final 7%) and frozen at -80°C.

2.2.2.13 Synthesis of dsRNA

For the synthesis of dsRNA the MEGASCRIP T7 transcription kit (Ambion) was used. The template for the dsRNA was generated before in a PCR reaction with a special T7-promotor sequence (gaa tta ata cga ctc act ata ggg aga). The kit was used according to the manufacturer's instructions. Therefore the reaction mixture containing 7 µl nuclease free H₂O, 2 µl ATP, 2 µl CTP, 2 µl GTP, 2 µl UTP, 1 µg DNA, 2 µl 10x buffer, 2 µl T7-Polymerase was incubated for 2-4 h at 37°C. Afterwards the RNA was precipitated. 115 µl nuclease free H₂O, 15 µl ammonium acetate stop solution from the kit and 150 µl Chloroform/ Phenol (Phenol H₂O saturated) mixture were added. After 5 min incubation the mixture was loaded onto a Phase-Lock-Eppi (Eppendorf) and RNA was purified according to the manufacturer's instruction. RNA was precipitated from collected upper phases by addition of an equal volumes of isopropanol. After 15 min at -20°C and 15 min centrifugation (13000 rpm, 4°C), the supernatant was carefully removed and RNA pellet was washed once with 70 % ethanol, followed by 15 min centrifugation (13000 rpm, 4°C). The RNA pellet was dried on ice and finally diluted in 20 µl nuclease free H₂O. The RNA was stored at -80°C.

2.2.2.14 Agarose gel electrophoresis of RNA

For electrophoresis analysis 6 µg of RNA were mixed with 20 µl autoclaved ddH₂O and 5 x loading buffer (4 mM EDTA, 2.5 % formaldehyde, 20 % glycerol, 30 % formamide, 2.5 x FA-buffer, 1 % bromphenol blue). RNA was separated on a 1.0 % agarose gel. The agarose was dissolved in 1 x FA buffer (200 mM MOPS, 50 mM sodium acetate, 10 mM

EDTA, pH 7,0) including 1 µg/ml ethidium bromide. The mixture was boiled and after cooling down 2 % (v/v) 37 % formaldehyde was added. As running buffer 1 x FA buffer containing 5 % (v/v) 37 % formaldehyde was used. Before loading the samples were denatured for 10 min at 65°C and immediately loaded on the agarose gel. The gel was electrophoresed at 7-10 V/cm for 90 min and analysed using the AlphaImager (Alpha Innotech).

2.2.3 Biochemical techniques

2.2.3.1 Immunoprecipitation

HEK293 cells transiently transfected as described above (2.2.1.1), were lysed for 30 min at 4°C using 750 µl of lysis buffer (2 mM EDTA, 50 mM Tris/HCl pH 8.0, 1 mM MgCl₂ 1% NP-40, supplemented with a protease inhibitor mixture from Roche Applied Science) After centrifugation for 30 min at 12 000 x g, anti-HA antibody 12CA5 coupled to sepharose A beads was added to supernatants and incubated for 3 h at 4 °C on a rotating wheel. Immunocomplexes were pelleted by centrifugation (300 x g for 5 min) followed by washing: twice with washing buffer I (50 mM Tris/HCl pH 8.0, 1% NP-40), twice with washing buffer II (50 mM Tris/HCl pH 8.0, 500 mM NaCl, 1% NP-40) and once with washing buffer I. Immunoprecipitated proteins were separated in SDS-PAGE, blotted onto PVDF-membranes (Waters) and stained with the anti-FLAG tag antibody M5 or anti-rat HA antibody.

2.2.3.2 Analyses of proteins from transfected HEK293 cells

Protein samples for Western blot analyses were isolated from transient transfected HEK293 (2.2.1.1) or S2 cells by dissolving 1 x 10⁷ cells in 750 µl of lysis buffer (2mM EDTA, 50mM Tris/HCl pH 8.0, 1mM MgCl₂ 1% NP-40, supplemented with a protease inhibitor mixture from Roche Applied Science). The lysates were incubated for 30 min at 4°C on a rotating wheel and centrifuged at 13000 rpm for 30 min at 4°C to remove cell debris. The lysates were mixed with 2 x Laemmli buffer and heated for 10 min at 95°C. 15 µl of these samples were separated on a SDS-PAGE and analysed by Western blotting (2.2.3.4).

2.2.3.3 Polyacrylamide gelelectrophoresis (SDS-PAGE)

SDS-PAGE was performed according to Laemmli (Laemmli, 1970). Protein samples were separated on SDS-polyacrylamide gels composed of a 5 % stacking gel (125 mM Tris/HCl pH 6.8, 0.1 % SDS, 5 % polyacrylamide) and a 12 % separating gel (375 mM Tris/HCl pH 8.8, 0.1 % SDS, 7-14 % polyacrylamide). Gels were prepared by mixing buffer, SDS and the acrylamide stock solution (37.5 % acrylamide, 1 % bisacrylamide) and polymerisation was initiated by adding 0.1 % TEMED and 1 % ammonium persulfate. Samples were mixed with 2x Laemmli buffer or Urea buffer by transmembrane proteins and heated to 95 °C for 10 min or to 50°C for 10 min to devoid big aggregates in the case of multi-transmembrane proteins. Electrophoresis was performed in SDS-electrophoresis buffer (50 mM Tris, 350 mM glycine, 0.1 % SDS) at 70 Volt (stacking gel) and 100 Volt (separating gel) per gel.

2.2.3.4 Western blot

Proteins separated by SDS-PAGE were transferred to PVDF-membranes using a *semidry* blotting chamber (Biometra) at 2 mA/cm² for 1 h. Before blotting the membrane was activated by dipping in methanol, then washed with H₂O and finally stored in blotting buffer. Gel and membrane were placed between two layers of *Whatman* filter paper soaked in blotting buffer (48 mM Tris, 39 mM glycine). The transfer activity was checked by the visible prestained protein marker (broad range 6-175 kDa, New England Biolabs).

2.2.3.5 Immunostaining of Western blots

The PVDF-membranes (2.2.3.4) were blocked overnight or for 1h in Odyssey blocking buffer diluted (1:2) with PBS. Afterwards the membranes were incubated for 1.5 h with the primary antibodies in blocking solution (anti-lacdiNAc 259-2A1 mAb 1:300, mouse α -Flag M5 mAb 1:1000, mouse α -myc 9E10 mAb 1:1000, rat α -HA 3F10 mAb 1:500). The blots were washed three times for 5 min with TBS/0.05 % Tween and incubated with secondary antibody (goat anti mouse IRDye 800 1:20 000, goat anti rat IRDye 800) in blocking buffer for 30 min at RT. After three washing steps with 2 x TBS/0.05 % Tween a 1 x PBS, the secondary antibody was directly detected on an Odyssey Infrared Imaging System from LI-COR Biosciences.

2.2.3.6 Protein estimation

Protein concentrations were estimated using the 'BCA Protein Assay Reagent' (Pierce) according to the manufacturer's instructions. Briefly, reagents A and B were mixed 50:1 immediately before use. 200 μ l of the mixture were added to 10 μ l of sample and incubated at 55°C for 30 min in 96-well microtiter plates. As reference, a dilution series of 25-200 μ g/ml BSA was included. The absorbance of all samples was measured at 540 nm using the ELISA-Reader 'DigiScan' (Asys Hitech) and protein concentrations were calculated from the BSA standard curve.

2.2.3.7 Golgi preparation

HEK293 cells were transiently transfected as described above (2.2.1.1). In the first step the cell layer was washed once with PBS and the cells were collected by centrifugation (5 min at 2000 x g). The cell pellets from three 175 cm² plates (9 x 10⁷ cells) were resuspended in 7 ml of lysis buffer (10 mM Hepes-Tris, pH 7.4; 0.8 M sorbitol, 1 mM EDTA) containing an EDTA-free protease inhibitor mixture (Roche Applied Science). After homogenization with 10 strokes in a Dounce homogenizer, the lysate was centrifuged (10 min at 1,500 x g) to remove unlysed cells and debris. The supernatant was collected and the pellet, after addition of 7 ml of lysis buffer, subjected to a second homogenization round with 7 strokes in the Dounce homogenizer. Debris were removed by centrifugation (10 min at 1,500 x g) and the ER/Golgi rich fraction was obtained by centrifugation of the combined supernatants at 100 000 x g for 1 h. Pelleted microsomal fraction were carefully resuspended in 500 μ l of assay buffer (0.1 M MOPS pH 7.5) and 20 μ l aliquots snap-frozen and kept at -80°C. Protein concentrations were determined using the BCATM kit (2.2.3.2).

2.2.3.8 *In vitro* assay for β 4GalNAc transferases

Standard enzyme assays were carried out with of the ER/Golgi preparations in 50 μ l of assay buffer (0.1 MOPS pH 7.5, 20 mM MnCl₂, 10 mM ATP, 100 mM GalNAc (Sigma), 0.1% bovine serum albumine (BSA), and 0.01% Saponin). Therefore, 20 μ l aliquots of the ER/Golgi vesicle preparation were supplemented to obtain the appropriate buffer composition and 0.5 mM of the radio-labelled nucleotide sugars UDP-6[³H]Gal (NEM Life Science) (specific activity 32 Bq/nmol) or UDP-1[³H]GalNAc (NEM Life Science) (specific activity 36 Bq/nmol). Before addition of the radiolabelled sugar, the mixture was sonicated for 3 sec to facilitate a good mixture and smaller vesicles. Reactions were started

by addition of the acceptor substrate p-nitrophenyl-N-acetyl- β -D-glucosaminide (GlcNAc-O-pNP; Sigma) in a final concentration of 1 mM. To determine incorporation of radioactive substrates into endogenous acceptors, control samples were incubated in the absence of GlcNAc-O-pNP. During the incubation time (2 h at 28°C) samples were gently mixed. Reactions were terminated by addition of 1 ml ice-cold water and synthesis products isolated by reverse-phase chromatography on Sep-Pak[®] Plus C₁₈ columns (Waters Corporation) as described (Palcic et al., 1988). The elutes were dried and resuspended in 2 ml scintillation cocktail (Luma Safe[™] Plus, Lumac LSC). Incorporated radioactivity was measured in a LS 6500 Multi-Purpose scintillation counter (Beckman Coulter).

2.2.3.9 Reverse-phase chromatography (*in vitro* assay)

The radioactively labelled products after incubation in the *in vitro* assay were separated from not incorporated UDP-6[³H]Gal or UDP-1[³H]GalNAc sugars, using reverse-phase chromatography. Therefore a Sep-Pak[®] Plus C₁₈ column (1 ml volume) was equilibrated with 5 ml methanol, followed by a washing step with 20 ml H₂O. The sample was loaded on the column with 4 ml H₂O and the column was washed twice with 10 ml H₂O. Radioactive sugars were eluted using 5 ml methanol.

2.2.3.10 Glycosphingolipid preparation from HEK293 cells

Transiently transfected HEK293 cells (2.2.1.1) were washed with PBS, scraped of the plates, and collected by centrifugation (5 min at 2000 x g). RNAi treated Schneider Drosophila cells were harvested by centrifugation and extracted in the same way. The cell pellets (1 x 10⁷ HEK293 cells and 1 x 10⁶ S2 cells) were resuspended in 300 μ l of water and sonicated for 5 min in a bath sonicator. 2-propanol and hexane were added to obtain a solvent ration of 55 : 25 : 20 (2-propanol : hexane : water) and the mixtures were sonicated again for 5 min in a bath sonicator. The samples were centrifuged to remove insoluble material for 10 min at 11 000 x g and the clarified supernatants were dried under nitrogen. The extracts were resuspended in 3 : 47 : 48 (chloroform : methanol : water). Salt and hydrophilic contaminants were removed from extractions by reverse-phase chromatography (Sep-Pak[®] Plus C₁₈ columns (Williams and McCluer, 1980). The eluted glycolipids were dried under nitrogen. Samples were analysed by high-performance thin-layer chromatography (HPTLC) (2.2.3.13) or by MALDI-TOF MS (2.2.3.14).

2.2.3.11 Glycosphingolipid preparation from *D. melanogaster*

Drosophila melanogaster flies of wild-type strain (Oregon R) and knock out strains β GalNAcTA^{4.1}, β GalNAcTB^{GT} and the double mutant β GalNAcTA^{4.1}; β GalNAcTB^{GT} (Haines and Irvine, 2005) were collected and frozen. 1,5 g of frozen material were extracted by the method of Folch (Folch et al., 1957). Therefore the flies were disrupted in a Dounce homogenizer in 3 volumes (4 ml per g wet weight) of ice-cold, deionized water. After sonification of the suspension 4 volumes of methanol were added and again homogenized, followed by the addition of 8 volumes of chloroform, homogenization and sonification. The 8 : 4 : 3 (chloroform/ methanol/ water) extract was vigorously shaken and then centrifuged to remove insoluble material. After centrifugation the upper phase was collected, dried under a nitrogen-stream and re-dissolved in 3 : 47 : 48 (chloroform/ methanol/ water). Salt and hydrophilic contaminants were removed from extractions by reverse-phase chromatography (Sep-Pak[®] Plus C₁₈ columns, Waters Corporation, Milford, MA, USA) (Williams and McCluer, 1980). The column was equilibrated with 5 column volumes of 3 : 47 : 48 and the sample was applied. Subsequently, the column was washed twice with 10 column volumes of water. The glycolipids were eluted with 10 column volumes of 10 : 10 : 1 and dried under a nitrogen-stream. For further analysis the samples were dissolved in chloroform/ methanol/ water (30 : 60 : 8).

2.2.3.12 High-performance thin-layer chromatography (HPTLC)

Glycolipid preparations corresponding to 2.5×10^6 cells or 50 mg of flies were spotted onto nanosilica-gel 60 plates and developed in running solvent composed of chloroform/ methanol/ 0.25 % aqueous KCl (5 : 4 : 1). Glycosphingolipids were visualised chemically by 0.5 % orcinol (w/w) / 62.5 % methanol / 10 % H₂SO₄-staining or by immunostaining.

2.2.3.13 Immunostaining of HPTLC

The HPTLC plates were dried and fixed for 90 s in 0.1% poly-isobutylmethacrylate (Sigma) in acetone. Afterwards plates were blocked overnight or for 1h in Odyssey blocking buffer. The membranes were incubated for 2-4 h with the primary antibody in blocking solution (anti-lacdiNAc 259-2A1 mAb 1:250). The blots were washed three times for 5 min with TBS Tween and incubated with secondary antibody (goat anti mouse IRDye 800 1:20 000) in blocking buffer for 1 h at RT. After two washing steps with TBS and one with PBS, the secondary antibody was directly detected on an Odyssey Infrared Imaging System from LI-COR Biosciences.

2.2.3.14 Matrix assistance laser desorption (MALDI) mass spectrometry

Matrix-assisted laser-desorption/ionization time-of-flight mass spectrometry (MALDI-TOF-MS) of extracted glycosphingolipids was performed on an Ultraflex II TOF/TOF mass spectrometer (Bruker Daltonics, Bremen, Germany) in the reflector negative-ion mode using 2,5-Dihydroxybenzoic acid (DHB) (20 mg/ml in 30% acetonitrile) as matrix and in the reflector positive-ion mode using 6-aza-2-thiothymine (ATT) (5 mg/ml in water) as matrix for sample preparation. Fragment-ion spectra were acquired by laser-induced decay in the LIFT mode as described by Manfred Wührer (Wührer and Deelder, 2005).

3 Results

3.1 Function of $\beta 4\text{GalNAcTA}$ and $\beta 4\text{GalNAcTB}$ *in vivo*

In *Drosophila melanogaster* two $\beta 4\text{GalNAcTs}$, $\beta 4\text{GalNAcTA}$ and $\beta 4\text{GalNAcTB}$ have been identified, which in theory are able to synthesize the lacdiNAc disaccharide unit (Haines and Irvine, 2005). To study the impact of each enzyme on lacdiNAc biosynthesis, $\beta 4\text{GalNAcTA}$ and $\beta 4\text{GalNAcTB}$ have been inactivated to generate single and double mutant ($\beta 4\text{GalNAcTA};\beta 4\text{GalNAcTB}$) flies. While flies with deleted $\beta 4\text{GalNAcTA}$ gene displayed abnormal locomotion due to defects in the neuromuscular system (Haines and Stewart, 2007), inactivation of $\beta 4\text{GalNAcTB}$ (Chen et al., 2007) induced abnormal oogenesis, implying that the two enzymes have different targets and eventually function *in vivo*. To address this question, $\beta 4\text{GalNAcTA}$, $\beta 4\text{GalNAcTB}$, and double mutant flies ($\beta 4\text{GalNAcTA};\beta 4\text{GalNAcTB}$), kindly provided by the laboratory of K. Irvine, were used to determine the contribution of the different enzymes to glycosphingolipid biosynthesis.

3.1.1 High-performance thin-layer chromatography analysis

In the first step the GSLs of *Drosophila melanogaster* were analyzed by High-performance thin-layer chromatography (HPTLC). Adult flies of four genotypes (wild-type, $\beta 4\text{GalNAcTA}$, $\beta 4\text{GalNAcTB}$ and $\beta 4\text{GalNAcTA};\beta 4\text{GalNAcTB}$ double mutant) were collected and GSLs were extracted by the method of Folch (FOLCH et al., 1957). Folch upper phases were desalted and purified by reverse-phase chromatography and spotted onto silica-gel plates (2.2.3.9-12). After separation, GSLs were visualized chemically with 0.5% orcinol (w/w) / 62.5 % methanol / 10 % H_2SO_4 -staining (Figure 5).

GSL extracts prepared from wild-type and $\beta 4\text{GalNAcTA}$ mutant showed similar staining patterns (Figure 5, lanes 2 and 3), indicating that mutation of $\beta 4\text{GalNAcTA}$ had no significant influence on the overall GSL composition. In contrast, staining of GSLs extracted from $\beta 4\text{GalNAcTB}$ mutant revealed a reduction of the high molecular weight GSL pool while additional bands with higher mobility became visible (marked with arrows, Figure 5 lane 4). GSL extracted from the $\beta 4\text{GalNAcTA};\beta 4\text{GalNAcTB}$ double mutant showed a similar profile to the GSLs of $\beta 4\text{GalNAcTB}$ single mutant (Figure 5 lane 5). Compared to the mobility of G_{M1} lipid, which is part of the standard GSL mixture

(Figure 5 lane 1), the upperband seen in GSLs of $\beta 4GalNAcTB$ and double mutants may represent the trisaccharide precursor, which are accumulated in these mutant flies.

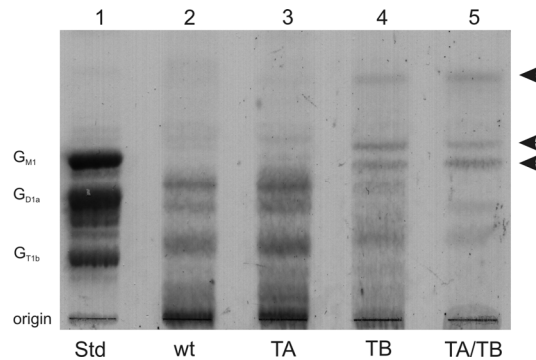


Figure 5: HPTLC analysis of glycosphingolipids from *Drosophila melanogaster*. GSLs were extracted from adult flies of four genotypes: wild-type (lane 2), $\beta 4GalNAcTA$ mutant (lane 3), $\beta 4GalNAcTB$ mutant (lane 4) and $\beta 4GalNAcTA/\beta 4GalNAcTB$ double mutant (lane 5) using the method described by Folch. Upper phases were resolved by HPTLC and chemically stained with 0.5 % orcinol (w/w) / 62.5 % methanol / 10 % H_2SO_4 . Type III gangliosides from bovine brain were used as references (lane 1). The arrows point at structures appearing in the $\beta 4GalNAcTB$ and double mutant. Based on the relative position to G_{M1} the upper band runs at a position matching the trisaccharide precursor structure expected to accumulate in $\beta 4GalNAcT$ mutants.

3.1.2 Matrix-assisted laser-desorption/ionization time-of-flight mass spectrometry (MALDI-TOF-MS)

To characterize the observed changes in the GSL patterns in detail, GSLs of wild type and mutant flies were analyzed by MALDI-TOF-MS. Studies including the MALDI-TOF-MS technology were carried out by myself in the Leiden Medical Center, Institute for Parasitology, in collaboration with Dr. Manfred Wuhler. Isolation of GSLs was again carried out according to Folch (FOLCH et al., 1957) (2.2.3.11). Upper phases were analyzed by MALDI-TOF-MS in the negative-ion and positive-ion mode (2.2.3.14). In the negative-ion mode all PE-modified zwitterionic and glucuronic acid-modified GSLs were detectable (Figure 6). In the positive-ion mode neutral, zwitterionic and acidic GSL could be measured as sodium and/or potassium adducts (Figure 9). Together with the ceramide heterogeneity, this resulted in multiplets of signals for GSLs sharing the same oligosaccharide moiety.

The negative-ion mode spectra are shown in Figure 6 and, as summarized in Table 1, were largely in accordance with the results of Seppo *et al.* (Seppo et al., 2000). The major signal of zwitterionic GSLs was detected at m/z 1592.9 and corresponded to the $[M-H]^-$ ion of the ceramide pentahexoside (Nz5) modified with phosphoethanolamine (PE). The identity of

this structure was corroborated by MALDI-TOF/TOF-MS (Figure 7, A). In this analysis the fragment ions at m/z 731.0 (B_3 -ion, according to the nomenclature of Domon and Costello and m/z 1186.5 (Y_3 -ion) indicated the attachment of the PE to the innermost *N*-acetylhexosamine. All detected GSL masses were consistent with a ceramide composition of C14:1 tetradecasphingene and C20:0 arachidic acid (marked with **b**, Figure 6), which is the major ceramide found in insect GSLs (Seppo et al., 2000; Wiegandt, 1992). Next to this major ceramide species, the complex GSLs exhibited ceramides with a 28 Da lower mass (marked with **a**, Figure 6), which presumably corresponds to ceramides with two methylene groups (C_2H_4) less (m/z 1564.8 for PE-containing ceramide pentahexoside; Figure 6). A further ceramide species showed a 28 Da higher mass (marked with **c**; Figure 6), which is expected to reflect two additional methylene groups (m/z 1620.9 for PE-containing ceramide pentahexoside; Figure 6). The strong signal observed at m/z 1958.0 especially in $\beta 4GalNAcTB$ mutants (Figure 6, C), indicated a hepta-saccharide structure $Nz7$, which in MALDI-TOF/TOF-MS could be identified as $GlcNAc\beta,3Gal\beta,3GalNAc\alpha,4GalNAc\beta,4(PE-6)GlcNAc\beta,3Man\beta,4Glc\beta Cer$ (Figure 7, B). In agreement with earlier studies (Seppo et al., 2000) we found also glucuronic acid-containing GSLs as shown in Table 1.

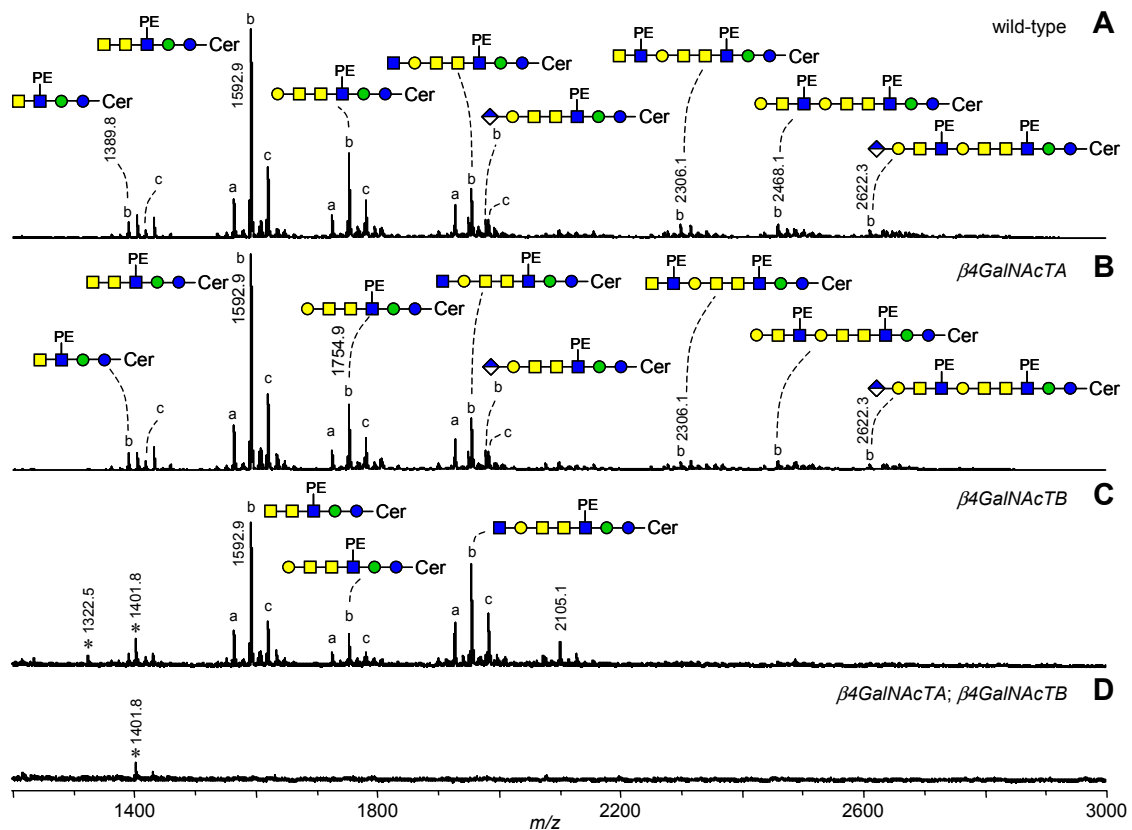


Figure 6: Negative-mode MALDI-TOF-MS of glycolipids from *Drosophila* wild-type and mutants.

Folch upper phases of wild-type (A), $\beta 4GalNAcTA$ (B), $\beta 4GalNAcTB$ (C) and $\beta 4GalNAcTA; \beta 4GalNAcTB$ (D) mutants were analyzed by negative-ion mode MALDI-TOF-MS in the reflectron mode. A complete list of registered masses and assigned glycolipid structures is given in Table 1. **b**, glycosphingolipid with ceramide composition of C14:1 tetradecasphinganine and C20:0 arachidic acid; **a** and **c**, glycosphingolipid with ceramide mass which is 28 Da (2 methylene groups, C_2H_4) lower (**a**) or higher (**c**) than for **b**; blue circle, glucose; green circle, mannose; yellow circle, galactose; yellow square, *N*-acetylgalactosamine; blue square, *N*-acetylglucosamine; white/blue diamond, glucuronic acid; PE, phosphoethanolamine; Cer, ceramide; *, no glycosphingolipid.

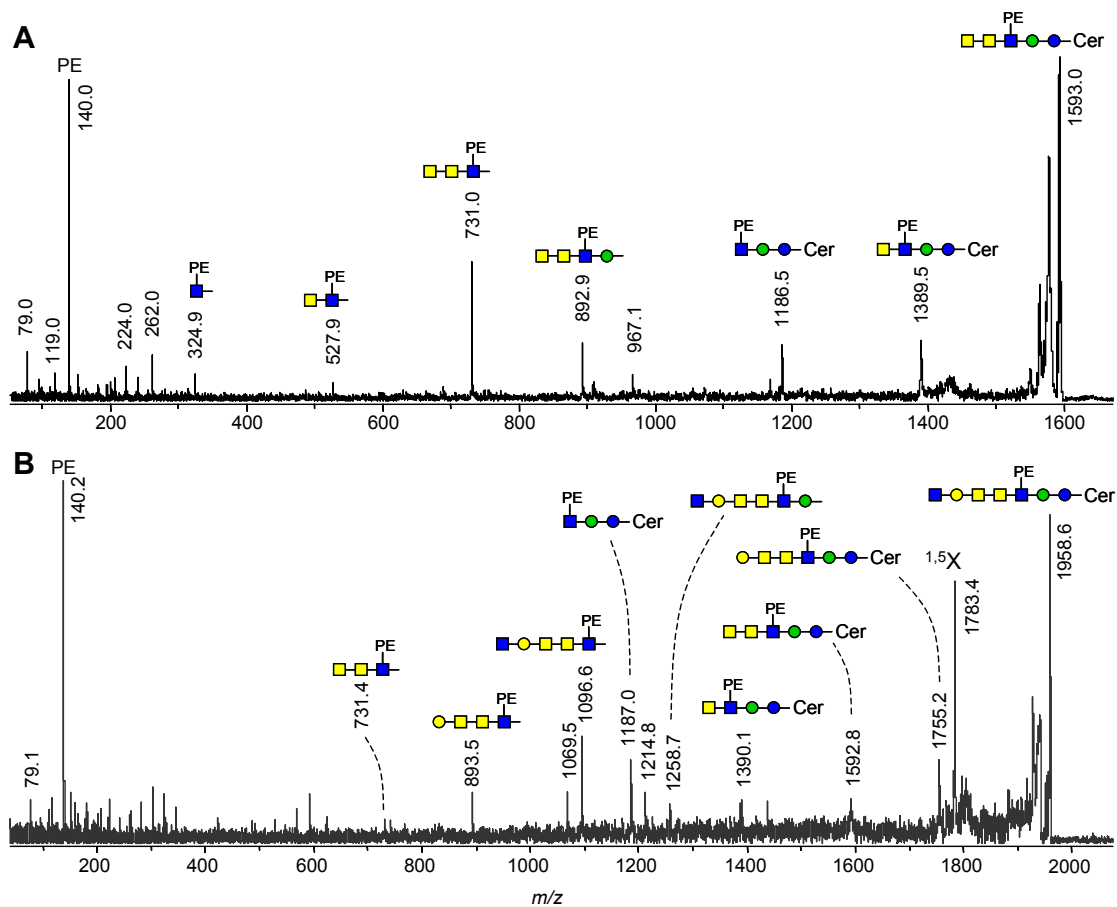


Figure 7: MALDI-TOF/TOF-MS analysis (negative-ion mode) of two zwitterionic glycolipid species. Zwitterionic glycolipid species (A) with a pentasaccharide glycan moiety (m/z 1592; from wild-type), and (B) with a heptasaccharide glycan moiety (m/z 1958; from the $\beta 4GalNAcTA$ mutant) were analyzed by MALDI-TOF/TOF-MS. For key see legend Figure 6. $^{1,5}X$, cross-ring cleavage of the terminal *N*-acetylglucosamine.

Detailed examination of all detectable signals displayed a possible variant of the Nz_28 structure with two PE-modifications. A signal at m/z 2446.2 was detected, which theoretically exhibited an additional hexose. This latter GSL species (Nz_29) was not identified in *Drosophila* before. The GSL structure was analyzed by MALDI-TOF/TOF-

MS in comparison to the fragmentation spectrum of Nz₂8 (m/z 2284.1) to evaluate the position of the additional hexose residue (Figure 8, A and B). The non-reducing end fragments observed in the region below m/z 1000 were largely the same for the two GSLs, indicating that the hexose modification was not attached to the terminal GalNAc β ,4(PE-6)GlcNAc β ,3Gal β ,3GalNAc-moiety. Two ions at m/z 1258.4 and m/z 1461.3 were observed for the hexose-modified GSL Nz₂9 (Figure 8, A), but not for Nz₂8 (Figure 8, B), which exhibited corresponding ions of a 162 Da lower mass at m/z 1096.9 and m/z 1299.9. This difference indicated the attachment of the hexose residue to the internal β -linked GalNAc residue, resulting in the Nz₂9 structure as listed in Table 1.

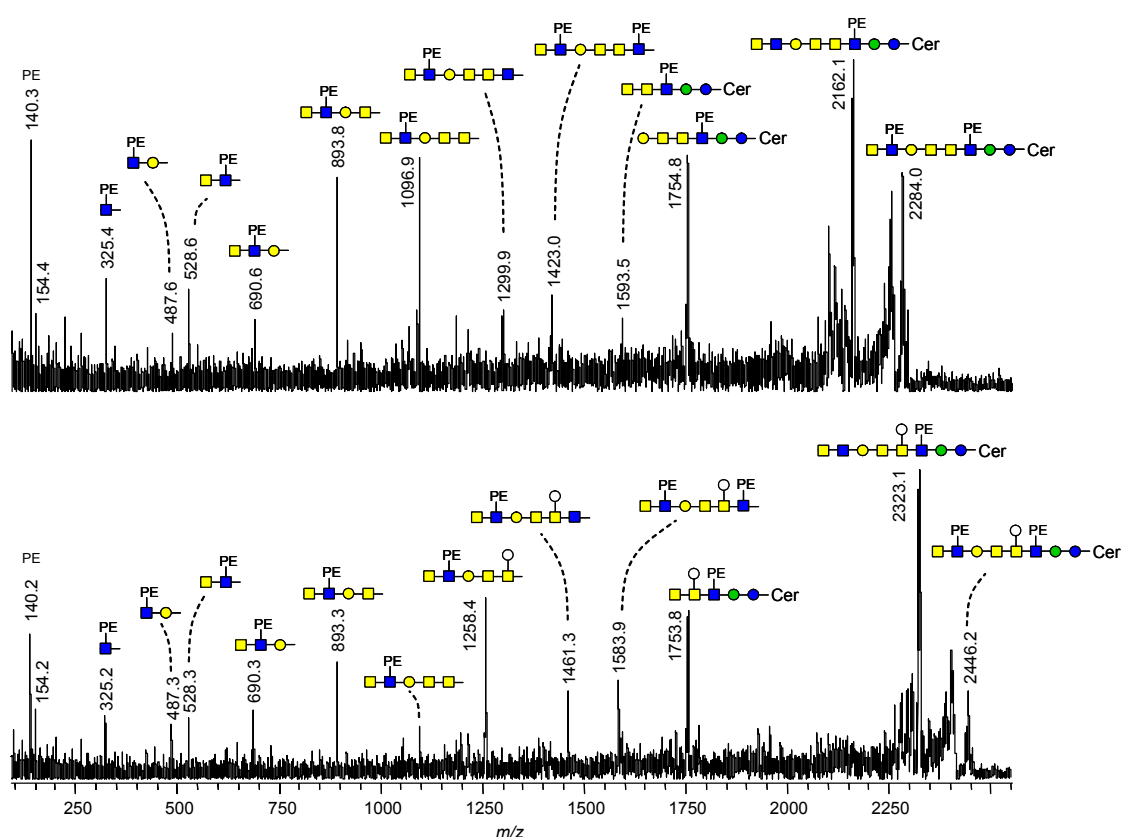


Figure 8: MALDI-TOF/TOF-MS analysis (negative-ion mode) of two zwitterionic glycolipids containing eight and nine monosaccharide residues. Zwitterionic glycolipid species (A) with an octasaccharide glycan moiety (m/z 2284; from wild-type), and (B) with a nonasaccharide glycan moiety (m/z 2446; from wild-type) were analyzed by MALDI-TOF/TOF-MS in deprotonated form. For key see legend Figure 6. Empty circle, hexose.

As in the HPTLC analysis, GSL pattern did not show any significant changes between wild-type and β 4GalNAcTA mutants (Figure 6). In contrast, an enrichment of the GlcNAc β ,3Gal β ,3GalNAc α ,4GalNAc β ,4(PE-6)GlcNAc β ,3Man β ,4Glc β Cer species (Nz7

at m/z 1958.0) was observed for GSLs isolated from $\beta 4GalNAcTB$ mutant. The fact that GSLs of higher molecular weight had almost disappeared indicated that $\beta 4GalNAcTB$ plays a major role in glycolipid biosynthesis in *D. melanogaster*. In the negative-ion mode no zwitterionic GSL were visible in the $\beta 4GalNAcTA; \beta 4GalNAcTB$ double mutants, indicating the complete loss of these species (Figure 6). To complete the characterization of GSL samples, all genotypes were also analyzed in the positive-ion mode (Figure 9). In the positive-ion mode all neutral, zwitterionic and acidic GSL were detected as sodium and/or potassium adducts (Table 1). Again the GSL pattern of wild-type and $\beta 4GalNAcTA$ mutant showed no differences, whereas the spectrum of $\beta 4GalNAcTB$ mutant was changed (Figure 9). As in the negative-ion mode spectra, the Nz7 species with a terminal GlcNAc-residue was enriched. Importantly, an additional structure with a low molecular weight at m/z 1087.9 became visible. This structure was characterized by MALDI-TOF/TOF-MS and revealed the sodium adduct of the trisaccharide N3 GlcNAc β ,3Man β ,4Glc β Cer (at m/z 1087.9; Figure 9, C, Figure 10, Table 1). The oligosaccharide sequence was indicated by a series of Y-ions at m/z 884.7 ([Hex₂Cer+Na]⁺), at m/z 722.6 ([Hex₁Cer+Na]⁺), and at m/z 560.2 ([Cer+Na]⁺). The HexNAc-Hex-Hex-Cer sequence was additionally indicated by the B-ion series with signals at m/z 226.1 (HexNAc+Na]⁺), m/z 388.1 (HexNAc₁Hex₁+Na]⁺), and m/z 550.2 (HexNAc₁Hex₂+Na]⁺). In the $\beta 4GalNAcTA; \beta 4GalNAcTB$ double mutant fly this structure was the only visible GSL species (Figure 10, D), demonstrating the complete loss of lacdiNAc containing GSLs in this mutant.

$\beta 4GalNAcTB$ is the dominant enzyme for GSL biosynthesis *in vivo*

From the HPTLC and MS data it can be concluded that $\beta 4GalNAcTA$ plays a minor role in the overall GSL biosynthesis of *Drosophila* adult flies as no differences were observed between wild type and $\beta 4GalNAcTA$ mutant. On the background of a $\beta 4GalNAcTB$ mutant, $\beta 4GalNAcTA$ is, however, responsible for the residual production of complex GSLs longer than the GlcNAc β ,3Man β ,4Glc β Cer structure (Figure 6, C). The deficiency of both $\beta 4GalNAcTA$ and $\beta 4GalNAcTB$ is required to completely abolish production of GSLs elongated beyond the ceramide trihexoside structure (Figure 9, D).

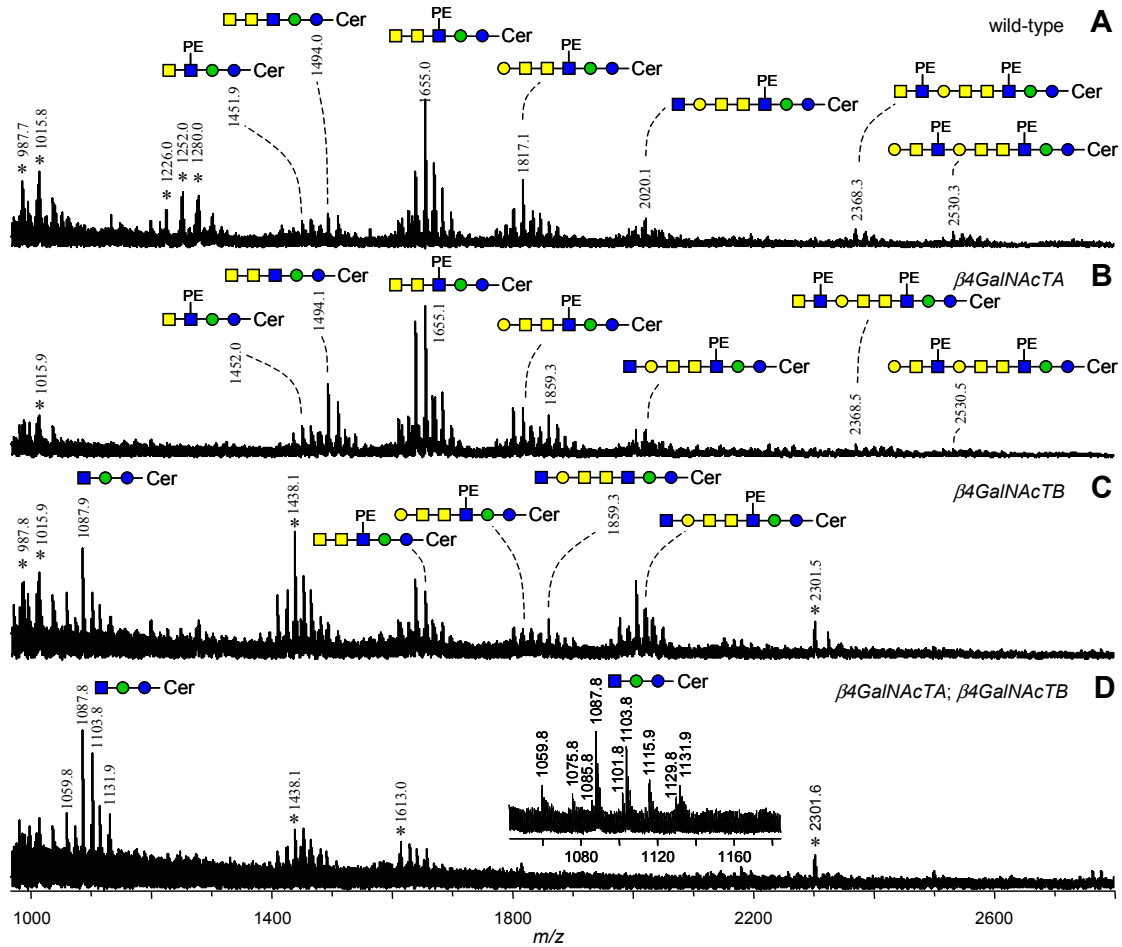


Figure 9: Positive-mode MALDI-TOF-MS of glycolipids from *Drosophila* wild-type and mutants. Folch upper phases of wild-type (A), $\beta 4GalNAcTA$ (B), $\beta 4GalNAcTB$ (C) and $\beta 4GalNAcTA; \beta 4GalNAcTB$ (D) mutants were analyzed by positive-mode MALDI-TOF-MS in the reflectron mode. A list of registered masses for assigned neutral glycolipid structures is given in Table 1. For key see legend Figure 6.

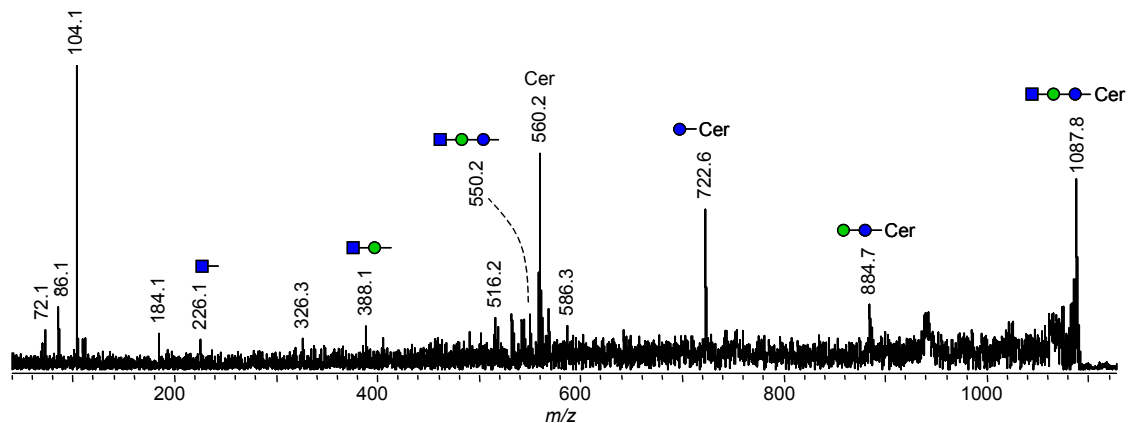


Figure 10: MALDI-TOF/TOF-MS analysis of the neutral glycolipid enriched in $\beta 4GalNAcTB$ and double knockout mutants. The neutral ceramide trisaccharide (sodium adduct at m/z 1087.8; $\beta 4GalNAcTA; \beta 4GalNAcTB$ double mutant) was analyzed by MALDI-TOF/TOF-MS in the positive-ion mode using ATT as matrix substance. For key see legend Figure 6.

Glycosphingolipid	Structure	Registered mass (m/z)
Zwitterionic		
Nz4	GalNAc β ,4(PE-6)GlcNAc β ,3Man β ,4Glc β Cer	1389.8
Nz5	GalNAc α ,4GalNAc β ,4(PE-6)GlcNAc β ,3Man β ,4Glc β Cer	1592.9
Nz6	Gal β ,3GalNAc α ,4GalNAc β ,4(PE-6)GlcNAc β ,3Man β ,4Glc β Cer	1754.9
Nz7	GlcNAc β ,3Gal β ,3GalNAc α ,4GalNAc β ,4(PE-6)GlcNAc β ,3Man β ,4Glc β Cer	1958.0
Nz ₂ 7	(PE-6)GlcNAc β ,3Gal β ,3GalNAc α ,4GalNAc β ,4(PE-6)GlcNAc β ,3Man β ,4Glc β Cer	2081.0
Nz8	GalNAc β ,4GlcNAc β ,3Gal β ,3GalNAc α ,4GalNAc β ,4(PE-6)GlcNAc β ,3Man β ,4Glc β Cer	2161.1
Nz ₂ 8	GalNAc β ,4(PE-6)GlcNAc β ,3Gal β ,3GalNAc α ,4GalNAc β ,4(PE-6)GlcNAc β ,3Man β ,4Glc β Cer	2284.1/2306.1#
Nz ₂ 9	GalNAc β ,4(PE-6)GlcNAc β ,3Gal β ,3GalNAc α ,4(Hex 1 \rightarrow)GalNAc β ,4(PE-6)GlcNAc β ,3Man β ,4Glc β Cer	2446.2/2268.1#
Acidic		
Az6	GlcA β ,3Gal β ,3GalNAc α ,4GalNAc β ,4(PE-6)GlcNAc β ,3Man β ,4Glc β Cer	1931.0
Az9	GlcA β ,3Gal β ,3GalNAc β ,4GlcNAc β ,3Gal β ,3GalNAc α ,4GalNAc β ,4(PE-6)GlcNAc β ,3Man β ,4Glc β Cer	2499.2
Az ₂ 9	GlcA β ,3Gal β ,3GalNAc β ,4(PE-6)GlcNAc β ,3Gal β ,3GalNAc α ,4GalNAc β ,4(PE-6)GlcNAc β ,3Man β ,4Glc β Cer	2622.3
Neutral		
N3	GlcNAc β ,3Man β ,4Glc β Cer	1087.9
N5	GalNAc α ,4GalNAc β ,4GlcNAc β ,3Man β ,4Glc β Cer	1494.1
N7	GlcNAc β ,3Gal β ,3GalNAc α ,4GalNAc β ,4GlcNAc β ,3Man β ,4Glc β Cer	1859.3

Table 1: Summary of detected GSL species in *Drosophila melanogaster*. For zwitterionic and acidic GSLs the masses of the $[M-H]^-$ species are listed in the table, whilst for neutral GSLs the masses of the registered $[M+Na]^+$ species are given. Various other adducts were registered, which are not listed in this table. #, $[M-2H+Na]^-$

3.2 *In vitro* characterization of β 4GalNAcTA and β 4GalNAcTB

In the previous section, β 4GalNAcTB was identified as the most important enzyme for the formation of lacdiNAc structures on glycolipids *in vivo*. However, in *in vitro* assays it had been shown to be, in contrast to β 4GalNAcTA, an almost inactive enzyme (Haines and Irvine, 2005). As mentioned before, cloning of β 4GalNAc transferases from *Drosophila melanogaster* in our laboratory was achieved by expression cloning. Since this methodology screens for functional activity (Bakker et al., 1997; Eckhardt et al., 1995; Eckhardt et al., 1996; Munster et al., 1998), the isolation of active enzymes was guaranteed. Particular in the case of cloning β 4GalNAcTB the detection of lacdiNAc

positive cells was dependent on the presence of a second cDNA harboring a multi-transmembrane protein of the DHHC protein family (Linder and Deschenes, 2007). The aim of this study was to differentially access the catalytic functions of β 4GalNAcTA and β 4GalNAcTB and to investigate how the DHHC-family protein called GABPI (β 4GalNAcTB Pilot Protein) influences their functionality.

3.2.1 Cell surface staining

Since earlier studies had shown that human embryonic kidney (HEK293) cells were most suitable for the expression for the cloned *Drosophila* proteins, these cells were used in all subsequent experiments to measure activity and to isolate materials (membrane vesicles and GLSs) for *in vitro* testing. The detection of lacdiNAc structures was carried out with mAb 259-2A1 (van Remoortere et al., 2000) (2.2.1.4).

To comparatively test activity a very first expression experiment was carried out by transient transfection of HEK293 cells as shown in Figure 11, whereby the β 4GalNAc transferase from *C. elegans* (Ce β 4GalNAcT) (Kawar et al., 2002) was used as a positive control. No activity was detectable in cells transfected with β 4GalNAcTB only (Figure 11, B), but co-expression of GABPI resulted in lacdiNAc production (Figure 11, D) comparable to the level of Ce β 4GalNAcT transfectants. β 4GalNAcTA transfected cells showed clear activity (Figure 11, C), which could not be increased by co-expression of GABPI (not shown). HEK293 cells were also transfected with GABPI alone, but no lacdiNAc positive cells became visible (data not shown).

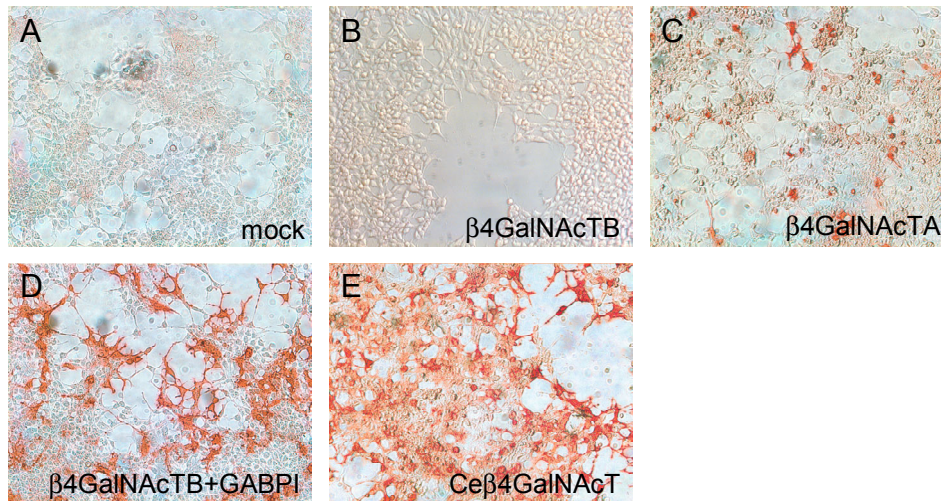


Figure 11: Immunohistochemical staining of GalNAc transferases transfected cells with mAb 259-2A1. HEK293 cells were transiently transfected with empty vector (A) β 4GalNAcTA (B), β 4GalNAcTB in absence (C) or presence of GABPI (D) and Ce β 4GalNAcT (D). Two days after transfection the cells were stained using the mAb 259-2A1. The negative, empty vector control (mock, A) showed no cell surface staining comparable to the β 4GalNAcTB expressing cells (B). β 4GalNAcTB activity was only visible in presence of GABPI (D) in contrast to the independently active β 4GalNAcTA (C). The Ce β 4GalNAc transferase was used as positive control (E).

3.2.2 Glycolipid specificity of β 4GalNAcTA and β 4GalNAcTB

In the next step the acceptor specificity of the *Drosophila* GalNAc transferases was investigated. Therefore, parallel cultures of HEK293 cells transiently transfected with the β 4GalNAc transferases in the presence and absence of GABPI were used to analyze (i) lipid-bound lacdiNAc via HPTLC and (ii) protein bound lacdiNAc by Western blotting. For HPTLC, glycolipids that were extracted with a 2-propanol-hexane-water mixture (2.2.3.10) were loaded onto HPTLC plates for separation (see 2.2.3.12). Protein analyses were carried out using total lysates on a 12% SDS-PAGE (see 2.2.3.3). To display lacdiNAc-linked structures the lipids and proteins were immunostained with mAb 259-2A1 and detected with goat anti-mouse IRdye 800 (2.2.3.5 and 2.2.3.13). In both experimental setups, extracts from HEK293 cells transfected with Ce β 4GalNAcT were used as positive and empty vector transfectants as negative control. In β 4GalNAcTA and especially in β 4GalNAcTB/GABPI transfected cells lacdiNAc-containing GSLs were detected (Figure 12, A). Moreover, in accordance with the observation made by cell surface staining, the β 4GalNAcTB/GABPI complex produced a stronger staining as compared to β 4GalNAcTA. The different staining pattern in GSLs from S2 cells compared to

transfected HEK293 cells was due to the different acceptor structures existing in mammalian cells. The main GSLs in HEK293 are gangliosides containing lactose as neutral carbohydrate moiety. With respect to available GSL structures in HEK293 cells, the tetrasaccharide core of ganglioside II and III (lacto-*N*-neotetraose) (GlcNAc β 3Gal β 4Glc β 1-Cer) turned out as potential acceptor structure for β 4GalNAc transferases from *Drosophila melanogaster*.

In Western blot analysis, no lacdiNAc structures were found on protein acceptors in either S2 cell lysates or HEK293 cells after transfection with the isolated *Drosophila* genes (β 4GalNAcTA; β 4GalNAcTB plus/minus GABPI). In lysates from *Schistosoma* egg and HEK293 cells transfected with Ce β 4GalNAcT, however, clear bands were detected, indicating that in HEK293 cells potential acceptors for the enzymatic activity exist, but are not used by the *Drosophila* enzymes. This result was in agreement with earlier studies, describing the presence of the lacdiNAc epitope on GLSs (Seppo et al., 2000) but not on glycoproteins (North et al., 2006) in *D. melanogaster*.

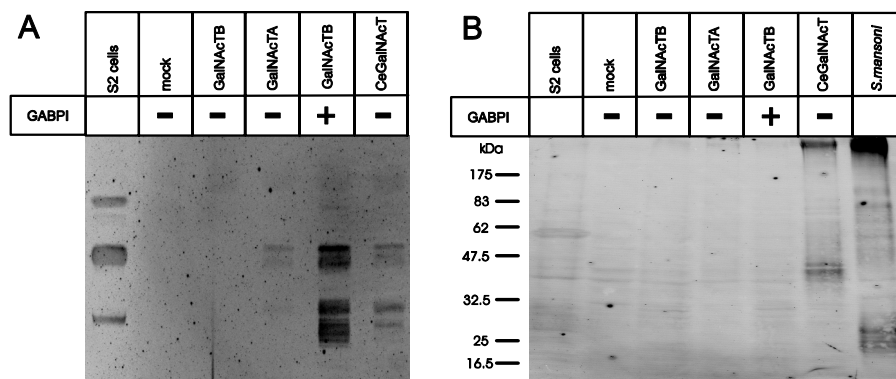


Figure 12: Immunostaining of lacdiNAc structures on glycolipids and glycoproteins. A: HPTLC analysis of extracted glycosphingolipids (GSLs) from HEK293 cells transfected with β 4GalNAcTA, β 4GalNAcTB with or without GABPI. The extracts were separated on an HPTLC plate and stained with mAb 259-2A1. *Drosophila* S2 cells and HEK293 cells transfected with Ce β 4GalNAcT were used as positive controls and exhibited lacdiNAc positive GSL staining. Only in extracts from cells transfected with β 4GalNAcTA and β 4GalNAcTB/GABPI, lacdiNAc positive GSLs were detected. B: Western blot analysis of protein extracts isolated from the same cells as in A. Total cells lysates were separated on a 12% SDS- PAGE and the same antibodies were used for immunostaining as described for HPTLC analysis. Total lysate of HEK293 cells after transfection with Ce β 4GalNAcT and isolated proteins from *Schistosoma mansoni* eggs were used as positive controls and showed lacdiNAc containing glycoproteins, whereas the other samples are lacdiNAc negative.

3.2.3 *In vitro* testing of β 4GalNAc transferases using Golgi vesicles

Because the comparative testing of the two *Drosophila* β 4GalNAc transferases so far indicated differences in their activity level, the next assay system was designed to quantify the enzymatic activities. For this, the 100.000 x g pellet of post nuclear supernatant of transfected HEK293 cells, containing both ER and Golgi vesicles, were used in a standard glycosyltransferase assay system with UDP-GalNAc as donor and p-nitrophenyl- β -*N*-acetylglucosamine (GlcNAc-pNP) as acceptor substrate (Palcic et al., 1988) (2.2.3.8). During the establishment of the assay it was observed that application of the detergent Triton X-100 in the standard concentration of 0.5% (used in glycosyltransferase assays to permeabilize the membrane and improve substrate accessibility) selectively destroyed activity in vesicles isolated from cells co-transfected with β 4GalNAcTB and GABPI. In contrast β 4GalNAcTA activity was readily measurable. Speculating that the deleterious effect of Triton X-100 was due to membrane destruction and in parallel to destruction of the potential β 4GalNAcTB/GABPI complex, the milder detergent saponin, (Goldenthal et al., 1985) which perforates membranes, but leaves intact protein complexes, was tested. The results are shown in Figure 13. Addition of saponin positively affected the measured activity for both enzymes in concentrations between 0.004% - 0.5%. However, while in the case of β 4GalNAcTA both detergents had similar positive effects, only saponin increased β 4GalNAcTB activity with a maximal effect in the concentration range 0.02% - 0.5%. Triton X-100 increased activity at relatively low concentrations only and completely disturbed activity at standard assay concentrations of 0.5% (Figure 13, B). The improved activity in the presence of detergent is most probably due to improved transport of the substrates over the vesicle membrane.

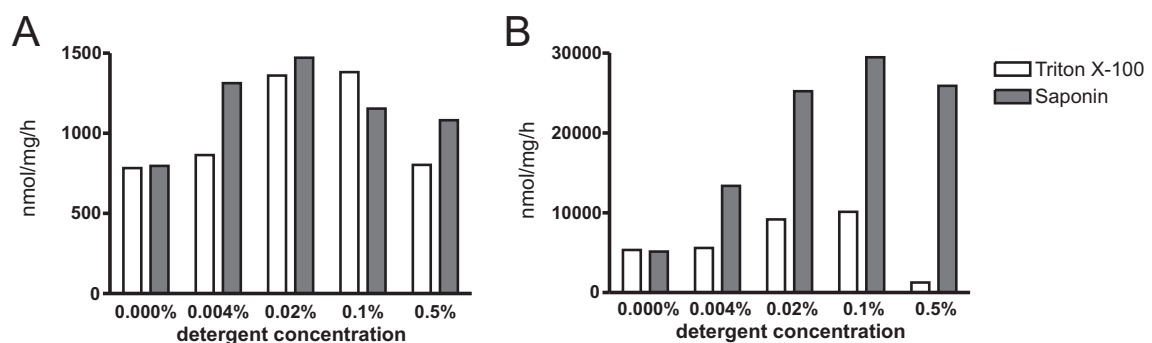


Figure 13: Influence of different detergents on the *in vitro* activity of β 4GalNAcTA and TB. Microsomal fractions of HEK293 cells transfected with β 4GalNAcTA (A) or the combination β 4GalNAcTB/GABPI (B)

were treated with Triton X-100 and saponin in various concentrations and assayed for activity with GlcNAc-pNP as acceptor and [3 H]UDP-GalNAc and [3 H]UDP-Gal as donor substrates. While β 4GalNAcTA activity significantly increased with both detergents (up to 0.1%), the activity of β 4GalNAcTB was negatively influenced or completely destroyed at 0.5%. In contrast, treatment of vesicles with saponin, drastically increased also β 4GalNAcTB activity (mind the different scales of Y-axis in A and B). Values represent the average of two independent test series each measured in triplicates.

In the optimised *in vitro* glycosyltransferase assay using 0.01% saponin it was confirmed that β 4GalNAcTB was directly dependent on GABPI for activity (Figure 14), whereas β 4GalNAcTB alone showed no activity. For β 4GalNAcTA, independent activity was detectable, but no increase in presence of GABPI was observed. Comparable to the observation made by cell surface staining (Figure 11) and HPTLC analysis (Figure 12), β 4GalNAcTB in co-expression with GABPI showed higher activity than β 4GalNAcTA (Figure 14).

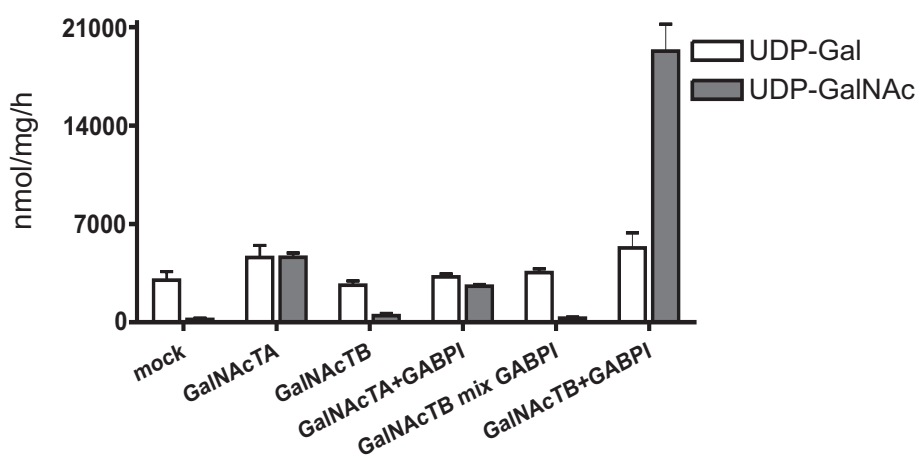


Figure 14: *In vitro* activity determined for β 4GalNAcTA and TB in the absence and presence of GABPI. HEK293 cells were transfected with β 4GalNAcTA or β 4GalNAcTB in the presence and absence of GABPI and activity was determined with optimized assay conditions using 0.01% saponin. Gal-transferase activity was used to control the quality of vesicles. In contrast to β 4GalNAcTB, cotransfection of GABPI was however not able to augment β 4GalNAcTA activity. Each value represents the average of three test series carried out with independent vesicle preparations.

In the next experiment it was analyzed whether β 4GalNAcTB and GABPI, expressed in separate cells, have the capacity to assemble into a functional complex. Therefore, the 100.000 x g pellet of post nuclear supernatants of HEK293 cells transfected with either β 4GalNAcTB or GABPI, were isolated and mixed. The heterogeneous microsome

fractions were mildly treated with saponin (0.01%) and sonicated before and after addition of reaction mixture (2.2.3.8). In this experiment no activity was detected (Figure 14), although postnuclear pellet of β 4GalNAcTA transfected HEK293, identically treated with detergent, showed activity (data not shown). In conclusion the experiments demonstrated that the complex formation of the β 4GalNAcTB and GABPI is essential for activity and cannot be formed *in situ*.

3.2.4 Physical interaction between β 4GalNAcTB and GABPI

The *in vitro* activity of β 4GalNAcTB in presence of GABPI and the importance to maintain membrane integrity raised the question, whether a direct protein-protein interaction exist between these proteins. Co-immunoprecipitation experiments were performed with C-terminally HA-tagged GABPI and Flag-tagged β 4GalNAcTB in HEK293 cells to investigate the interaction behavior. As negative control, Flag-tagged β 4GalNAcTA in co-expression with GABPI was used. Two days after transfection, cells were lysed with buffer containing 1% NP-40 (2.2.3.1). A small sample of total lysate was reserved as expression control and the main part was immunoprecipitated with anti-HA antibody coupled sepharose A beads. Total lysates and immunoprecipitates were separated by SDS-PAGE (2.2.3.3) and immunoblotted with either mouse anti-Flag or rat anti-HA antibodies (2.2.3.5).

HA-tagged GABPI were detected in total cell lysates of single and double transfected cells. After immunoprecipitation more intense, but still identical bands were obtained (Figure 15, A). Interestingly, exclusively β 4GalNAcTB (Figure 15, B) and not β 4GalNAcTA (Figure 15, C) could be co-precipitated via HA-tagged GABPI from lysates of double transfected cells. These results confirmed the specific physical interaction between β 4GalNAcTB and GABPI.

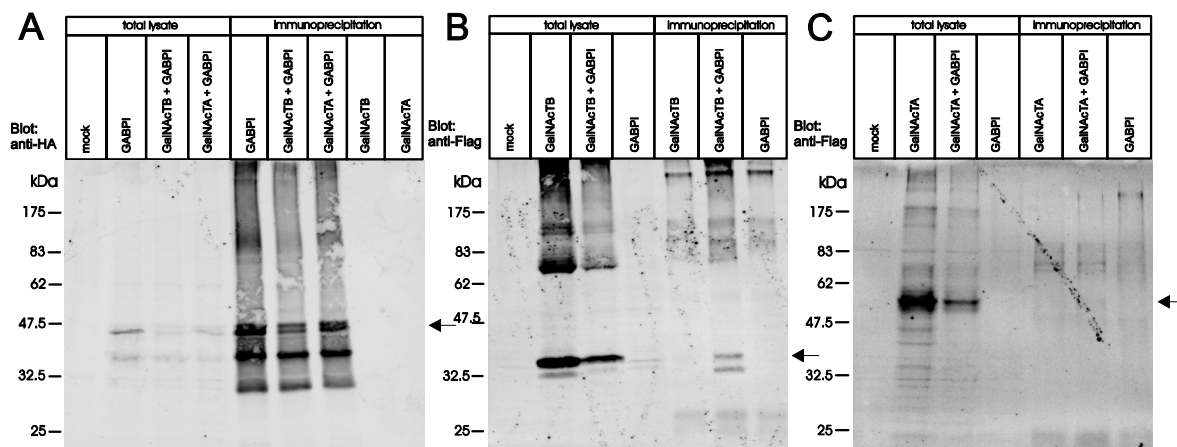


Figure 15: Immunoprecipitation of $\beta 4$ GalNAcTB and $\beta 4$ GalNAcTA with GABPI. HEK293 cells were transfected with C-terminally HA-tagged GABPI and N-terminally Flag-tagged $\beta 4$ GalNAcTB or $\beta 4$ GalNAcTA. Two days after transfection, cells were lysed with buffer containing 1% NP-40 and lysates were immunoprecipitated with anti-HA coupled beads. The beads were washed and precipitates were analyzed by Western blot. Small samples of total lysates before precipitation were loaded as expression controls. Expression and precipitation of HA-tagged GABPI was investigated by immunoblotting using the rat anti-HA antibody (A), whilst $\beta 4$ GalNAcTB (B) and $\beta 4$ GalNAcTA (C) were incubated with mouse anti-Flag antibody M5. In contrast to $\beta 4$ GalNAcTA (C), immunoprecipitation of $\beta 4$ GalNAcTB with GABPI could be detected (B).

3.3 Biosynthesis of lacdiNAc in $\beta 4$ GalNAcTA, $\beta 4$ GalNAcTB, or GABPI depleted *Drosophila* S2 cells

3.3.1 GSL structures in RNAi treated S2 cells

To investigate whether the biosynthesis of the lacdiNAc structure in *Drosophila* is dependent on GABPI *in vivo*, *Drosophila* S2 cells were used in an RNAi based approach (Caplen et al., 2000). S2 cells were incubated with double stranded (ds) RNA corresponding to a central region of $\beta 4$ GalNAcTA, $\beta 4$ GalNAcTB, GABPI and $\beta 4$ GalNAcTB in combination with GABPI (2.2.1.3). The presentation of the lacdiNAc epitope on the cell surface of depleted cells was comparatively detected with the mAB 259-2A1 (2.2.1.4) (van Remoortere et al., 2000). To confirm the effect of dsRNA treatment on GSL biosynthesis, glycolipids of depleted cells were additionally extracted and analyzed by MALDI-TOF-MS in negative- and positive-ion mode (2.2.3.14).

In untreated S2 cells high expression of the lacdiNAc epitope on the cell surface (Figure 16, A) was observed and the complete set of already characterized GSL structures were identified by negative-ion MALDI-TOF-MS analysis (Seppo et al., 2000; Stolz et al.,

2007) (see also Table 1). The depletion of β 4GalNAcTA resulted in only slight decreased immunostaining (Figure 16, B) and the GSL pattern, analyzed by MALDI-TOF-MS, did not indicate any significant change. In contrast, dsRNA treated cells corresponding to either β 4GalNAcTB or GABPI (Figure 16, C and D, respectively) exhibited a strong reduction of lacdiNAc positive cells, which was additionally reflected in the MALDI-TOF mass spectra. In negative-ion mode analyses, glycolipids of β 4GalNAcTB and GABPI depleted cells showed a slight enrichment of the GlcNAc β ,3Gal β ,3GalNAc α ,4GalNAc β ,4(PE-6)GlcNAc β ,3Man β ,4Glc β Cer species (m/z 1958.4) and GSLs with higher molecular weight were hardly detectable (Figure 16, C and D). The positive-ion mode analyses, moreover, revealed the accumulation of the precursor structure GlcNAc β ,3Man β ,4Glc β Cer (at m/z 1087.6; Figure 16, C and D). Finally, double incubation with dsRNA against β 4GalNAcTB and GABPI led to a nearly complete absence of detectable lacdiNAc structures on the cell surface. In MALDI-TOF-MS analyses, lacdiNAc containing GSLs were still detectable, but similarly changed as in β 4GalNAcTB and GABPI depleted cells with accumulation of the trisaccharide structure (at m/z 1087.6; Figure 16, E).

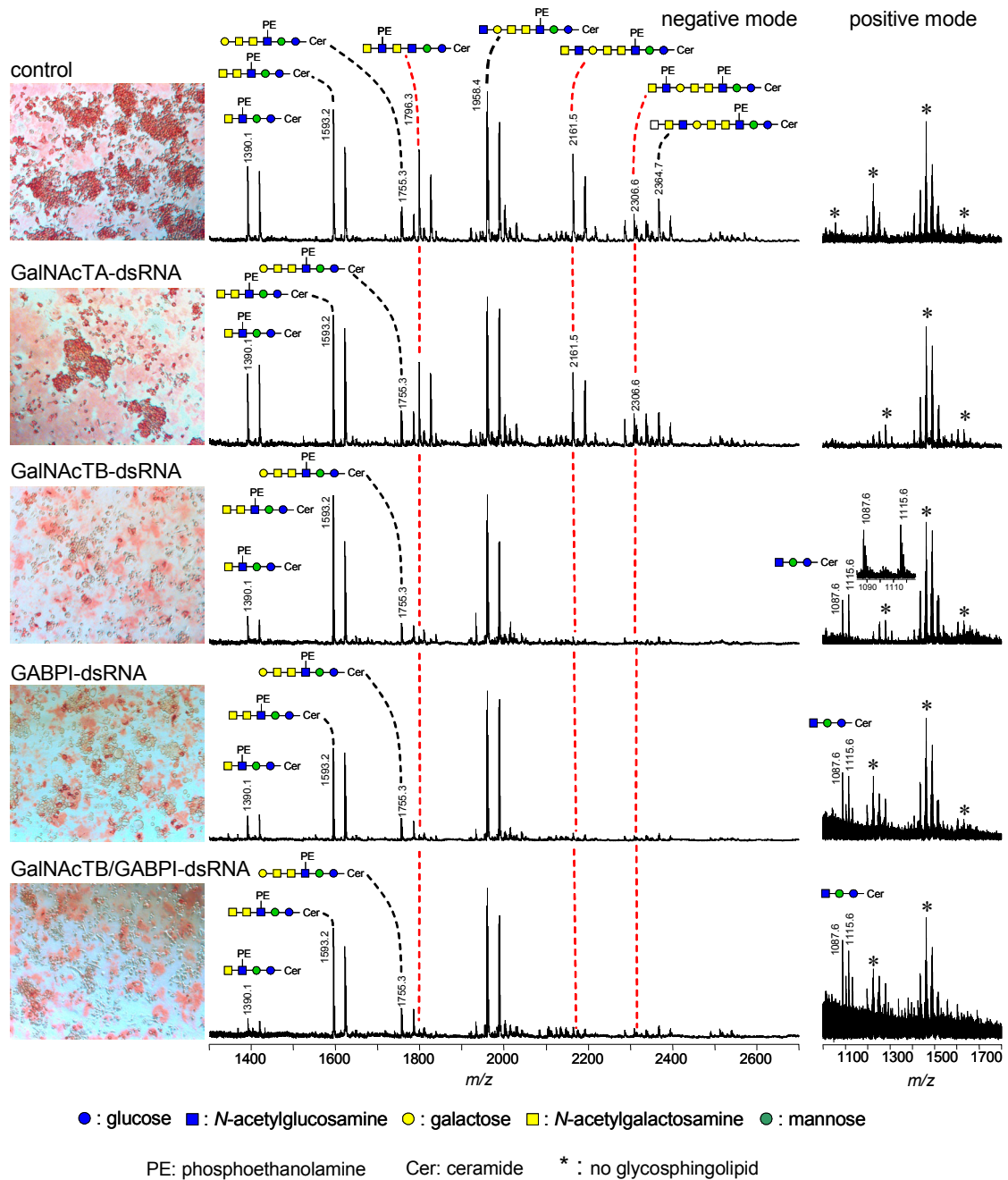


Figure 16: Depletion of GalNAc transferases and GABPI in *Drosophila* S2 cells. Cells were incubated for 3 days with dsRNA corresponding to β 4GalNAcTA (B), β 4GalNAcTB (C), GABPI (D) or the combination of β 4GalNAcTB and GABPI (E). The lacdiNac epitope presentation on the cells surface was detected with mAb 259-2A1. Additionally, GSL extracts of depleted cells were obtained and analyzed with MALDI-TOF-MS in negative- and positive mode. Red lines sign at most changed glycolipid signals.

3.3.2 New glycosphingolipid structures in *Drosophila* S2 cells

In comparison to already characterized GSL structures in adult wild type flies of *Drosophila melanogaster* (see chapter 3.1, Table 1), GSLs from *Drosophila* S2 cells were mainly identical (Seppo et al., 2000; Stolz et al., 2007). However, closer examination of all signals exposed one additional major peak at m/z 1796.4 (Figure 16, A). This signal could not be assigned to a known structure, but corresponded to a ceramide carrying two hexose and four *N*-acetylhexosamine residues modified with one phosphoethanolamine (PE). In addition, the signal at m/z 1919.4 corresponded to a ceramide carrying two hexose and four *N*-acetylhexosamine sugars with two phosphoethanolamine (PE) residues (Figure 16, A), was detected. This structure was analyzed by MALDI-TOF/TOF-MS (Figure 17, A and B) revealing the $Nz6^*$ and Nz_26^* structures that both contained stretches of four *N*-acetylhexosamine residues (Table 2). These structures were interpreted as lacdiNAc tandem repeats that might be in part ($Nz6^*$) or fully modified with PE (Nz_26^* ; Table 2). The $Nz6^*$ species was expected to represent a mixture of isomers differing in the location of the PE on the outer or inner lacdiNAc unit. Furthermore, GSLs containing a stretch of five *N*-acetylhexosamine residues were observed containing one ($Nz7^*$) and two PE units (Nz_27^* ; Table 2). MALDI-TOF/TOF-MS analysis revealed an ion of m/z 1137.1, which corresponds to a PE-modified HexNAc5 unit (Figure 18, A). In analogy to other *Drosophila* zwitterionic GSL structures, $Nz7^*$ was interpreted as $Nz6^*$ with an additional outer HexNAc, probably a GalNAc residue in α 1,4-linkage (Table 2) (Seppo et al., 2000; Stolz et al., 2007). Moreover, an $Nz9^*$ species (m/z 2364.7) with one PE modification and an Nz_29^* signal (m/z 2487.7) with two PE residues were registered, which were assumed to be built by addition of a GalNAc in α 1-4-linkage to the outer β -linked GalNAc of Nz_28 with one and two PE modifications (Figure 18, B; Table 2). This structure describes the largest, so far identified GSL structure in *D. melanogaster*.

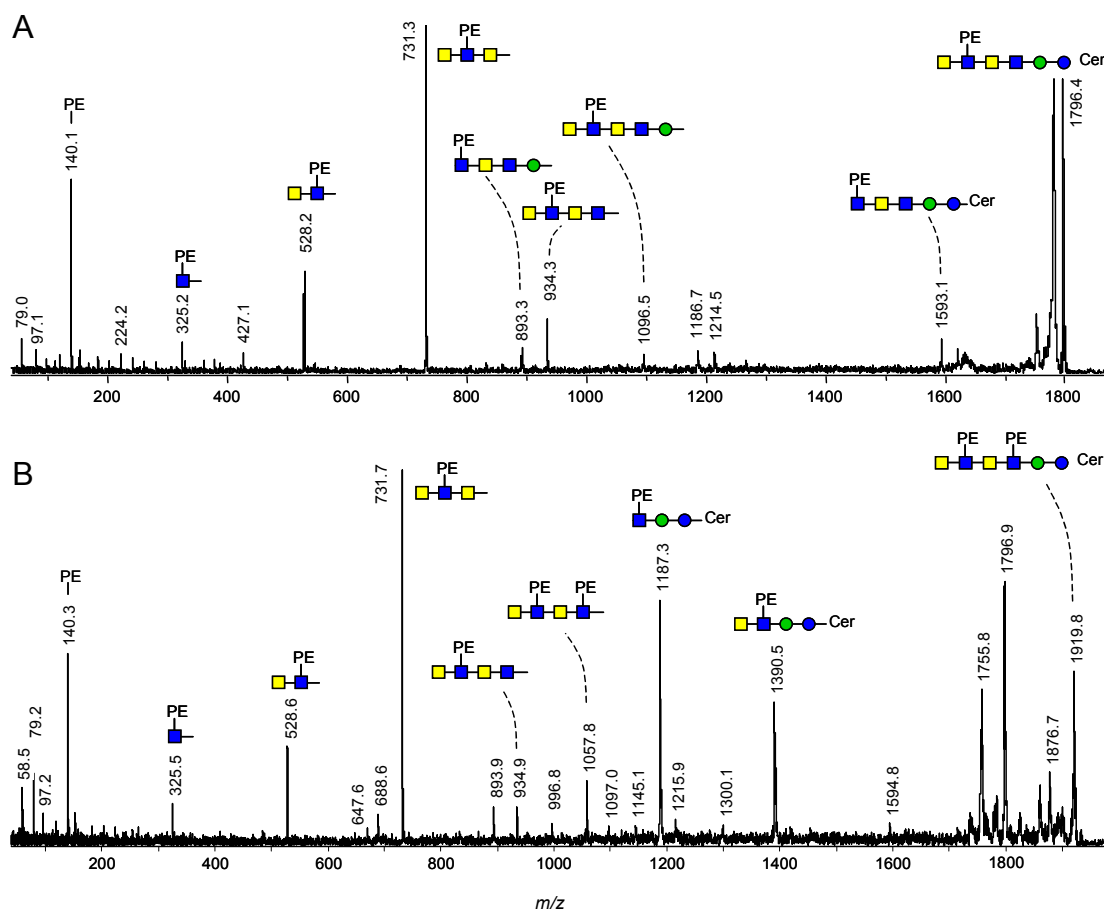


Figure 17: MALDI-TOF/TOF-MS analysis of zwitterionic GSL species. Glycolipid species A with a hexasaccharide glycan moiety with one PE-substitution (m/z 1796; from β 4GalNAcTA depleted cells) and B the hexasaccharide glycan moiety (m/z 1919) containing two PE residues were analyzed by MALDI-TOF/TOF-MS in deprotonated form. Because of isomerism in the case of single PE-substitution, the localization of the PE-residue could not be assigned exactly. For key see legend Figure 6.

Glycosphingolipid Zwitterionic	Proposed structure	Registered mass (m/z)
Nz6*	GalNAc β ,4(PE-6)GlcNAc β ,3GalNAc β ,4GlcNAc β ,3Man β ,4Glc β Cer, GalNAc β ,4GlcNAc β ,3GalNAc β ,4(PE-6)GlcNAc β ,3Man β ,4Glc β Cer	1796.3/1824.4#
Nz ₂ 6*	GalNAc β ,4(PE-6)GlcNAc β ,3GalNAc β ,4(PE-6)GlcNAc β ,3Man β ,4Glc β Cer	1919.4
Nz7*	(HexNAc1-)GalNAc β ,4GlcNAc β ,3GalNAc β ,4(PE-6)GlcNAc β ,3Man β ,4Glc β Cer	1999.5/2027.5#
Nz ₂ 7*	(HexNAc1-)GalNAc β ,4(PE-6)GlcNAc β ,3GalNAc β ,4(PE-6)GlcNAc β ,3Man β ,4Glc β Cer	2122.5
Nz9*	(HexNAc1-)GalNAc β ,4GlcNAc β ,3Gal β ,3GalNAc α ,4GalNAc β ,4(PE-6)GlcNAc β ,3Man β ,4Glc β Cer	2364.7
Nz ₂ 9*	(HexNAc1-)GalNAc β ,4(PE-6)GlcNAc β ,3Gal β ,3GalNAc α ,4GalNAc β ,4(PE-6)GlcNAc β ,3Man β ,4Glc β Cer	2487.7

Table 2: Newly registered zwitterionic glycosphingolipid species in S2 cells. Zwitterionic GSLs were registered as $[M-H]^-$ species, # GSL with a ceramide species with a 28 Da higher mass, which is to reflect two additional methylene groups.

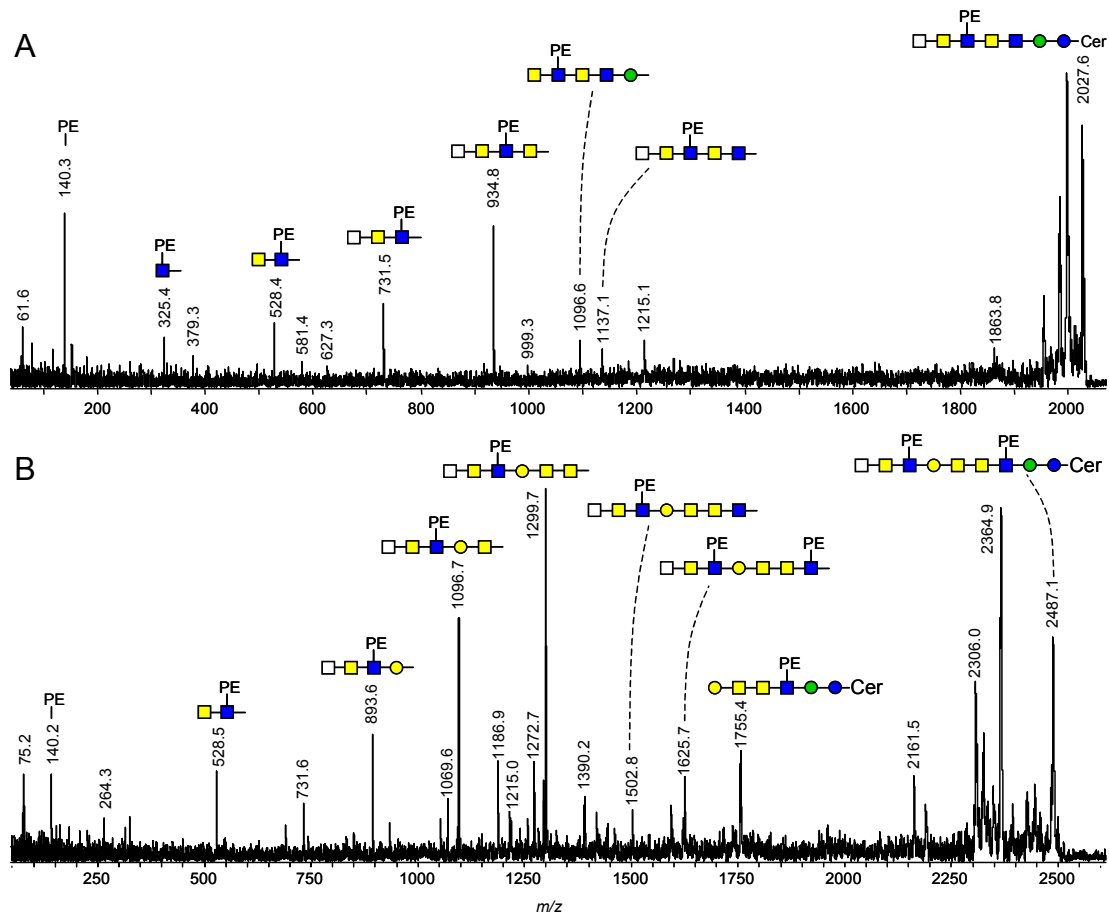


Figure 18: MALDI-TOF/TOF-MS analysis of two zwitterionic GSL species. Glycolipid species A with a hexasaccharide glycan moiety (m/z 1919; from β 4GalNAcTA depleted cells) and B with a nonasaccharide glycan moiety (m/z 2487; from β 4GalNAcTA depleted cells) were analyzed by MALDI-TOF/TOF-MS in deprotonated form. For key see legend Figure 6.

3.4 Characterization of GABPI

3.4.1 Determination of the minimal functional unit

The multi-transmembrane protein GABPI contains six transmembrane spanning regions. To determine the minimal functional unit of GABPI, different deletion constructs were generated. Based on the topology prediction derived from the aminoacid sequence of GABPI generated with the program TopPred II (Claros and von Heijne, 1994) (Figure 19), the protein was truncated from the N- or C-terminal site between the transmembrane domains (TMDs) (Table 3). Truncated GABPI proteins were tested for their ability to activate β 4GalNAcTB by immunocytochemistry staining with mAb 259-2A1 as described in 2.2.1.4. It was ascertained that the last four transmembrane domains (TMD 3-6) comprise essential parts for activation of β 4GalNAcTB (Table 3). Further deletions of the

fourth N-terminal (TMD 3) or the last C-terminal (TMD 6) domain affected functionality. The determined minimal functional unit of four TMDs was additionally investigated by reconstitution of single TMDs. Constructs containing TMD 3+4 and TMD 5+6 were generated, co-expressed in HEK293 cells and tested for functionality, but no activity was observed (Table 3).

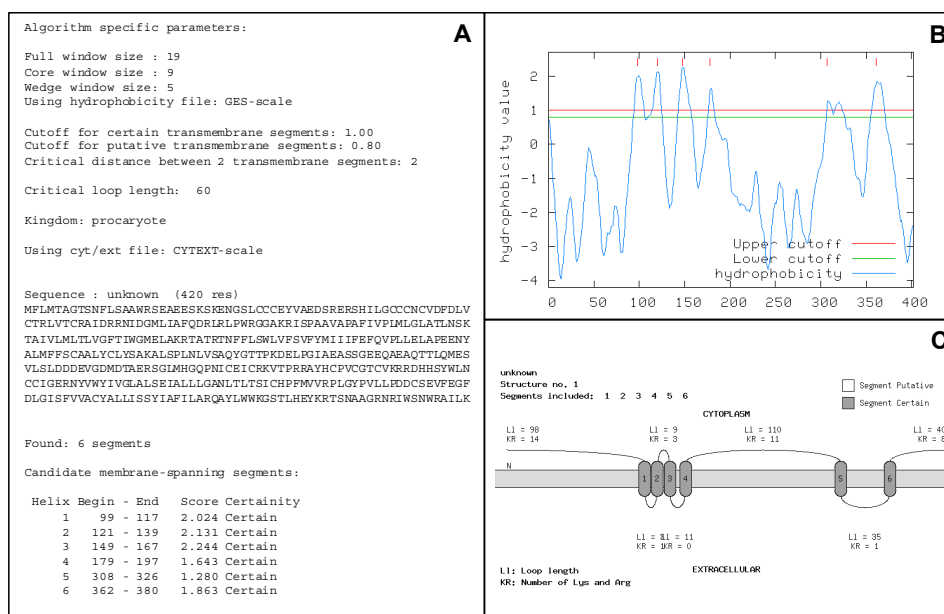


Figure 19: Topology prediction of GABPI. The number and orientation of six transmembrane spanning regions was derived from the aminoacid sequence of GABPI using TopPred II (<http://bioweb.pasteur.fr/seqanal/interfaces/toppred.html>). A: Algorithm specific parameters. B: Hydrophobicity graph image based on the hydrophobicity scale of Goldman Engelman Steitz. C: Image of the calculated topology model

deletion constructs	scheme	functionality
full length		+
NΔ90		+
NΔ117		+
NΔ141		+
NΔ167*		-
NΔ141CΔ80*		-

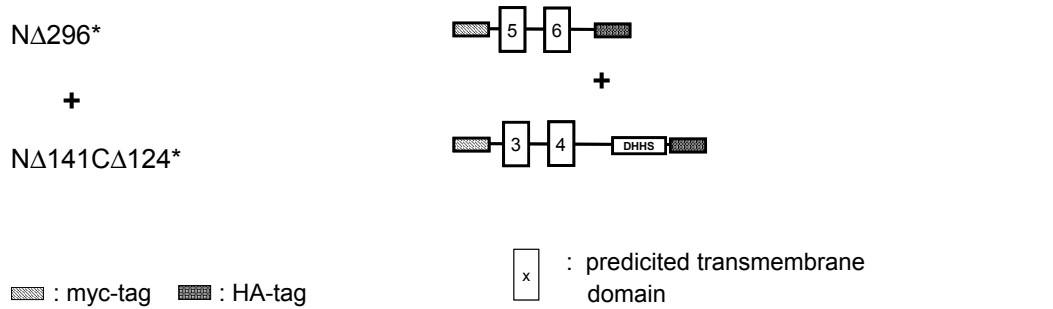


Table 3: Summary of deletion constructs of GABPI. Different deletion constructs generated based on the sequence information and the topology prediction of full length GABPI. The N-terminal deletions are marked with NΔ and the C-terminal deletions with CΔ. For a better imagination the constructs are shown as schemata. The functionality of the different proteins were tested in co-expression with β4GalNAcTB by immunocytochemistry staining with mAb 259-2A1. * Constructs were generated and tested by Benjamin Kraft. Functional positive means that the construct is able to activate β4GalNAcTB as determined by positive cell surface staining with anti lacdiNAc.

3.4.2 Transmembrane topology of GABPI

For a better understanding of the structure-function relationship of multi-transmembrane proteins the knowledge of the organisation in the lipid bilayer is very important. In the previous section, GABPI was predicted as protein that contains six TMDs (Figure 19) with cytoplasmic orientated N- and the C-terminus. This model was in accordance with other DHHC protein topology models (Linder and Deschenes, 2004; Politis et al., 2005). An epitope-insertion approach was used to investigate and confirm the membrane topology of GABPI. Indirect immunofluorescence experiments were performed to map the orientation of introduced tags. Semi-stably transfected cells were treated either with the detergent saponin to permeabilize all cellular membranes (Seeman, 1967) or with digitonin, which is only able to perforate the plasma membrane (Katz and Wals, 1985) (2.2.1.5). The usage of saponin facilitated the detection of all tags and served as a control for the accessibility of the epitopes. With digitonin only cytoplasmically oriented tags were detected. To evaluate the membrane topology of GABPI the first immunofluorescence experiments were done with semi-stable cell lines transfected with deletion constructs with N-terminal myc- and C-terminal HA-tags (Table 3).

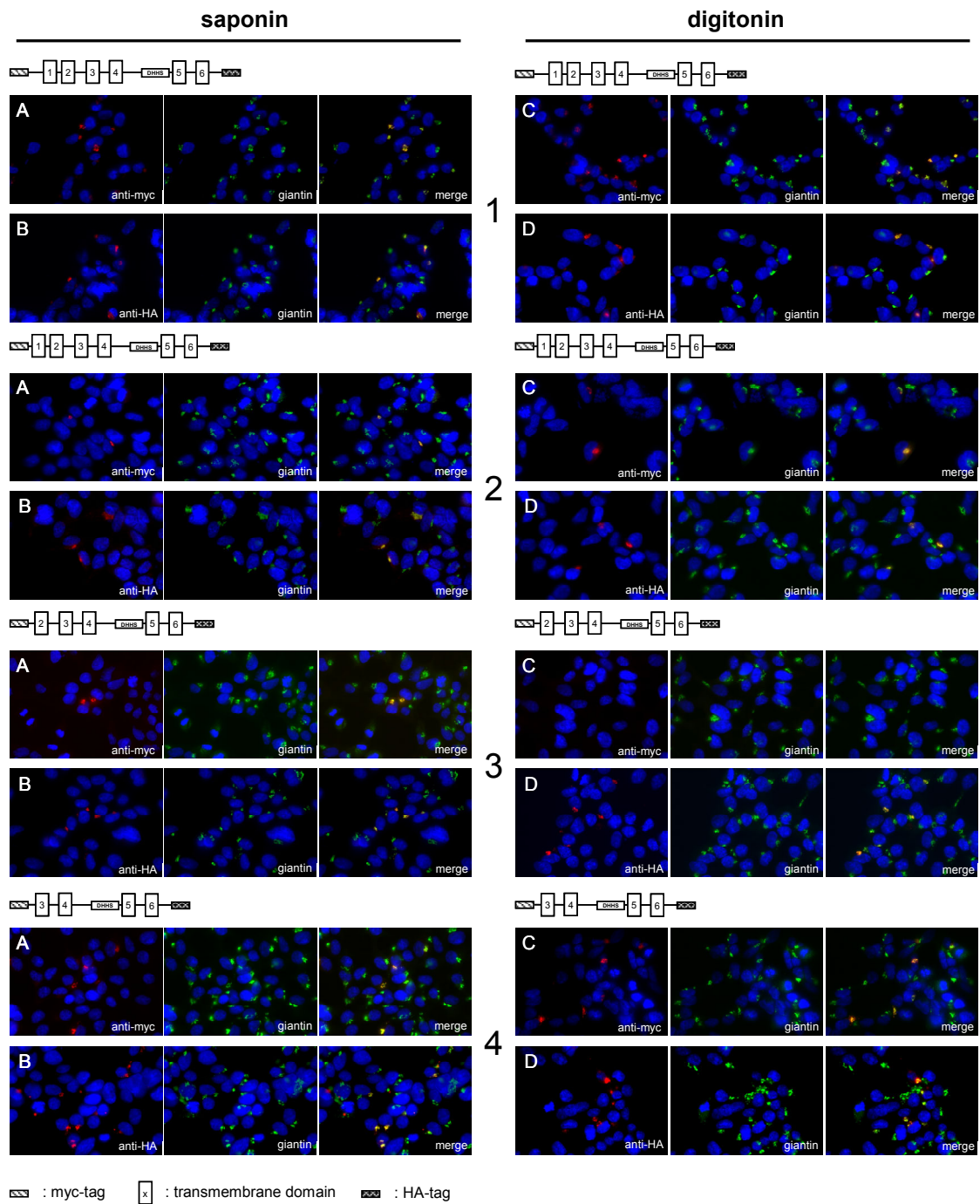

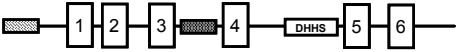
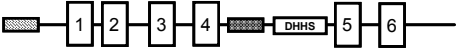
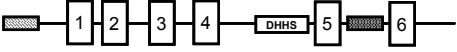


Figure 20: Orientation of the N-and the C-terminus of GABPI deletion constructs. HEK293 cells were semi-stably transfected with different truncated constructs of GABPI. 1: full length; 2: NΔ90; 3: NΔ117; 4: NΔ141. All these constructs carry N-terminal myc- and C-terminal HA-tags. For immunofluorescence detection of these tags saponin (A,B) or digitonin (C,D) treated cells were incubated with the mouse anti-myc mAb 12CA5 (A,C) or the rat anti-HA mAb 3F10 (B,D). Simultaneously, all cells were stained with rabbit anti-giantin polyclonal antibody to visualize the Golgi apparatus. Bound primary antibodies were visualized using anti-mouse Cy3, anti-rat Cy3 or anti-rabbit Alexa488 conjugated antibodies, respectively. Cell nuclei were stained with HOECHST 33258.

The HA-epitopes at the C-terminus of all constructs could be detected after saponin as well as after digitonin treatment (Figure 20, 1-4 B, D), by which was shown that the C-terminus was oriented towards the cytoplasm. The localization of the N-terminus, detected via the myc-tag, changed with different truncation states. Whereas the myc-tag in the full length and the N Δ 90 construct remained detectable with saponin and digitonin, the myc-tag of construct N Δ 117 was exclusively visible in saponin treated cells (Figure 20, 3). According to this, deletion of the first transmembrane spanning region resulted in a luminal orientation of the N-terminus in the Golgi-apparatus. By further deletion of the second TMD, the myc-tag of the construct N Δ 141 was detectable again under both saponin and digitonin treatment (Figure 20, 4).

To investigate the orientation of predicted loop regions, GABPI constructs containing internal HA-tags inside the loop regions and N-terminal myc-tags were generated (Table 4). As described before, indirect immunofluorescence was used to detect the tags in semi-stable HEK293 cells. In addition to membrane orientation, these constructs were tested for functionality by cell surface detection of the lacdiNAc epitope (Table 5).

internal HA-tag constructs	scheme	functionality
HA Δ 143-145		+
HA Δ 170-176		-
HA222		+
HA Δ 346-353		-




Table 4: Summary of GABPI constructs with internal HA-tags. Different internally HA-tagged constructs were generated based on the sequence information and the topology prediction of full length GABPI. The tags were inserted into predicted loop regions. For a better imagination the constructs are shown as scheme. The functionality of the proteins were tested in co-expression with β 4GalNAcTB by immunocytochemistry staining with mAb 259-2A1. Functional constructs are marked with +, non functional constructs with -.

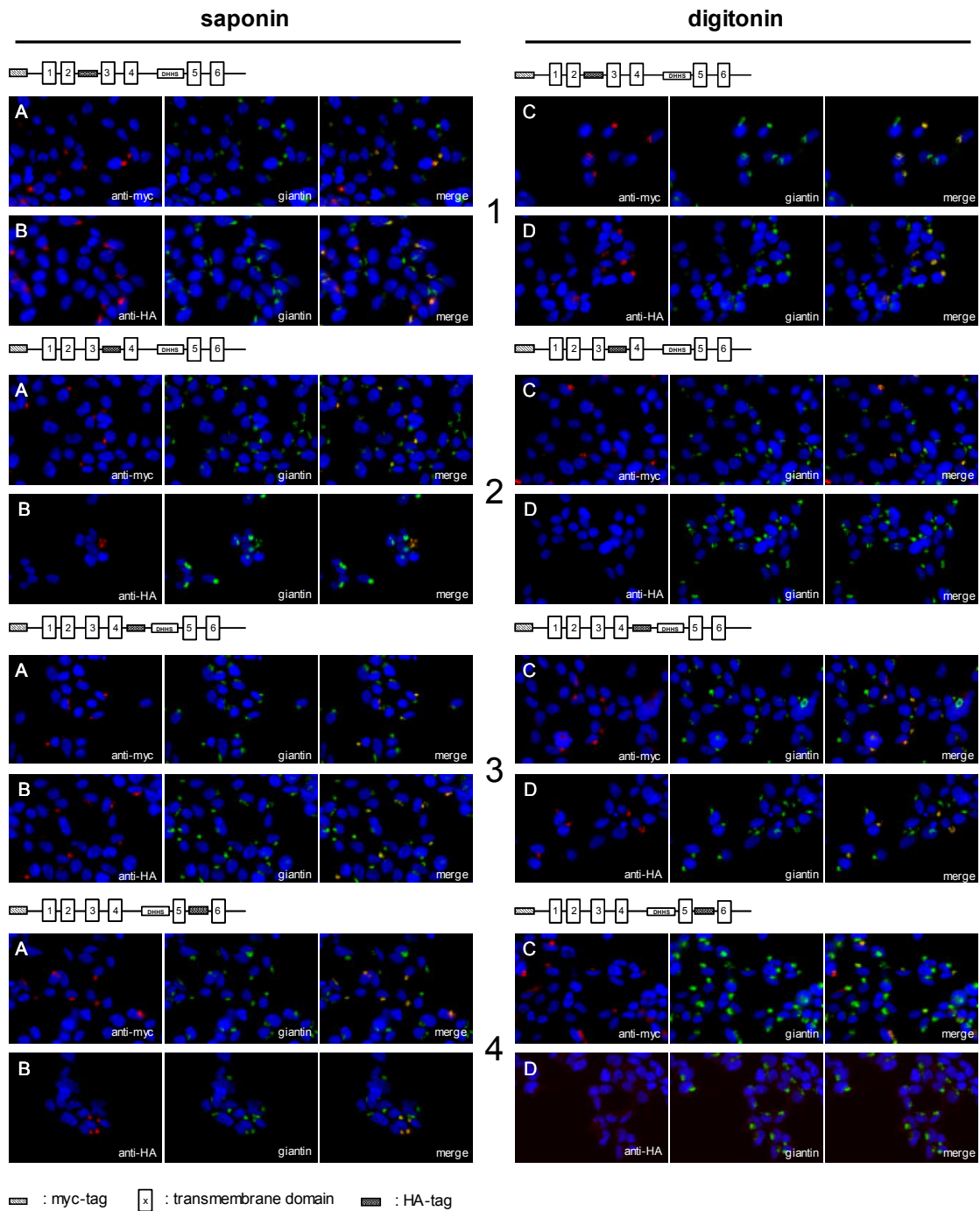


Figure 21: Orientation of myc- and internal HA-tags of different GABPI constructs. HEK293 cells were semi-stably transfected with different constructs of GABPI. 1: HA Δ 143-145; 2: HA Δ 170-176; 3: HA Δ 222; 4: HA Δ 346-353. All these constructs carry an N-terminal myc-tag. For indirect immunofluorescence detection, saponin (A,B) or digitonin (C,D) treated cells were incubated with the mouse anti-myc mAb 12CA5 (A,C) or the rat anti-HA mAb 3F10 (B,D). Simultaneously, all cells were stained with anti-giantin polyclonal antibody to visualize the Golgi apparatus. Bound primary antibodies were visualized using anti-mouse Cy3, anti-rat Cy3 or anti-rabbit Alexa488 conjugated antibodies, respectively. Cell nuclei were stained with HOECHST 33258.

In this immunofluorescence experiment all N-terminal myc-tags and internal HA-tags of GABPI constructs were detected under saponin treatment (Figure 21, A and B). The N-terminal myc-tag of all constructs was also visible in digitonin treated cells (Figure 21, C). The HA-tag of construct HA Δ 170-176 (Figure 21, 2 D) and HA Δ 346-353 could not be stained after digitonin treatment, indicating that these tags were located on the luminal side of the Golgi membrane. In contrast, the HA-tags of HA Δ 143-145 (Figure 21, 1 D) and HA222 (Figure 21, 3 D) could be detected in digitonin treated cells. In Table 5 the results of the immunofluorescence experiments and the functionality assays are summarized.

construct	N-terminal myc-epitope	HA-epitope	functionality	subcellular localization
<u>Deletions with C-term. HA</u>				
full length	cytosolic	cytosolic	+	Golgi
N Δ 90	cytosolic	cytosolic	+	Golgi
N Δ 117	luminal	cytosolic	+	Golgi
N Δ 141	cytosolic	cytosolic	+	Golgi
N Δ 167*			-	cytoplasm
N Δ 296*			-	cytoplasm
N Δ 141C Δ 80*			-	cytoplasm
N Δ 141C Δ 124*			-	cytoplasm
N Δ 296 + N Δ 141C Δ 124*			-	cytoplasm
<u>internal HA</u>				
HA Δ 143-145	cytosolic	cytosolic	+	Golgi
HA Δ 170-176	cytosolic	luminal	-	Golgi
HA222	cytosolic	cytosolic	+	Golgi
HA Δ 346-353	cytosolic	luminal	-	Golgi

Table 5: Membrane topology of GABPI. Orientation of N-terminal myc and C-terminal or internal HA tags in the Golgi membrane. Functionality was tested by cell surface staining with the mAb 259-2A1. * Constructs were generated and tested by Benjamin Kraft. Functional constructs are marked with +, non functional constructs with -.

These experiments could confirm the predicted transmembrane topology of GABPI with six transmembrane regions, the N- and C-terminal ends located to the cytoplasm and three luminal and two cytoplasmic loop regions (see also Figure 23).

3.4.3 The loop regions of GABPI

Functional tests of the internal HA-tag constructs demonstrated that insertions of HA-tags between the third and the fourth (loop 3/4) and between the fifth and the sixth (loop 5/6) transmembrane domain resulted in proteins that were not able to activate β 4GalNAcTB (Table 5). In contrast, the insertion of an HA-tag in the DHHS loop region did not affect functionality. In a sequence alignment of the loop regions of GABPI with related insect DHHC proteins high similarity were shown. In contrast, the human DHHC homolog was significantly different, especially in the loop 5/6, which is shorter than the loop of GABPI (Figure 22). For detailed functional analyses of the loop regions of GABPI, conserved amino acids of the insect proteins, which were different to the human homolog, were selected for site-directed mutagenesis (see Table 6, 2.2.2.2).

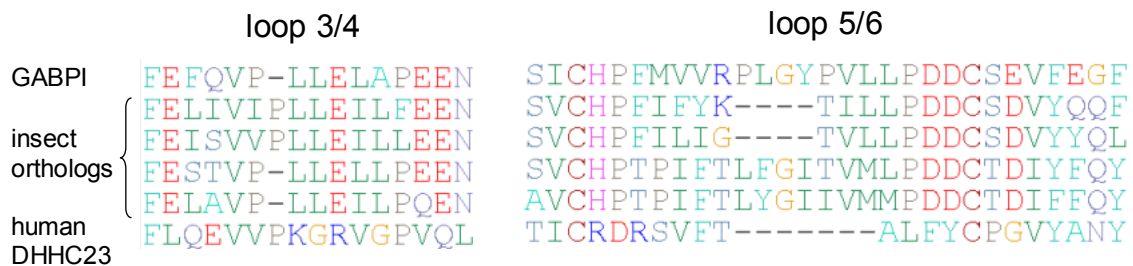


Figure 22 : Sequence alignment of the loop regions 3/4 and 5/6 of GABPI with other DHHC proteins.

Listed species (top down): *Drosophila melanogaster*, *Tribolium castaneum*, *Apis mellifera*, *Aedes aegypti*, *Anopheles gambia*, *Homo sapiens*

All mutants were tested in transient transfected HEK293 cells for their ability to activate β 4GalNAcTB (2.2.1.4). Localization studies using the N-terminal myc-tag were performed to exclude that mutations led to misfolded and because of that unfunctional proteins (summarized in Table 6, primary data not shown).

Although GABPI is clearly a member of the DHHC protein family, an unexpected feature of this protein is that the DHHC sequence is represented by a DHHS motif. With respect to the fact that the cysteine residue in the DHHC motif is absolutely required for the activity of DHHC proteins (Lam et al., 2006; Lobo et al., 2002b; Roth et al., 2002b; Smotrys et al., 2005; Valdez-Taubas and Pelham, 2005), individual aminoacids of the DHHS motif were replaced by cysteine or alanine (see Table 6). This approach was used to investigate, whether this motif was as essential as in other DHHC proteins. Immunocytochemical staining was used for functional analyses.

region	mutation	function	subcellular localization
<u>loop 3/4</u> EFQVPLLELAPEEN	<u>AA 166-179</u> A FQVPLLELAPEEN	+	Golgi
	EFQV A LLELAPEEN	+	Golgi
	EFQVPLLE A LAPEEN	+	Golgi
	EFQVPLLELA A EEN	-	cytoplasm
	EFQVPLLELAP A AN	-	Golgi
	EFQVPLLELAP Q QN	-	Golgi
<u>DHHS motif</u> DHHS	<u>AA 193-196</u> DH H C	+	Golgi
	DH H A	+	Golgi
	D A HS	+	Golgi
	DH A S	+	Golgi
	A HHS	+	Golgi
	A AAA	+	Golgi
<u>loop 5/6</u> SICHPFMVVRPLGYPVLLNPDDCSEVFEGF	<u>AA 332-360</u> SIC A PFMVVRPLGYPVLLNPDDCSEVFEGF	-	Golgi
	SIC H AFMVRPLGYPVLLNPDDCSEVFEGF	+	Golgi
	SICHPFMVVRPLG A VLLNPDDCSEVFEGF	-	Golgi
	SICHPFMVVRPLGYPVLL N ADDCEVFEGF	+	Golgi
	SICHPFMVVRPLGYPVLLNP A ACSEVFEGF	+	Golgi
	SICHPFMVVRPLGYPVLLNPDD A SEVFEGF	-	Golgi
	SICHPFMVVRPLGYPVLLNPDDCSEVFEGF	-	Golgi

Table 6: Site-directed mutagenesis constructs of GABPI. Mutated amino acids are shown in bold letters. Functionality of the constructs was tested in co-expression with β 4GalNAcTB via immunocytochemical staining with the mAb 259-2A1. Functional positive means that the construct is able to activate β 4GalNAcTB as determined by positive cell surface staining with anti lacdiNAc. Subcellular localization was investigated by immunofluorescence experiments.

The investigation of site-directed mutated GABPI proteins confirmed, that the luminal regions of GABPI comprise important elements to activate β 4GalNAcTB. Furthermore, individual amino acids were identified to be essential for the activation process. In contrast, mutations of any amino acid of the DHHS motif did not affect functionality, indicating that this sequence, unlike in other DHHC family members, has no relevance for GABPI function.

In Figure 23, the evaluated topology model of GABPI based on the Toppred II calculation and the immunofluorescence experiments is shown. The sites of deletion and internal HA-tag constructs are marked with arrows and functional important amino acids (in bold) are summarized (Figure 23).

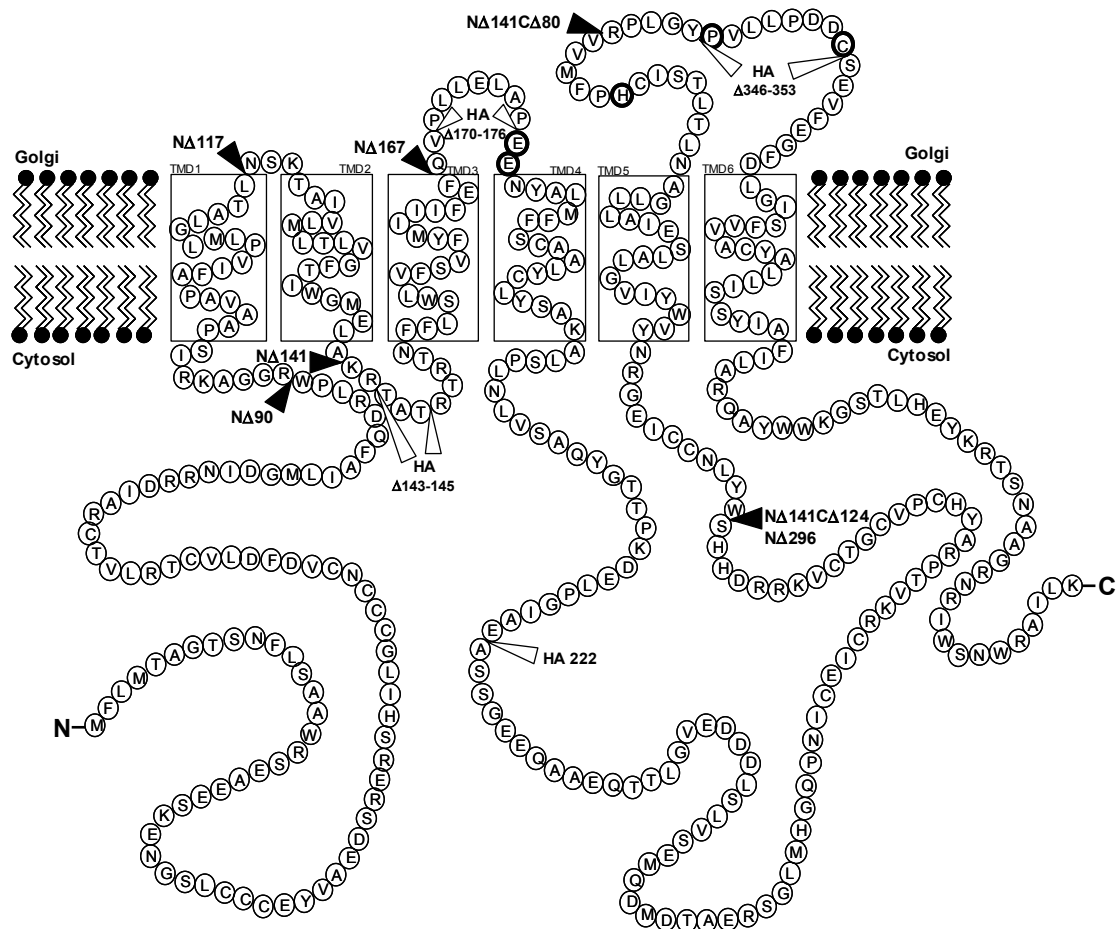


Figure 23: Topology and functional amino acids of GABPI. This illustration is build based on the Toppred II calculation and indirect immunofluorescence experiments. The sites of deletion and internal HA-tag constructs are indicated with arrows. The bold amino acids were determined to be important for activation of β 4GalNAcTB by GABPI.

3.4 The function of GABPI

3.4.1 Palmitoyltransferase activity of the DHHC family member GABPI

The DHHC protein family members that are characterized by now, have been shown to be protein acyltransferase (PAT) (Fernandez-Hernando et al., 2006; Fukata et al., 2006; Mitchell et al., 2006). As already mentioned, the conserved DHHC motif is essential for PAT activity. GABPI contains a DHHS instead of a DHHC motif and site-directed mutagenesis experiments demonstrated that this sequence does not affect its effects on β 4GalNAcTB. We therefore concluded that GABPI does not function as a protein acyltransferase. To additionally confirm this hypothesis a β 4GalNAcTB mutant was generated, in which the cysteine-residue (C29) at the N-terminal end of the predicted

transmembrane domain was mutated by site-directed mutagenesis to alanine (C29A). This residue was the only cysteine residue that theoretically could serve as a target for palmitoylation although it was located in the predicted transmembrane domain rather than in the cytoplasmic domain of $\beta 4\text{GalNAcTB}$, where palmitoylation takes place and the DHHC domain of GABPI is localized. The activity of the mutant was investigated by transfection of HEK293 cells in presence of the full length GABPI, but no change in lacdiNAc presentation could be observed. From this experiment and the other observations we concluded that GABPI, although a member of the DHHC protein family, has no protein acyltransferases activity.

3.4.2 GABPI is required for Golgi targeting of $\beta 4\text{GalNAcTB}$, but not of $\beta 4\text{GalNAcTA}$

In the next experiments the subcellular localization of the GalNAc transferases and GABPI was investigated. HEK293 cells were stably transfected with N-terminally Flag-tagged GalNAc transferases and N-terminally myc-tagged GABPI. The proteins were detected by indirect immunofluorescence in combination with the respective ER and Golgi markers calnexin and mannosidase-II.

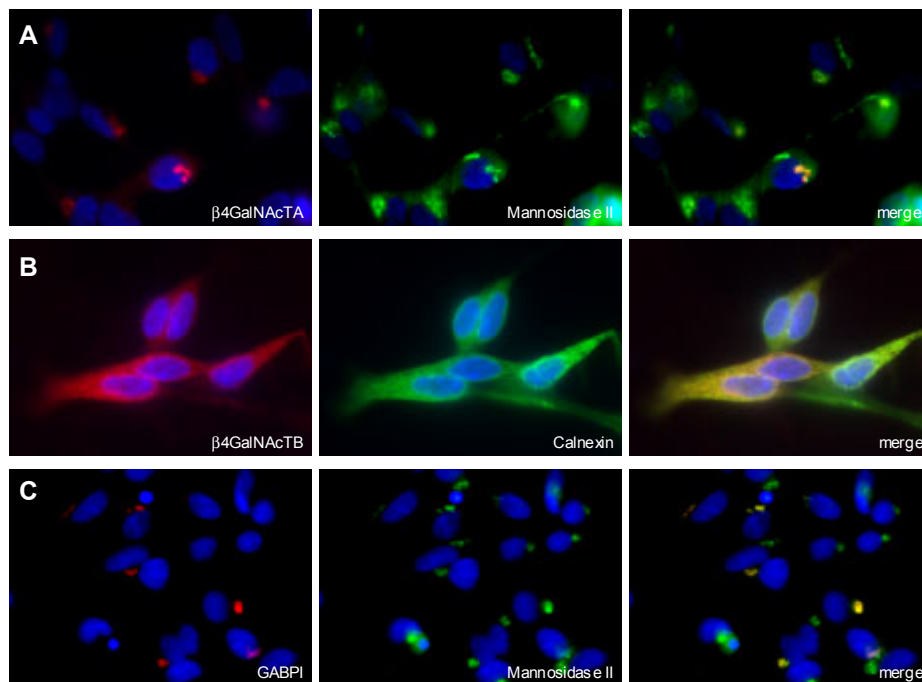


Figure 24: Subcellular localization of $\beta 4\text{GalNAcTA}$, $\beta 4\text{GalNAcTB}$ and GABPI. HEK293 cells were stably transfected with N-terminally Flag-tagged $\beta 4\text{GalNAcTA}$ (A), $\beta 4\text{GalNAcTB}$ (B) and N-terminally myc-tagged GABPI (C). $\beta 4\text{GalNAcTA}$ and GABPI show co-localization with the Golgi maker

mannosidase II (A and C), whereas β 4GalNAcTB merges with the ER resident protein Calnexin (B). The cell nuclei were stained with HOECHST 33258.

Surprisingly, a defined difference in the subcellular localization was observed. In contrast to β 4GalNAcTA and GABPI (Figure 24, A and C), which co-localized with the Golgi marker, β 4GalNAcTB perfectly overlapped with the ER resident protein Calnexin (Figure 24, B).

In the next experiment, it was tested whether subcellular localization of β 4GalNAcTB was effected by the presence of GABPI. Therefore, HEK293 cells that stably expressed β 4GalNAcTB were transiently transfected with GABPI. The proteins were detected via indirect immunofluorescence as described before.

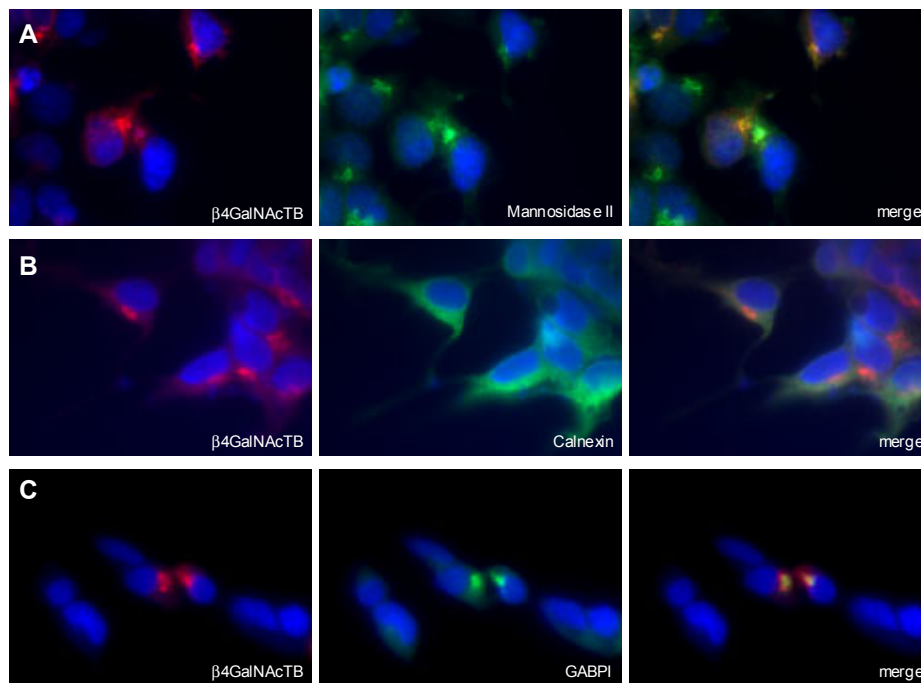


Figure 25: Subcellular localization of β 4GalNAcTB and GABPI. HEK293 cells were stably transfected with N-terminally Flag-tagged β 4GalNAcTB and after a few weeks of expression the cells were transiently cotransfected with myc-tagged GABPI. The subcellular localization was detected via indirect immunofluorescence using anti-Flag antibody M5 and anti-myc antibody 9E10. Two days after transfection, β 4GalNAcTB in presence of GABPI showed co-localization with the Golgi marker mannosidase II (A and B). Additionally a co-localization of the transferases and GABPI could be observed (C). The cell nuclei were stained with HOECHST 33258.

In presence of GABPI a shift of $\beta 4\text{GalNAcTB}$ from the ER to the Golgi apparatus was detected (Figure 25, A and B) and co-localization of the transferase with GABPI became visible.

To evaluate the effect of GABPI on $\beta 4\text{GalNAcTB}$ in a more natural environment, subcellular localization experiments were repeated in *Drosophila* S2 cells. S2 cells were transiently transfected with Flag-tagged $\beta 4\text{GalNAcTA}$ and $\beta 4\text{GalNAcTB}$. For visualization of the ER and Golgi, already characterized specific organelle resident proteins were co-transfected. KDEL-GFP (Okajima et al., 2005) was used as ER marker and dGrasp-GFP (Kondylis et al., 2005) as Golgi marker. In the immunofluorescence images, $\beta 4\text{GalNAcTA}$ and $\beta 4\text{GalNAcTB}$ overlapped with the Golgi-resident protein dGrasp-GFP (Figure 26, A and C), no co-localization with the ER marker KDEL-GFP was visible (Figure 26, B and D).

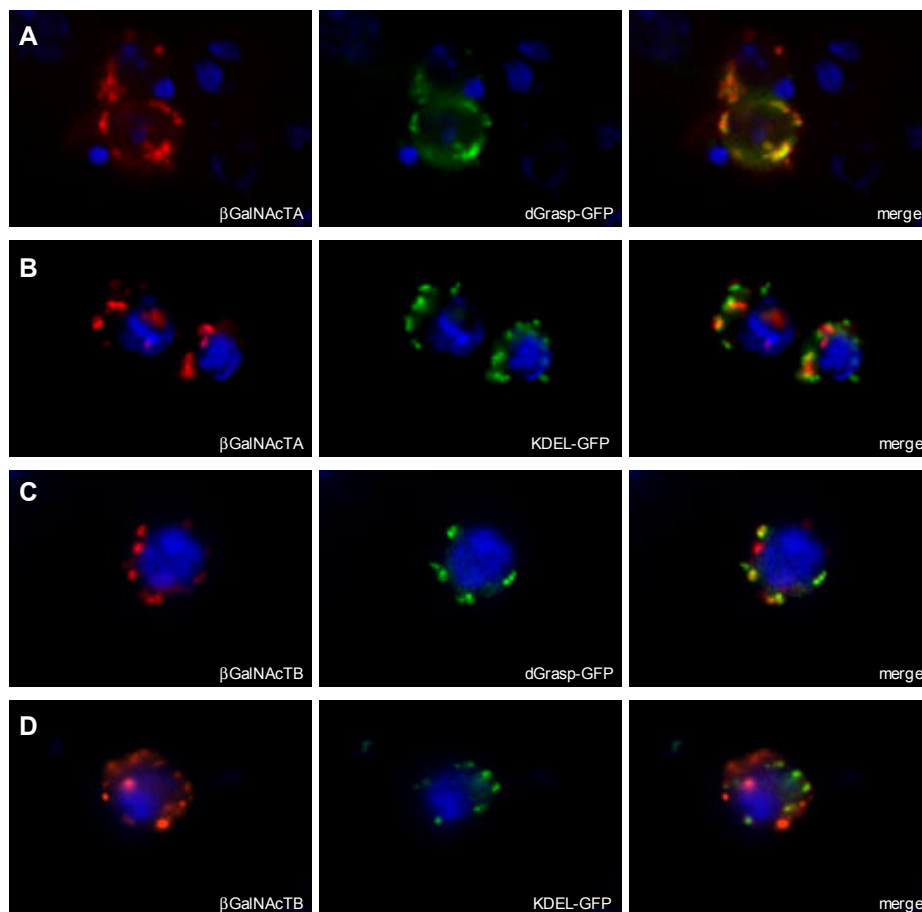


Figure 26: : Subcellular localization of $\beta 4\text{GalNAcTA}$, $\beta 4\text{GalNAcTB}$ in *Drosophila* S2 cells. S2 Schneider cells were transiently transfected with N-terminally Flag-tagged $\beta 4\text{GalNAcTA}$ (A and B), $\beta 4\text{GalNAcTB}$ (C and D) and the Golgi marker dGrasp-GFP or the ER marker KDEL-GFP. Both GalNAc transferases are co-localized with the Golgi resident protein (A and C). The cell nuclei were stained with HOECHST 33258.

In a second step, localization of $\beta 4\text{GalNAcTA}$ and TB was investigated in cells, in which GABPI was downregulated by RNAi. For this, *Drosophila* S2 cells were incubated with dsRNA corresponding to a central region of GABPI (2.2.1.3). Three days after the first incubation, the cells were washed and transfected with the different GalNAc transferases and organelle markers. After transfection, the cells were washed and RNAi treatment was repeated. Two days after transfection the cells were investigated by immunofluorescence as described before.

As shown in Figure 27 C, the RNAi treatment dissected Flag-tagged $\beta 4\text{GalNAcTB}$ from the signal produced by the Golgi marker. Instead, the signal of $\beta 4\text{GalNAcTB}$ overlapped with the ER marker KDEL-GFP (Figure 27, D). In contrast, changes in subcellular localization of $\beta 4\text{GalNAcTA}$ were not observed in dsRNA treated cells (Figure 27, A).

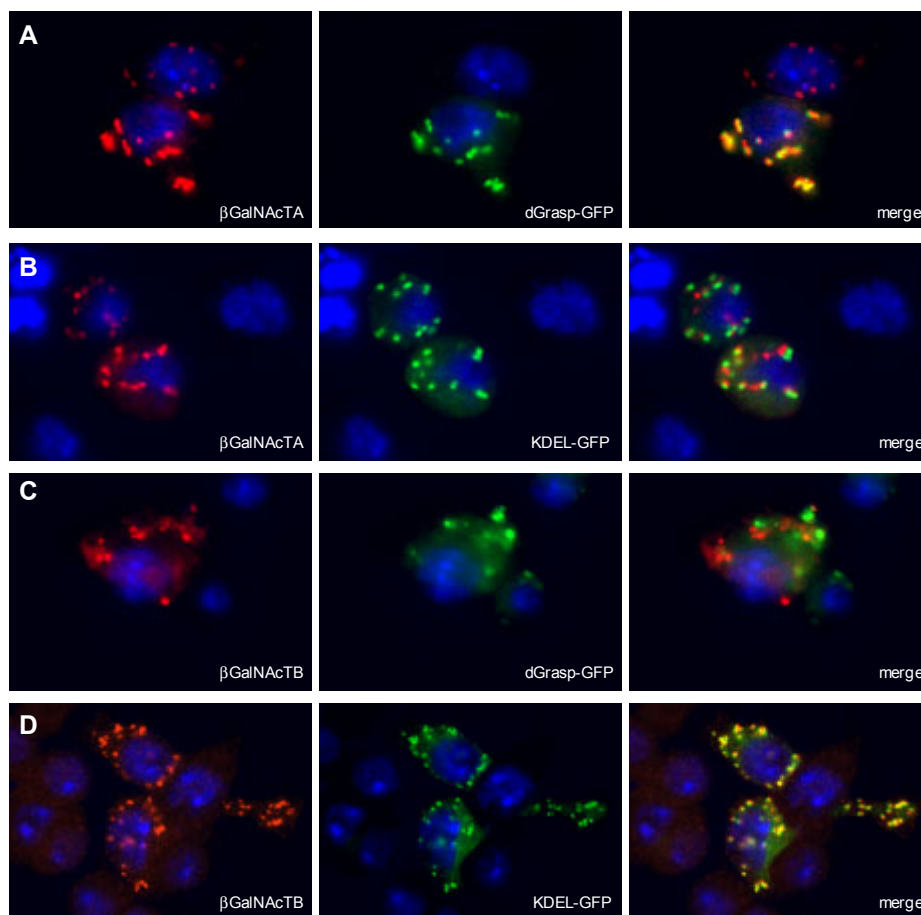


Figure 27: Subcellular localization of $\beta 4\text{GalNAcTA}$, $\beta 4\text{GalNAcTB}$ in *Drosophila* S2 cells under influence of dsRNA. S2 cells were incubated for three days with dsRNA corresponding to a central region of GABPI. Afterwards, cells were transiently transfected with N-terminally Flag-tagged $\beta 4\text{GalNAcTA}$ (A and B), $\beta 4\text{GalNAcTB}$ (C and D) and the Golgi maker dGrasp-GFP or the ER marker KDEL-GFP. After transfection, RNAi treatment was repeated and two days later the cells were analyzed by immunofluorescence. Whereas $\beta 4\text{GalNAcTA}$ stayed co-localised with the Golgi marker (A), $\beta 4\text{GalNAcTB}$ showed redistribution to the ER (C). The cell nuclei were stained with HOECHST 33258.

3.5 Interactions domains of β 4GalNAcTB and GABPI

A detailed look at the sequence alignment of β 4GalNAcTA and β 4GalNAcTB generated with the program MegAlign (Figure 28) demonstrated that the primary sequence of these enzymes mainly differ in the first region until the catalytic domain. The stem region of GalNAcTB comprises 30 amino acids, whereas the stem of β 4GalNAcTA consists of 105 amino acids. Like other β 4GalT family members, both *Drosophila* β 4GalNAcTs have the first conserved cysteine residue that marks the start of the catalytic domain (Boeggeman et al., 1993). The C-terminal region downstream of this cysteine was mainly conserved.

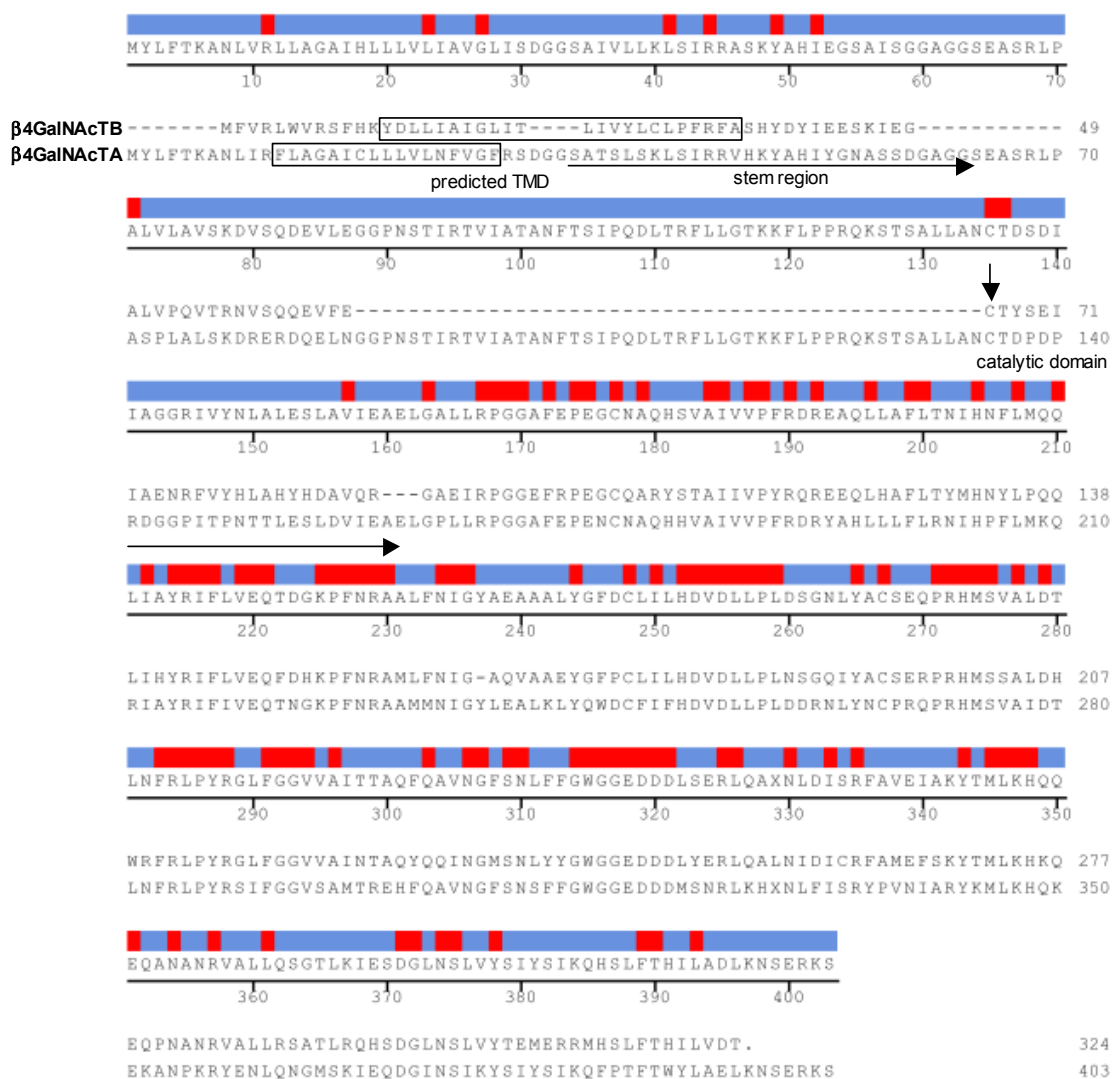


Figure 28: Sequence alignment of β 4GalNAcTA and -TB. Identical amino acids are marked with red bars.

To investigate the region of interaction between GABPI and β 4GalNAcTB, hybrid constructs from β 4GalNAcTA and β 4GalNAcTB were generated. Therefore, the transferases were subdivided into three functional parts: the cytoplasmic tail plus the transmembrane domain (1), the stem region (2), and the catalytic domain (3) starting from the conserved cysteine residue. These parts from both GalNAc transferases were combined in different ways. All constructs are listed in Table 7. The hybrid constructs were investigated for activity, using immunocytochemical staining as described before (2.2.1.4). For this purpose, HEK293 cells were transfected with hybrid constructs in presence or absence of GABPI and lacdiNAc epitope presentation on the cells surface was detected using mAb 259-2A1.









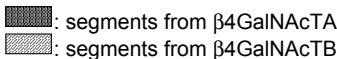
construct	scheme			activity without GABPI	activity with GABPI
	(1) cytpl. TMD domain	(2) stem	(3) catalytic domain		
β 4GalNAcTA				+	/
hybrid B-A-A				+	/
hybrid B-B-A				+	/
hybrid A-B-A				+	/
β 4GalNAcTB				-	+
hybrid A-B-B				-	+
hybrid A-A-B				-	-
hybrid B-A-B				-	-
					

Table 7: Different hybrid constructs of β 4GalNAcTA and β 4GalNAcTB. The two GalNAc transferases from *Drosophila melanogaster* were divided in three domains: the cytoplasmic tail plus the transmembrane domain (1), the stem region (2) and the catalytic domain (3). These domains were combined in different ways. For better imagination the constructs are also shown as scheme. The activities of the different proteins were tested with and without co-expression of GABPI via immunocytochemical staining with the mAb 259-2A1. Active constructs are marked with +, inactive constructs with - and not tested with /.

All constructs containing the catalytic domain of β 4GalNAcTA showed independent activity. For chimeras with the catalytic domain of β 4GalNAcTB, the lacdiNAc epitope on the cell surface was only detectable in presence of the stem region the B enzyme and in co-expression with GABPI.

In the next step, subcellular localization studies of the hybrid constructs were performed. HEK293 cells were semi-stably transfected with the N-terminally Flag-tagged hybrid B-B-A alone and with the Flag-tagged hybrids A-B-B and A-B-B in presence or absence of N-terminally myc-tagged GABPI. The transferases were detected by indirect immunofluorescence in combination with the ER and Golgi markers Calnexin and mannosidase-II (2.2.1.5). The hybrid B-B-A with the catalytic domain of β 4GalNAcTA was co-localized with the Golgi resident protein (Figure 29, E). In contrast, the hybrids A-B-B and A-A-B were co-localized with the ER marker Calnexin (Figure 29, A and C). Exclusive hybrid A-B-B was able to shift from the ER to the Golgi in presence of GABPI (Figure 29, B).

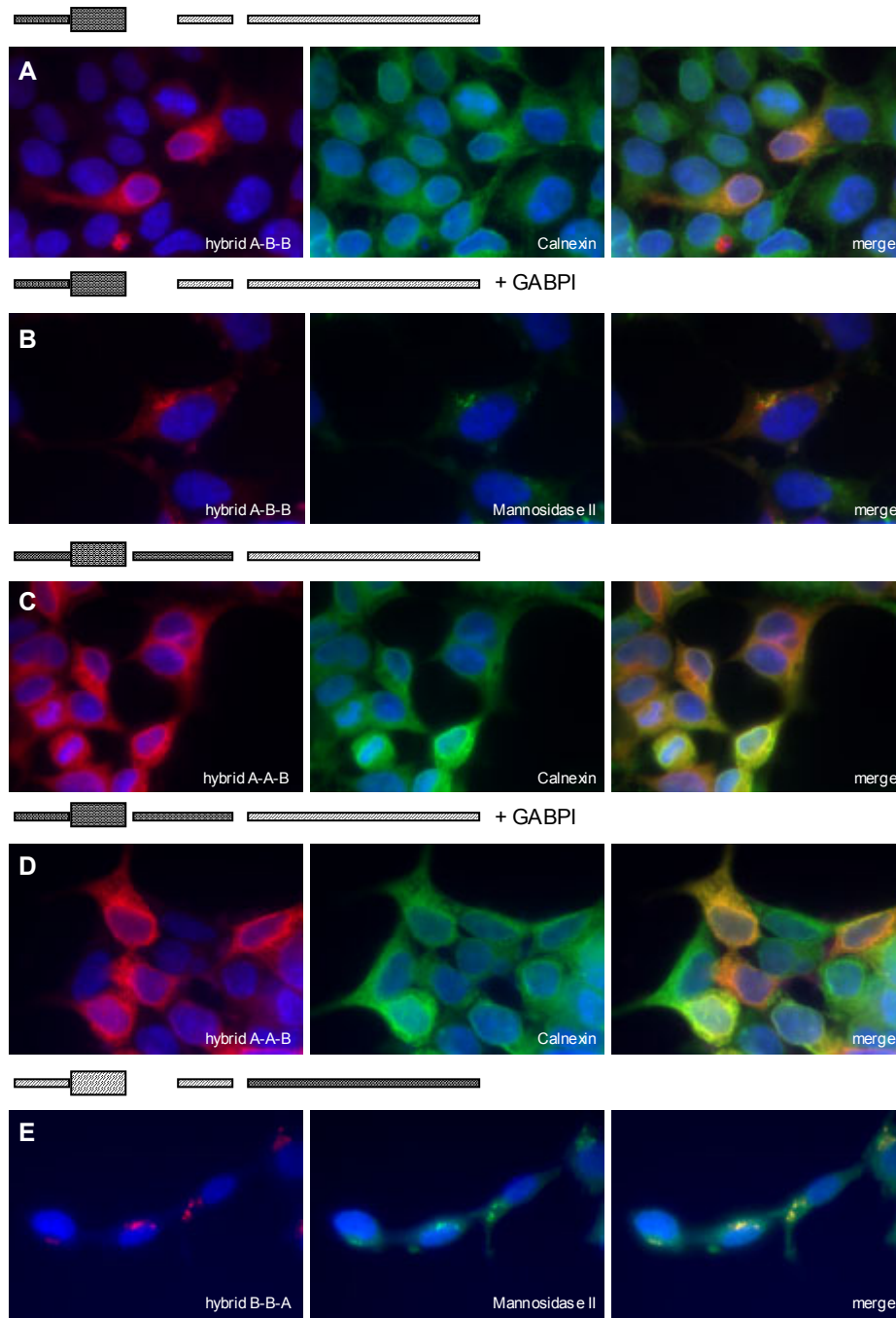


Figure 29: Subcellular localization of hybrid constructs. HEK293 cells were stably transfected with N-terminally Flag-tagged hybrid A-B-B (A and B) and A-A-B (C and D) in absence and presence (B and D) of GABPI. HEK293 cells were stably transfected with N-terminally tagged hybrid constructs and transiently co-transfected with GABPI. Hybrid B-B-A (E) with the catalytic part of β 4GalNAcTA was additionally investigated. Subcellular localization was analyzed via indirect immunofluorescence using anti-Flag antibody M5. Hybrid A-B-B, containing the stem and the catalytic domain of β 4GalNAcTB, merged with the ER marker (A), whereas in presence of GABPI showed co-localization with the Golgi marker mannosidase II (B). Exchange of the stem region (hybrid A-A-B) led to exclusive co-localization with Calnexin (C and D). Hybrid B-B-A merged with mannosidase II. The cell nuclei were stained with HOECHST 33258.

These experiments demonstrated that the stem region of $\beta 4\text{GalNAcTB}$ played an important role in the activation and localization process by GABPI. A further question was, whether the distance between the catalytic domain and the membrane would be a second limiting factor. Additional hybrids were generated, in which the stem region of $\beta 4\text{GalNAcTA}$, introduced in enzyme B, was shortened from the N- or C-terminal side to the exact length of the stem region of $\beta 4\text{GalNAcTB}$ (Table 8). The construct A-A_{short}-A served as control to determine whether the shortened stem region of $\beta 4\text{GalNAcTA}$ affects activity. Hybrids were tested for activity in HEK293 cells as described before (Table 8).

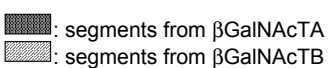
construct	scheme	activity without GABPI	activity with GABPI
A-A _{short} -A		+	/
hybrid A-A _{short} -B		-	-
hybrid A- _{short} A-B		-	-
hybrid A-A _{short} B-B		-	-

Table 8: Different hybrid constructs of $\beta 4\text{GalNAcTA}$ and $\beta 4\text{GalNAcTB}$. The two GalNAc transferases from *Drosophila* were divided in three domains: the cytoplasmic tail plus the transmembrane domain (1), the stem region (2) and the catalytic domain (3). The stem region of $\beta 4\text{GalNAcTA}$ was shortened from the N- or C-terminal side to the exact length of the stem region of $\beta 4\text{GalNAcTB}$. $\beta 4\text{GalNAcTA}$ with a short stem was used as positive control. The short stem regions were fused to the catalytic domain of $\beta 4\text{GalNAcTB}$ and an additional construct, containing the short stem of the A enzyme and the complete stem of the B enzyme, were generated. For better imagination the constructs are shown as scheme. The activity of the different proteins was tested with and without co-expression of GABPI via immunocytochemical staining with the mAb 259-2A1. Active constructs are marked with +, inactive constructs with -, and not tested with /.

All generated chimeras containing the catalytic domain of $\beta 4\text{GalNAcTB}$ were inactive in absence or presence of GABPI. Moreover, the hybrid A-A_{short}B-B with the elongated stem region, which contains the full length stem region of $\beta 4\text{GalNAcTB}$, did not show any activity. This indicated that both, the sequence and the length of the stem region together, played an important role in interaction process of $\beta 4\text{GalNAcTB}$ and GABPI.

The generated constructs were additionally investigated for subcellular localization in absence of GABPI as described before. All hybrids containing the catalytic domain of $\beta 4\text{GalNAcTA}$ were Golgi localized, whereas hybrids with the catalytic domain of $\beta 4\text{GalNAcTB}$ were co-localized with Calnexin. A summary of the generated hybrids, the activity and subcellular localization is given in Table 9.

construct	scheme	activity	activity with GABPI	localisation	localisation with GABPI
$\beta 4\text{GalNAcTA}$	(1) (2) (3)	+	/	Golgi	/
hybrid B-A-A		+	/	Golgi	/
hybrid B-B-A		+	/	Golgi	/
hybrid A-B-A		+	/	Golgi	/
$\beta 4\text{GalNAcTB}$		-	+	ER	Golgi
hybrid A-B-B		-	+	ER	Golgi
hybrid A-A-B		-	-	ER	ER
hybrid B-A-B		-	-	ER	ER
A-A _{short} -A		+	/	Golgi	/
hybrid A-A _{short} -B		-	-	ER	/
hybrid A _{short} -A-B		-	-	ER	/
hybrid A-A _{short} -B-B		-	-	ER	/



 ■: segments from $\beta 4\text{GalNAcTA}$
 ▨: segments from $\beta 4\text{GalNAcTB}$

Table 9: Summary of generated hybrid constructs of $\beta 4\text{GalNAcTA}$ and $\beta 4\text{GalNAcTB}$, the activity and subcellular localization. The two GalNAc transferases were divided in three domains: the cytoplasmic tail

plus the transmembrane domain (1), the stem region (2) and the catalytic domain (3). These domains were combined in different ways. For better imagination the constructs are also shown as scheme. The activity of the different proteins was tested with or without co-expression of GABPI via immunocytochemical staining with the mAb 259-2A1. Active constructs are marked with +, inactive constructs with –, and not tested with /. Localization experiments were performed in semi-stably expressing HEK293 cells with or without transient expression of GABPI.

4 Discussion

In this study the β 4GalNAc transferases A and B from *Drosophila melanogaster* were characterized. Both enzymes are responsible for the biosynthesis of the lacdiNAc structure, but differ in activity. In contrast to the cofactor independent enzyme β 4GalNAcTA, we demonstrated in different *in vitro* assay systems that β 4GalNAcTB needs a type III transmembrane protein for activity. This protein is a member of the DHHC protein gene family and during this study referred to as β 4GalNAcTB **P**ilot protein (GABPI). The *in vivo* function of β 4GalNAcTA and β 4GalNAcTB in lacdiNAc biosynthesis on GSL was confirmed by detailed MALDI-TOF-MS analysis of *Drosophila* mutants and we demonstrated that GABPI also directly influences lacdiNAc biosynthesis in *Drosophila* S2 cells. Finally, localization studies highlighted the important function of GABPI in β 4GalNAcTB Golgi localization and investigations of chimeras between β 4GalNAcTA and TB identified the stem region to mediate the selective interaction.

4.1 *In vivo* characterization of β 4GalNAcTA and β 4GalNAcTB

At the beginning of this study β 4GalNAcTA and β 4GalNAcTB mutants were already generated and the phenotypes were characterized by Nicola Haines and Kenneth Irvine (Haines and Irvine, 2005). The mutant larvae and flies of β 4GalNAcTA and β 4GalNAcTB exhibited a mild phenotype compared to the lethal mutants lacking *brainiac* or *egghead* (Goode et al., 1992; Goode et al., 1996), the enzymes responsible for the synthesis of the trisaccharide acceptor structure. β 4GalNAcTA mutants showed defects in behaviour and in the neuromuscular system (Haines and Irvine, 2005; Haines and Stewart, 2007), whilst a small proportion of β 4GalNAcTB mutants displayed a defect in epithelial morphogenesis (Chen et al., 2007). During this study, further analytical characterizations of these flies with HPTLC and MALDI-TOF-MS were performed. The pattern of GSLs of *Drosophila* wild-type flies was largely in accordance with the results of Seppo et al. (Seppo et al., 2000). Additionally, besides the already described Nz₂8 GSL species (see Table 1) a possible variant structure exhibiting an additional hexose linked to the internal β -GalNAc residue was detected and corroborated (Stolz et al., 2007). This branched structure has not been described in insects, but theoretically one of the *Drosophila* β 3-galactosyltransferases acting on GalNAc residues could transfer a hexose in this position (Wiegandt, 1992).

Based on the GSL structures in *C. elegans* (Griffitts et al., 2005), the hexose could be also interpreted as a β 6-linked glucose residue. Additional analyses are necessary for the exact identification of this sugar and could not be performed during this study.

The MALDI-TOF-MS analyses of the GalNAc transferase mutants revealed that the GSL composition of β 4GalNAcTA mutants was not significantly different from wild-type. Therefore, the role of β 4GalNAcTA in GSL biosynthesis of *Drosophila* is uncertain. On the other hand, as elongated GSLs were still detectable in the β 4GalNAcTB mutant, but not in the double β 4GalNAcTA; β 4GalNAcTB mutant, β 4GalNAcTA is able to transfer GalNAc to GSL and may contribute to the generation of these structures in wild-type flies. β 4GalNAcTB seems to play the major role in GSL biosynthesis, because mutation of this gene resulted in the accumulation of the N3 (GlcNAc β ,3Man β ,4Glc β Cer at m/z 1087.9) and Nz7 species

(GlcNAc β ,3Gal β ,3GalNAc α ,4GalNAc β ,4(PE-6)GlcNAc β ,3Man β ,4Glc β Cer at m/z 1958.0), carrying terminal GlcNAc residues that form acceptor structures for β 4GalNAcTs. The fact, that the N3 GSL species was the only detected structure in β 4GalNAcTA; β 4GalNAcTB double mutants demonstrated that β 4GalNAcTA and β 4GalNAcTB are the only enzymes involved in transfer of β 4-linked GalNAc. The exclusive presence of the trisaccharide structure in double mutant flies in combination with the mild phenotype showed that this trisaccharide product is already sufficient for relatively normal development of *Drosophila*. The inability to generate the N3 GSL results even in lethality (*Brainiac*).

In contrast to β 4GalNAcTB mutants, the behavioural phenotype and the defect in neuromuscular system of β 4GalNAcTA mutants without changes in GSL pattern suggest that β 4GalNAcTA is involved in lacdiNAc biosynthesis of other important glycoconjugates, so far not identified. It could also be explained by β 4GalNAcTA being the dominant enzyme in only a limited number of cells, not contributing measurable to the overall GSL pattern.

4.2 *In vitro* activity of β 4GalNAcTA and β 4GalNAcTB

The mass spectrometric analyses of *Drosophila* β 4GalNAcTA and β 4GalNAcTB mutants demonstrated that β 4GalNAcTB was the most active enzyme in GSL biosynthesis but that both transferases were involved in lacdiNAc formation. In the *in vivo* characterization, no evidence could be obtained for the requirement of β 4GalNAcTB for a cofactor. The fact that Haines and Irvine could detect very low activity for β 4GalNAcTB (Haines and Irvine, 2005) was contradictory to the observation made by structural analyses of GSLs from the mutant flies (Stolz et al., 2007). Due to the complementation cloning strategy of Dr. Hans Bakker the multi-transmembrane protein GABPI required for activity of the B enzyme could be identified. The major role of β 4GalNAcTB in lacdiNAc formation compared to β 4GalNAcTA was reflected by the lower expression of lacdiNAc on the cell surface of β 4GalNAcTA transfected HEK293 cells than on cells expressing the B enzyme in presence of GABPI (see Figure 11). This was probably also the reason why the expression cloning strategy resulted in the cloning of β 4GalNAcTB and GABPI and not β 4GalNAcTA; Dr. Hans Bakker selected the clones resulting in most intensely stained cells. In more quantitative *in vitro* assays using Golgi preparation, GlcNAc-pNP as acceptor and UDP-[3 H]GalNAc as substrate, the approximate 4-fold higher activity of β 4GalNAcTB with GABPI in comparison to β 4GalNAcTA was confirmed (Figure 14). Moreover, it was shown that the activation effect of GABPI was only restricted to β 4GalNAcTB, because activity of β 4GalNAcTA did not increase in co-expression with GABPI (see Figure 14). If this lower activity is an intrinsic property of the enzymes of reflecting different expression level of the single enzymes was not further investigated.

4.2.1 Substrate specificity

Analysis of lacdiNAc containing glycoconjugates in GalNAc transferases expressing HEK293 cells confirmed the glycolipid specificity of these enzymes (see chapter 3.2.2). This findings corresponds with the observation that the lacdiNAc epitope in *Drosophila melanogaster* was exclusively found on glycolipids and not on glycoproteins (North et al., 2006). On the other hand, the fact that several insect species have lacdiNAc containing *N*-glycans (Kubelka et al., 1993; Park et al., 1999) and that enzymes, which are able to act on glycoproteins acceptors, have been identified (Vadaie and Jarvis, 2004; van Die et al., 1996) point towards the possibility that *Drosophila* also process lacdiNAc containing glycoproteins. Additionally, Sasaki et al. reported the activity of β 4GalNAcTA on *N*- and

O-glycans (Sasaki et al., 2007b), but, with critical respect to this publication, it remains unclear if β 4GalNAcTA is able to synthesize lacdiNAc on glycoproteins *in vivo*. The characterization of a *Drosophila* sialyltransferase that exhibits transferase activity on lacdiNAc at the nonreducing end of oligosaccharides and glycoproteins, but not on glycolipids (Koles et al., 2004), suggested the presence of β 4-linked GalNAc residues on glycoproteins. The very recent publication about sialylated *N*-glycan structures in *Drosophila*, however, reported the occurrence of sialic acid on lacNAc (Gal β 1,4GlcNAc) of *N*-glycans (Koles et al., 2007). It remains unclear, whether one of the GalNAcTs is also involved in the generation of the galactose serving as sialyltransferase acceptor. This question might be resolved by evaluating the presence of sialic acid in the GalNAcT mutant flies.

4.2.2 The activation of β 4GalNAcTB by GABPI

With an RNAi approach in *Drosophila* Schneider cells the dependency of β 4GalNAcTB on GABPI was confirmed *in vivo*. The depletion of this protein resulted in a sharp change in glycolipid pattern, comparable to the change in β 4GalNAcTB down regulated cells (see chapter 3.3) and demonstrated the direct influence of GABPI on the lacdiNAc containing glycolipid biosynthesis. During the establishment of the *in vitro* assay with ER and Golgi vesicles a detergent sensitivity for β 4GalNAcTB in presence of GABPI could be observed. Under usage of saponin, which is rather forming pores in the membrane than disrupting it (Schulz, 1990), a prominent activity was detectable, whereas in the presence of Triton X-100 the transfer ability of β 4GalNAcTB was completely abolished (see chapter 3.2.3, Figure 13). Because of this observation we suggest that the maintenance of membrane integrity is essential for activation of β 4GalNAcTB by GABPI and moreover that the physical contact of these proteins is needed for the transfer reaction.

Most glycosyltransferase can be produced as active soluble secreted enzymes if the transmembrane domain is replaced by a cleaved secretion signal (Haines and Irvine, 2005), but GABPI was not able to activate a soluble secreted form of β 4GalNAcTB neither in *Drosophila* S2 cells, nor in GABPI transfected HEK293 cells (data not shown). Furthermore it was shown in this study, that single expression of both proteins and subsequent fusion of the microsomes of these cells did not result in measurable enzymatic activity (see chapter 3.2.3, Figure 14). The formation of the complex between β 4GalNAcTB and GABPI seems to start co-translationally in the ER requesting

synchronous presence of the nascent proteins and anchoring of β 4GalNAcTB in the membrane.

Several glycosyltransferases acting in glycolipid biosynthetic pathways exhibit very low activity (de Vries et al., 1995; Togayachi et al., 2001) or no activity (Amado et al., 1998; Schwientek et al., 2002b; Steffensen et al., 2000) as truncated soluble recombinant proteins. One example is the *Drosophila* β 3GlcNAc transferase brainiac, which can not be expressed as an active soluble secreted protein (Schwientek et al., 2002b). Comparable to β 4GalNAcTB, the detergent solubilization of microsome fractions is also a critical parameter for brainiac activity. It seems that the anchorage of the enzymes in the membrane represents an important factor in glycolipid synthesis. Not much is known about the lipid recognition by glycosyltransferases and factors involved in this process. In analogy to lysosomal glycosphingolipid degradation, where the sphingolipid activator protein is required to present the glycolipid substrates to the glycosidases (Kolter and Sandhoff, 2005), it has been suggested that membrane bound activator proteins are required for presentation of glycolipid acceptors to modifying glycosyltransferases (Ramakrishnan et al., 2002). With respect to the glycosphingolipid biosynthesis pathway, GABPI seems to accomplish the role of a membrane bound activator protein for β 4GalNAcTB and discloses so far unknown aspects of the complex glycolipid biosynthetic machinery.

4.2.3 The possibility of multi-enzyme complexes

The physical interaction between β 4GalNAcTB and GABPI could be demonstrated by co-immunoprecipitation experiments (see chapter 3.2.4, Figure 15), supporting the specific relationship between GABPI and the glycosyltransferase. Homo- and heterodimerization are common themes in the organization of glycosylation events (van Meer, 2001). The association between the UDP-Galactose transporter and the UDP-Galactose:ceramide galactosyltransferase (Sprong et al., 2003) already describes the interaction between a multi-transmembrane protein and a glycosyltransferase and encourages the hypothesis about the function of GABPI as a part of a multi-enzyme complex in glycolipid biosynthesis. Other multi-enzyme complexes involved in heparan synthesis that assemble in the ER and exert their function in the Golgi apparatus (McCormick et al., 2000; Pinhal et al., 2001) have been described. For the ganglioside biosynthesis in the distal Golgi it has been shown that the sequentially acting UDP-GalNAc:lactosylceramide/GM3/GD3- β 4GalNAc transferase and the UDP-Gal: GA2/GM2/GD2- β 3Gal transferase were

associated (Giraud et al., 2001). Further experiments demonstrated the physical contact between transferases GalT1, SialT1 and SialT2 and suggested the organization of ganglioside synthesis in distinct units (Giraud and Maccioni, 2003b). Referring to these observations and the confirmed complex formation between β 4GalNAcTB and GABPI, these proteins may also form a multi-enzyme platform in GSL biosynthesis of *Drosophila melanogaster*. To verify and complete this hypothesis, further experiments were started in this study (data not shown). Therefore, egghead and brainiac were cloned from a *Drosophila* cDNA library. Both enzymes were clearly Golgi localized in HEK293 cells. Because Schwientek et al. reported that brainiac could not be expressed as an active soluble secreted protein (Schwientek et al., 2002b), we suggested that GABPI could also be involved in activation of brainiac. The influence of GABPI on brainiac activity was investigated, but no increase of activity was observed (single experiment, data not shown). Furthermore, the fact that the product of brainiac was still present in GABPI downregulated S2 cells, contradicts a function of GABPI for brainiac activation. Nevertheless, more glycosyltransferases could be associated with GABPI, without being dependent on it for activity.

β 4GalT-1, a mammalian homolog of the *Drosophila* GalNAc transferases, acting on terminal GlcNAc residues, forms a heterodimer with α -lactalbumin, thereby presenting the acceptor glucose to the enzyme to allow it to synthesize lactose (Ramakrishnan et al., 2001). The functional complex of β 4GalT-1 with α -lactalbumine has been crystallized and investigated in detail and exhibit an example of a co-factor protein:glycosyltransferase interaction (Ramakrishnan and Qasba, 2001). We suggest that the interaction with α -lactalbumine can reflect in part the physical contact between β 4GalNAcTB and GABPI. β 4GalNAcTB, however, is completely inactive without GABPI, and α -lactalbumine and GABPI are unrelated proteins, but seen from an evolutionary point of view, members of this gene family have a history of interacting with other proteins to perform specific reactions. As described in the introduction, other mammalian members of this family are reacting different with glycolipids and glycoproteins. Proteins like GABPI, might be responsible for this change in specificity.

4.3 Characteristics of GABPI

During this study it was possible to determine the topology of GABPI as protein with six TMDs. Politis et al. already described the transmembrane topology of Akrl, a yeast DHHC protein family member. In this study the insertion of a 46- or 511-residue-long invertase

segment was used, which includes three NX(S/T) sites for glycosylation (Politis et al., 2005). The glycosylation event was easily detected by Western blot analysis, but with respect to the glyco-modifications that are known to change physical properties of proteins and compete with folding in the ER (Holst et al., 1996; Ruddock and Molinari, 2006), this approach bears the high risk that topogenic organisation might have changed. Therefore, in this study, deletion constructs with N- and C-terminal tags and constructs with very short inserted or replaced HA-tags were generated and investigated by indirect immunofluorescence (see chapter 3.4.1 and 3.4.2). With this approach the influence on the protein was relatively small and the monitored functional activity of the protein reflected correct molecular organization.

The analysis of deletion constructs revealed that the first and the second TMD were not necessary for GABPI to activate β 4GalNAcTB. In the literature, DHHC proteins with four TMDs were already described. For example the proteins Erf2, SW1, Ydr459c, Ynl326c and Yol003c of *Saccharomyces cerevisiae* and the protein GODZ from *Rattus norvegicus* were predicted to contain only four TMDs (Politis et al., 2005), and this is the minimal number of TMDs found in all DHHC proteins. The fact that TMD 3-6 are essential for functionality of GABPI was not surprising, but raises the question which function TMD 1 and 2 possess. In Western blot analysis of full length GABPI, no evidence of posttranslational cleavage was found, but in analyses of different deletion constructs, distinct expression levels were detected (data not shown). Additionally, the first clone of GABPI, which was cloned *via* expression cloning by Dr. Hans Bakker, was already a deletion construct, missing the first TMD. Interestingly the deletion of the TMD 1 resulted in the highest expression level that could be observed in Western blot analysis. The expression level of GABPI might depend on the number of TMDs. Therefore, posttranscriptional cleavage could regulate the number of GABPI proteins and indirectly control the activity of β 4GalNAcTB.

4.3.1 The loop regions of GABPI

In the topology study of the DHHC protein member Akr1 from *Saccharomyces cerevisiae*, it was shown that insertion of glycosylation sites in regions mapped to cytoplasmic domains disrupted protein acyl transferase (PAT) activity (Politis et al., 2005), whereas the luminal insertion mutants were fully functional. It was suggested that the cytoplasmic domains play a more critical role in Akr1 function than the luminal domains. With respect to the palmitoylation transfer event, occurring at the cytoplasmic site, this observation

could be explained. In contrast, the insertion or the replacements of HA-tags in the luminal orientated loops of GABPI caused lost of functionality (see chapter 3.4.3 Fig. 18), whereas the insertion in the cytoplasmic DHHS loop region did not change the activation of β 4GalNAcTB. This result indicated that GABPI fulfills another function than palmitoylation (see chapter 3.4.1). The fact that GABPI carries a DHHS motif instead of a DHHC sequence in this highly conserved region, which is essential for PAT activity, verified this assumption. Even the complete mutation of this sequence into the aminoacids AAAA (see chapter 3.4.3 Table 6) did not influence the function of GABPI. By point mutation experiments of amino acids in the loop regions between the third, and fourth and the fifth, and sixth TMD, single residues were identified to be important for the activation process (see chapter 3.4.3 Table 6). In conclusion, the luminal orientated loops of GABPI are essential for activation of β 4GalNAcTB and the interaction between these proteins might occur inside the organelle and seems to depend on specific residues.

4.4 Role of GABPI in subcellular localization

The function of GABPI became clearer after the subcellular localization experiments of β 4GalNAcTA, β 4GalNAcTB and GABPI. β 4GalNAcTA and GABPI exhibited an expected Golgi localization. With the knowledge about the Golgi localization of egghead and brainiac, we anticipated that the acceptor structure for the β 4GalNAc transferases is present in the Golgi and apparently the glycosyltransferases should act there. Surprisingly, β 4GalNAcTB expressed as a single protein showed an explicit co-localization with Calnexin, a well known ER marker (see chapter 3.4.2 Figure 24), but in presence of GABPI switched localization to the Golgi apparatus (see chapter 3.4.2 Figure 25). The same was observed in *Drosophila* S2 cells. Under endogenous expression of GABPI, β 4GalNAcTB was located in the Golgi, but depletion of GABPI with dsRNA caused redistribution of this transferase to the ER (see chapter 3.4.2; Figure 26 and 27). Different signals that direct protein ER export and Golgi localization have been analyzed and described for different proteins. Specific signals in the cytoplasmic sequences or in the transmembrane domain of transmembrane proteins have been found to enhance or to be required for their ER export (Colley, 1997). Giraudo and Maccioni identified the sequence, rich in Arg and Lys residues, ([RK](X)[RK]), which is found in the cytoplasmic tail of different glycosyltransferases, as important for Golgi localization (Giraudo and Maccioni, 2003a). The sequence of the cytoplasmic tails of β 4GalNAcTA and β 4GalNAcTB contain both a potential ER export/Golgi localization signal. In β 4GalNAcTA the sequence is

MYLFTKANLIRF“ and in β 4GalNAcTB „MFVRLWVRSFHK“. Because β 4GalNAcTA was already targeted to the Golgi, the question remained whether the amino acids in the cytoplasmic tail of β 4GalNAcTB really act as an ER export signal. The hybrid construct of the N-terminal part of β 4GalNAcTB including the stem region and the catalytic domain of β 4GalNAcTA were directly located in the Golgi apparatus (see chapter 3.5, Table 9). This indicated the presence of a functional ER export signal in the tail of β 4GalNAcTB. Finally, Golgi localization of a fusion construct from the N-terminal part of β 4GalNAcTB and the catalytic domain of the non homologue core 3 fucosyltransferase from *Arabidopsis thaliana* confirmed this signal function (data not shown).

If β 4GalNAcTB has a functional Golgi localization signal, why does it remain in the ER?

In general, the maturation of secretory proteins starts in the ER. There, a special system exists to proof the folding state of a protein, which is also called “quality control” (Helenius, 2001). Ari Helenius wrote in his review: “As a rule, only proteins that have reached a native, folded and assembled structure are transported to their target organelles and compartments within the cell.” (Helenius, 2001). With respect to the quality control system of the ER, the localization of β 4GalNAcTB despite having a functional Golgi localization signal indicates that β 4GalNAcTB remains in the ER, because of uncompleted maturation. Correct folding is not accomplished by the resident protein folding machinery and chaperones. The necessity of client specific chaperones is already demonstrated by the description of Cosmc, a protein required for activity of the mammalian core 1 β 3-galactosyltransferase (Ju and Cummings, 2002). Cosmc (**c**ore 1 β 3Gal-T-**s**pecific **m**olecular **c**haperon) is essential for folding and transport to the destination in the Golgi of its single client the core 1 β 3GalT, which is involved in generation of the core 1 O-glycan (T-antigen). Another example is the O-fucosyltransferase1 (OFUT1), which promotes Notch receptor folding (Okajima et al., 2005). The depletion of OFUT1 leads to a accumulation of the Notch protein in the ER and inhibits transport to the cell surface (Okajima et al., 2005).

The importance of GABPI for the Golgi localization of β 4GalNAcTB suggests that this DHHC protein family member is also a client specific chaperone and might function in glycosyltransferase maturation. It is not known, if GABPI modifies or really folds the transferases in the ER, but without its help β 4GalNAcTB is not able to be targeted to the Golgi apparatus. Importantly, GABPI seems to move with β 4GalNAcTB to the Golgi, which is not the property of a classical chaperone. The function of GABPI, therefore,

seems to go beyond that of a client specific chaperone. Indicative for that are the facts that GABPI can immunoprecipitate β 4GalNAcTB and that the activity of β 4GalNAcTB not only depends on membrane integrity, but also on the presence of GABPI in the same organelle. The exact role of GABPI after reaching the Golgi, however, remains unclear and requires further investigations.

4.5 The stem region of β 4GalNAcTB

The hybrid construct between β 4GalNAcTA and β 4GalNAcTB demonstrated that the stem region of β 4GalNAcTB was essential for activation by GABPI (see chapter 3.5). If this defined region was exchanged with the stem of β 4GalNAcTA, the mutant was not active any more and remained in the ER. Additionally, it was demonstrated, that the distance between the membrane and the catalytic domain seemed to influence the protein-protein interaction, because it was not possible to elongate the stem region of β 4GalNAcTB and get a GABPI dependent, active, Golgi localized enzyme.

The stem region of glycosyltransferases seems to be involved in Golgi retention by function in protein-protein interaction to form hetero- or homodimers (Colley, 1997). For example, Sasai et al. 2001 found that the stem region of GnT-V was responsible for the Golgi localization, forming disulfide linkage-mediated oligomers, but was not associated with enzymatic activity (Sasai et al., 2001).

In a very recent study, a dataset of experimentally characterized human Golgi glycosyltransferases with type II membrane topology was created and these transferases were classified into five functional categories. In a comparison of structural and sequential motifs it appeared that the stem region of glycosyltransferases involved in the biosynthesis of glycolipids and blood group antigens have a shorter stem region compared to those glycosyltransferases, which participate in the biosynthesis of *N*- and *O*-linked glycans and glycosaminoglycans (Patel and Balaji, 2007). In coherence with the different lengths in the stem region of β 4GalNAcTA (long stem) and the β 4GalNAcTB (short stem) this supports the predict function of β 4GalNAcTA in glycoprotein biosynthesis (see also chapter 4.2.1). Although the stem region is, for most glycosyltransferases, not required for activity, it seems to be important for folding and stabilizing of glycosyltransferases (personal communication of Pradman Qasba). For example the stem region of sialyltransferases is required for the stable expression of an active enzyme (Masibay et al., 1993). In further *in vitro* studies on β 4GalTs it was clearly shown that the stem region enhances the folding efficiency of the catalytic domain of these enzymes (Boeggeman et al., 2003). Clearly, the

stem region is not the only domain important for GABPI interaction. β 4GalNAcTA remains independent of GABPI and Golgi localized if its catalytic domain was fused to the cytoplasmic, TMD, and stem of β 4GalNAcTB. Also the catalytic domain of β 4GalNAcTB must contain essential elements for this interaction.

4.7 Outlook

4.7.1 The three-dimensional structure of β 4GalNAcTA and β 4GalNAcTB

From the current experiments it can be concluded that the catalytic domain of β 4GalNAcTA and β 4GalNAcTB contains essential elements determining the dependency on GABPI. The primary amino acid sequence provides regions that are highly or less conserved, but a three dimensional structure model will help to identify possible interaction domains with GABPI.

Many glycosyltransferases are already crystallized and structures are resolved (for review see (Breton et al., 2006)). Glycosyltransferases from the β 4GalT family show a characteristic GT-A fold (Chiu et al., 2004; Hu et al., 2003; Pedersen et al., 2003). To gain more information about the GABPI dependency of β 4GalNAcTB in comparison to β 4GalNAcTA, the three-dimensional structure of these proteins were predicted.

The program PHYRE (**P**rotein **H**omology/**a**nalog**Y** **R**ecognition **E**ngine) was used to calculate the three-dimensional structure for the catalytic domain of β 4GalNAcTA and β 4GalNAcTB (Bennett-Lovsey et al., 2007; Kelley et al., 2000). The folds were predicted based on the known structure of the homologous bovine β 4GalT (Figure 30).

The three-dimensional structure alignment of β 4GalNAcTA and β 4GalNAcTB indicated that both enzymes are structural similar. In the N-terminal region of the catalytic domain the primary structure shows differences (see chapter 3.5) and this is reflected also in the 3D-structure prediction, where this part of the catalytic domain exposes a striking loop region (Figure 30, A). A closer look at the amino acids in this domain demonstrates that β 4GalNAcTA (Figure 30, B) exhibits more neutral amino acids, whereas β 4GalNAcTB carries amino acids with big, aromatic residues (Figure 30, C). Furthermore, this region interacts with the extreme C-terminus of the glycosyltransferases. The three-dimensional structure prediction is going to form a platform for further analyses of the interaction

between β 4GalNAcTB and GABPI and will be used to design further hybrid enzymes and mutants to identify the elements in β 4GalNAcTB that determine GABPI dependency.

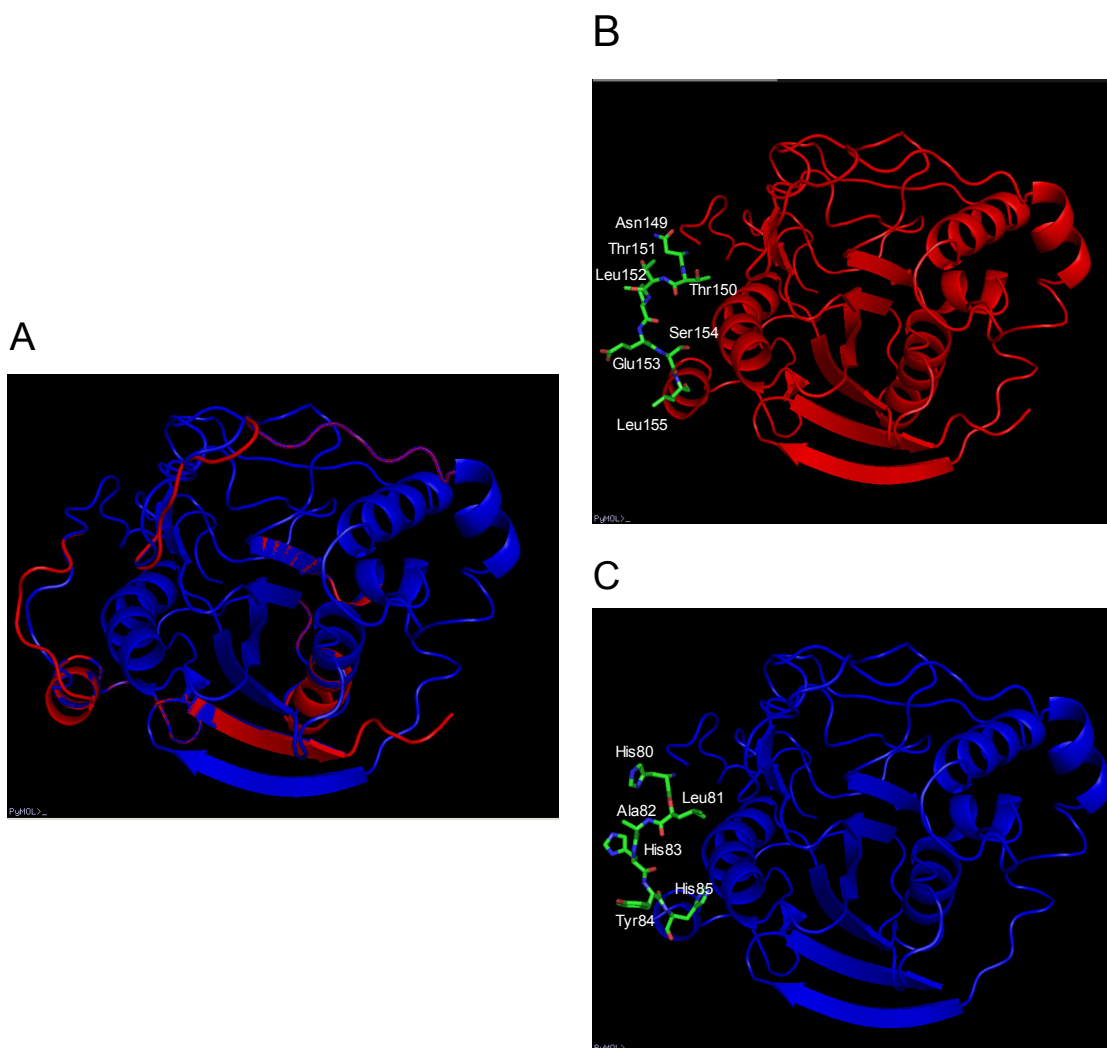


Figure 30: Prediction of the three-dimensional structure of β 4GalNAcTA and β 4GalNAcTB. (A) The 3D- structures of β 4GalNAcTA and β 4GalNAcTB were generated by the program phyre (<http://www.sbg.bio.ic.ac.uk/3dpssm>) and visualized with pyMOL (<http://pymol.sourceforge.net>). The β 4GalNAcTA is shown in red and the β 4GalNAcTB in blue. (B) 3D-structure of β 4GalNAcTA with exposed single amino acids of the N-terminal region. (C) 3D-structure of β 4GalNAcTB with exposed single amino acids of the N-terminal region.

4.7.2 The function of GABPI- a working hypothesis

Several experiments have shown that GABPI is required in several steps in the maturation and activity of β 4GalNAcTB. These processes are summarized in the current working model shown in Figure 31. GABPI is required for correct folding of β 4GalNAcTB in the ER, remains associated with the enzyme and forms the active complex of the enzyme in the Golgi, possibly required to present the glycolipid acceptor structure to the enzyme and to keep the enzyme in an active state.

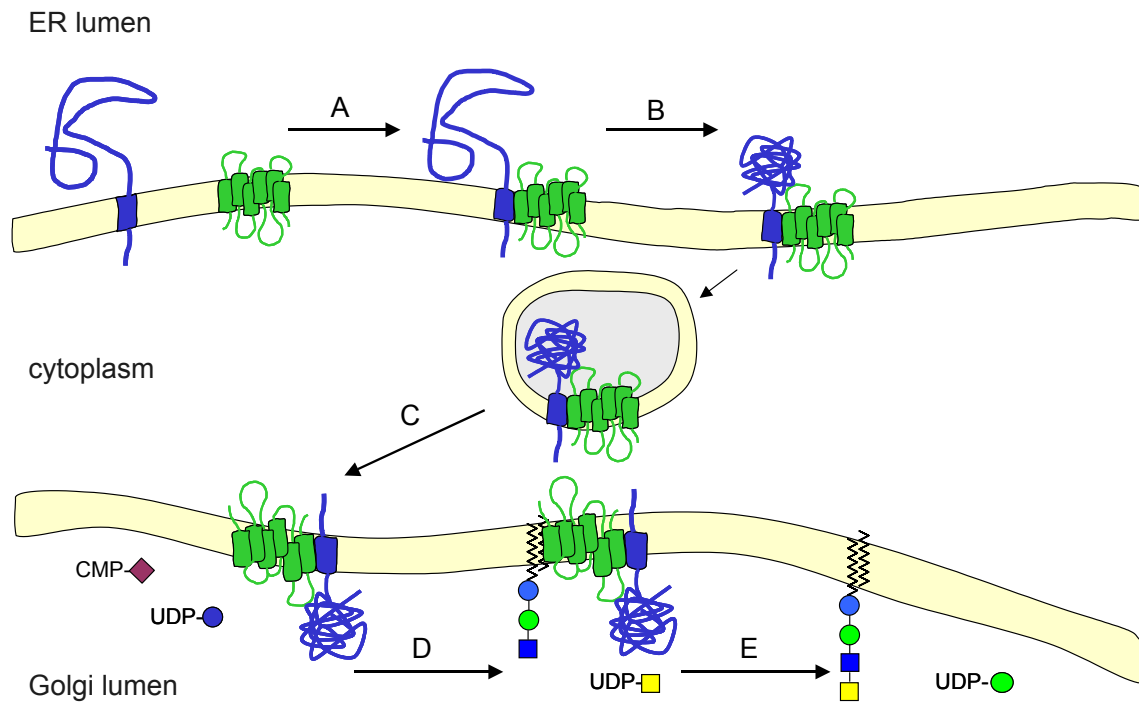


Figure 31: Scheme of interaction of GABPI with β 4GalNAcTB. Illustration of interaction and function of GABPI in lacdiNAc biosynthesis. (A) β 4GalNAcTB and GABPI interact in the ER (B) GABPI causes maturation of β 4GalNAcTB (C) and transport to the Golgi. (D) The active complex of GABPI and β 4GalNAcTB reaches the lipid acceptor (E) GABPI presents the trisaccharide acceptor to β 4GalNAcTB, which is able to synthesis the lacdiNAc epitope.

This type of interactions can display a general model for especially enzymes involved in glycolipid biosynthesis. Exactly the same enzyme as β 4GalNAcTB is not present in mammals, but a direct homologue of the *Drosophila* DHHC protein member exists. This protein was already investigated, but no palmitoylation activity on specific acceptor proteins could be observed (Dietrich and Ungermann, 2004; Mitchell et al., 2006). It remains possible that this DHHC protein member influences glycosyltransferases, in particular one of the six homologs of β 4GalNAcTA and TB, in mammals. With respect to congenital disorders of glycosylation (CDGs), diseases caused by genetic defects in

glycosyltransferases, or by mutations of their essential co-factor Cosmc (Schietinger et al., 2006; Ju and Cummings, 2002; Ju and Cummings, 2005) have been described. Furthermore, there are several CDGs caused by disordered glycosyltransferases, but no direct mutation could be demonstrated (Freeze, 2006; Kanagawa et al., 2004; Nguyen et al., 2002). The identification of co-factors in glycosylation like GABPI can therefore uncover so far unknown aspects, leading to a better understanding of the complex glycosylation machinery.

5 References

- (1999). IUPAC-IUB joint commission on biochemical nomenclature (JCBN) nomenclature of glycolipids recommendations 1997. *J. Mol. Biol.* *286*, 963-970.
- Abeijon, C. and Hirschberg, C.B. (1992). Topography of glycosylation reactions in the endoplasmic reticulum. *Trends Biochem. Sci.* *17*, 32-36.
- Almeida, R., Levery, S.B., Mandel, U., Kresse, H., Schwientek, T., Bennett, E.P., and Clausen, H. (1999). Cloning and expression of a proteoglycan UDP-galactose:beta-xylose beta1,4-galactosyltransferase I. A seventh member of the human beta4-galactosyltransferase gene family. *J. Biol. Chem.* *274*, 26165-26171.
- Amado, M., Almeida, R., Carneiro, F., Levery, S.B., Holmes, E.H., Nomoto, M., Hollingsworth, M.A., Hassan, H., Schwientek, T., Nielsen, P.A., Bennett, E.P., and Clausen, H. (1998). A family of human beta3-galactosyltransferases. Characterization of four members of a UDP-galactose:beta-N-acetylglucosamine/beta-N-acetyl-galactosamine beta-1,3-galactosyltransferase family. *J. Biol. Chem.* *273*, 12770-12778.
- Amado, M., Almeida, R., Schwientek, T., and Clausen, H. (1999). Identification and characterization of large galactosyltransferase gene families: galactosyltransferases for all functions. *Biochim. Biophys. Acta* *1473*, 35-53.
- Amara, J.F., Cheng, S.H., and Smith, A.E. (1992). Intracellular protein trafficking defects in human disease. *Trends Cell Biol.* *2*, 145-149.
- Antonny, B., Bigay, J., Casella, J.F., Drin, G., Mesmin, B., and Gounon, P. (2005). Membrane curvature and the control of GTP hydrolysis in Arf1 during COPI vesicle formation. *Biochem. Soc. Trans.* *33*, 619-622.
- Appenzeller-Herzog, C. and Hauri, H.P. (2006). The ER-Golgi intermediate compartment (ERGIC): in search of its identity and function. *J. Cell Sci.* *119*, 2173-2183.
- Argon, Y. and Simen, B.B. (1999). GRP94, an ER chaperone with protein and peptide binding properties. *Semin. Cell Dev. Biol.* *10*, 495-505.
- Aridor, M. and Balch, W.E. (1999). Integration of endoplasmic reticulum signaling in health and disease. *Nat. Med.* *5*, 745-751.
- Bakker, H., Agterberg, M., van Tetering, A., Koeleman, C.A., van den Eijnden, D.H., and van, D., I (1994). A *Lymnaea stagnalis* gene, with sequence similarity to that of mammalian beta 1-->4-galactosyltransferases, encodes a novel UDP-GlcNAc:GlcNAc beta-R beta 1-->4-N-acetylglucosaminyltransferase. *J. Biol. Chem.* *269*, 30326-30333.
- Bakker, H., Friedmann, I., Oka, S., Kawasaki, T., Nifant'ev, N., Schachner, M., and Mantei, N. (1997). Expression cloning of a cDNA encoding a sulfotransferase involved in the biosynthesis of the HNK-1 carbohydrate epitope. *J. Biol. Chem.* *272*, 29942-29946.
- Barlowe, C. (2003). Signals for COPII-dependent export from the ER: what's the ticket out? *Trends Cell Biol.* *13*, 295-300.
- Bennett-Lovsey, R.M., Herbert, A.D., Sternberg, M.J., and Kelley, L.A. (2007). Exploring the extremes of sequence/structure space with ensemble fold recognition in the program Phyre. *Proteins*.
- Boeggeman, E.E., Balaji, P.V., Sethi, N., Masibay, A.S., and Qasba, P.K. (1993). Expression of deletion constructs of bovine beta-1,4-galactosyltransferase in *Escherichia coli*: importance of Cys134 for its activity. *Protein Eng* *6*, 779-785.

- Boeggeman, E.E., Ramakrishnan, B., and Qasba, P.K. (2003). The N-terminal stem region of bovine and human beta1,4-galactosyltransferase I increases the in vitro folding efficiency of their catalytic domain from inclusion bodies. *Protein Expr. Purif.* *30*, 219-229.
- Bonifacino, J.S. and Glick, B.S. (2004). The mechanisms of vesicle budding and fusion. *Cell* *116*, 153-166.
- Breton, C., Snajdrova, L., Jeanneau, C., Koca, J., and Imberty, A. (2006). Structures and mechanisms of glycosyltransferases. *Glycobiology* *16*, 29R-37R.
- Brew, K., Vanaman, T.C., and Hill, R.L. (1968). The role of alpha-lactalbumin and the A protein in lactose synthetase: a unique mechanism for the control of a biological reaction. *Proc. Natl. Acad. Sci. U. S. A* *59*, 491-497.
- Campbell, J.A., Davies, G.J., Bulone, V., and Henrissat, B. (1997). A classification of nucleotide-diphospho-sugar glycosyltransferases based on amino acid sequence similarities. *Biochem. J.* *326 (Pt 3)*, 929-939.
- Caplen, N.J., Fleenor, J., Fire, A., and Morgan, R.A. (2000). dsRNA-mediated gene silencing in cultured *Drosophila* cells: a tissue culture model for the analysis of RNA interference. *Gene* *252*, 95-105.
- Chen, Y.W., Pedersen, J.W., Wandall, H.H., Levery, S.B., Pizette, S., Clausen, H., and Cohen, S.M. (2007). Glycosphingolipids with extended sugar chain have specialized functions in development and behavior of *Drosophila*. *Dev. Biol.* *306*, 736-749.
- Chiu, C.P., Watts, A.G., Lairson, L.L., Gilbert, M., Lim, D., Wakarchuk, W.W., Withers, S.G., and Strynadka, N.C. (2004). Structural analysis of the sialyltransferase CstII from *Campylobacter jejuni* in complex with a substrate analog. *Nat. Struct. Mol. Biol.* *11*, 163-170.
- Claros, M.G. and von Heijne, G. (1994). TopPred II: an improved software for membrane protein structure predictions. *Comput. Appl. Biosci.* *10*, 685-686.
- Colley, K.J. (1997). Golgi localization of glycosyltransferases: more questions than answers. *Glycobiology* *7*, 1-13.
- Coutinho, P.M., Deleury, E., Davies, G.J., and Henrissat, B. (2003). An evolving hierarchical family classification for glycosyltransferases. *J. Mol. Biol.* *328*, 307-317.
- de Vries, T., Srnka, C.A., Palcic, M.M., Swiedler, S.J., van den Eijnden, D.H., and Macher, B.A. (1995). Acceptor specificity of different length constructs of human recombinant alpha 1,3/4-fucosyltransferases. Replacement of the stem region and the transmembrane domain of fucosyltransferase V by protein A results in an enzyme with GDP-fucose hydrolyzing activity. *J. Biol. Chem.* *270*, 8712-8722.
- Dietrich, L.E. and Ungermann, C. (2004). On the mechanism of protein palmitoylation. *EMBO Rep.* *5*, 1053-1057.
- Easton, D.P., Kaneko, Y., and Subject, J.R. (2000). The hsp110 and Grp1 70 stress proteins: newly recognized relatives of the Hsp70s. *Cell Stress. Chaperones.* *5*, 276-290.
- Eckhardt, M., Muhlenhoff, M., Bethe, A., and Gerardy-Schahn, R. (1996). Expression cloning of the Golgi CMP-sialic acid transporter. *Proc. Natl. Acad. Sci. U. S. A* *93*, 7572-7576.
- Eckhardt, M., Muhlenhoff, M., Bethe, A., Koopman, J., Frosch, M., and Gerardy-Schahn, R. (1995). Molecular characterization of eukaryotic polysialyltransferase-I. *Nature* *373*, 715-718.
- Ellgaard, L. and Helenius, A. (2003). Quality control in the endoplasmic reticulum. *Nat. Rev. Mol. Cell Biol.* *4*, 181-191.
- Fenteany, F.H. and Colley, K.J. (2005). Multiple signals are required for alpha2,6-sialyltransferase (ST6Gal I) oligomerization and Golgi localization. *J. Biol. Chem.* *280*, 5423-5429.

- Fernandez-Hernando, C., Fukata, M., Bernatchez, P.N., Fukata, Y., Lin, M.I., Brecht, D.S., and Sessa, W.C. (2006). Identification of Golgi-localized acyl transferases that palmitoylate and regulate endothelial nitric oxide synthase. *J. Cell Biol.* *174*, 369-377.
- FOLCH, J., LEES, M., and SLOANE STANLEY, G.H. (1957). A simple method for the isolation and purification of total lipides from animal tissues. *J. Biol. Chem.* *226*, 497-509.
- Folch, J., Lees, M., and Sloane-Stanley, G.H. (1957). A simple method for the isolation and purification of total lipides from animal tissues. *J. Biol. Chem.* *226*, 497-509.
- Freeze, H.H. (2006). Genetic defects in the human glycome. *Nat. Rev. Genet.* *7*, 537-551.
- Fukata, M., Fukata, Y., Adesnik, H., Nicoll, R.A., and Brecht, D.S. (2004). Identification of PSD-95 palmitoylating enzymes. *Neuron* *44*, 987-996.
- Fukata, Y., Iwanaga, T., and Fukata, M. (2006). Systematic screening for palmitoyl transferase activity of the DHHC protein family in mammalian cells. *Methods* *40*, 177-182.
- Furukawa, K. and Sato, T. (1999). Beta-1,4-galactosylation of N-glycans is a complex process. *Biochim. Biophys. Acta* *1473*, 54-66.
- Gastinel, L.N., Cambillau, C., and Bourne, Y. (1999). Crystal structures of the bovine beta4galactosyltransferase catalytic domain and its complex with uridine diphosphogalactose. *EMBO J.* *18*, 3546-3557.
- Giraud, C.G., Daniotti, J.L., and Maccioni, H.J. (2001). Physical and functional association of glycolipid N-acetyl-galactosaminyl and galactosyl transferases in the Golgi apparatus. *Proc. Natl. Acad. Sci. U. S. A.* *98*, 1625-1630.
- Giraud, C.G. and Maccioni, H.J. (2003a). Endoplasmic reticulum export of glycosyltransferases depends on interaction of a cytoplasmic dibasic motif with Sar1. *Mol. Biol. Cell* *14*, 3753-3766.
- Giraud, C.G. and Maccioni, H.J. (2003b). Ganglioside glycosyltransferases organize in distinct multienzyme complexes in CHO-K1 cells. *J. Biol. Chem.* *278*, 40262-40271.
- Goldenthal, K.L., Hedman, K., Chen, J.W., August, J.T., and Willingham, M.C. (1985). Postfixation detergent treatment for immunofluorescence suppresses localization of some integral membrane proteins. *J. Histochem. Cytochem.* *33*, 813-820.
- Goode, S., Melnick, M., Chou, T.B., and Perrimon, N. (1996). The neurogenic genes egghead and brainiac define a novel signaling pathway essential for epithelial morphogenesis during *Drosophila* oogenesis. *Development* *122*, 3863-3879.
- Goode, S., Wright, D., and Mahowald, A.P. (1992). The neurogenic locus brainiac cooperates with the *Drosophila* EGF receptor to establish the ovarian follicle and to determine its dorsal-ventral polarity. *Development* *116*, 177-192.
- Griffitts, J.S., Haslam, S.M., Yang, T., Garczynski, S.F., Mulloy, B., Morris, H., Cremer, P.S., Dell, A., Adang, M.J., and Aroian, R.V. (2005). Glycolipids as receptors for *Bacillus thuringiensis* crystal toxin. *Science* *307*, 922-925.
- Haas, I.G. and Wabl, M. (1983). Immunoglobulin heavy chain binding protein. *Nature* *306*, 387-389.
- Haines, N. and Irvine, K.D. (2005). Functional analysis of *Drosophila* β 1,4-N-acetylgalactosaminyltransferases. *Glycobiology* *15*, 335-346.
- Haines, N. and Stewart, B.A. (2007). Functional roles for beta1,4-N-acetylgalactosaminyltransferase-A in *Drosophila* larval neurons and muscles. *Genetics* *175*, 671-679.
- Helenius, A. (2001). Quality control in the secretory assembly line. *Philos. Trans. R. Soc. Lond B Biol. Sci.* *356*, 147-150.

- Hirschberg, C.B. and Snider, M.D. (1987). Topography of glycosylation in the rough endoplasmic reticulum and Golgi apparatus. *Annu. Rev. Biochem.* *56*, 63-87.
- Holst, B., Bruun, A.W., Kielland-Brandt, M.C., and Winther, J.R. (1996). Competition between folding and glycosylation in the endoplasmic reticulum. *EMBO J.* *15*, 3538-3546.
- Holthuis, J.C., Pomorski, T., Raggars, R.J., Sprong, H., and van Meer, G. (2001). The organizing potential of sphingolipids in intracellular membrane transport. *Physiol Rev.* *81*, 1689-1723.
- Hu, Y., Chen, L., Ha, S., Gross, B., Falcone, B., Walker, D., Mokhtarzadeh, M., and Walker, S. (2003). Crystal structure of the MurG:UDP-GlcNAc complex reveals common structural principles of a superfamily of glycosyltransferases. *Proc. Natl. Acad. Sci. U. S. A* *100*, 845-849.
- Huang, K. and El Husseini, A. (2005). Modulation of neuronal protein trafficking and function by palmitoylation. *Curr. Opin. Neurobiol.* *15*, 527-535.
- Ju, T. and Cummings, R.D. (2002). A unique molecular chaperone Cosmc required for activity of the mammalian core 1 β 3-galactosyltransferase. *Proc. Natl. Acad. Sci. U. S. A* *99*, 16613-16618.
- Ju, T. and Cummings, R.D. (2005). Protein glycosylation: chaperone mutation in Tn syndrome. *Nature* *437*, 1252.
- Jungmann, J. and Munro, S. (1998). Multi-protein complexes in the cis Golgi of *Saccharomyces cerevisiae* with alpha-1,6-mannosyltransferase activity. *EMBO J.* *17*, 423-434.
- Kanagawa, M., Saito, F., Kunz, S., Yoshida-Moriguchi, T., Barresi, R., Kobayashi, Y.M., Muschler, J., Dumanski, J.P., Michele, D.E., Oldstone, M.B., and Campbell, K.P. (2004). Molecular recognition by LARGE is essential for expression of functional dystroglycan. *Cell* *117*, 953-964.
- Kapitonov, D. and Yu, R.K. (1999). Conserved domains of glycosyltransferases. *Glycobiology* *9*, 961-978.
- Katz, J. and Wals, P.A. (1985). Studies with digitonin-treated rat hepatocytes (nude cells). *J. Cell Biochem.* *28*, 207-228.
- Kawar, Z.S., van Die, I., and Cummings, R.D. (2002). Molecular cloning and enzymatic characterization of a UDP-GalNAc:GlcNAc(β)-R β 1,4-N-acetylgalactosaminyltransferase from *Caenorhabditis elegans*. *J. Biol. Chem* *277*, 34924-34932.
- Kelleher, D.J. and Gilmore, R. (2006). An evolving view of the eukaryotic oligosaccharyltransferase. *Glycobiology* *16*, 47R-62R.
- Kelley, L.A., MacCallum, R.M., and Sternberg, M.J. (2000). Enhanced genome annotation using structural profiles in the program 3D-PSSM. *J. Mol. Biol.* *299*, 499-520.
- Koles, K., Irvine, K.D., and Panin, V.M. (2004). Functional characterization of *Drosophila* sialyltransferase. *J. Biol. Chem.* *279*, 4346-4357.
- Koles, K., Lim, J.M., Aoki, K., Porterfield, M., Tiemeyer, M., Wells, L., and Panin, V. (2007). Identification of N-glycosylated proteins from the central nervous system of *Drosophila melanogaster*. *Glycobiology* *17*, 1388-1403.
- Kolter, T. and Sandhoff, K. (2005). Principles of lysosomal membrane digestion: stimulation of sphingolipid degradation by sphingolipid activator proteins and anionic lysosomal lipids. *Annu. Rev. Cell Dev. Biol.* *21*, 81-103.
- Kondylis, V., Sporendonk, K.M., and Rabouille, C. (2005). dGRASP localization and function in the early exocytic pathway in *Drosophila* S2 cells. *Mol. Biol. Cell* *16*, 4061-4072.
- Kubelka, V., Altmann, F., Staudacher, E., Tretter, V., Marz, L., Hard, K., Kamerling, J.P., and Vliegenthart, J.F. (1993). Primary structures of the N-linked carbohydrate chains from honeybee venom phospholipase A2. *Eur. J. Biochem.* *213*, 1193-1204.

- Laemmli, U.K. (1970). Cleavage of structural proteins during the assembly of the head of bacteriophage T4. *Nature* 227, 680-685.
- Lam, K.K., Davey, M., Sun, B., Roth, A.F., Davis, N.G., and Conibear, E. (2006). Palmitoylation by the DHHC protein Pfa4 regulates the ER exit of Chs3. *J. Cell Biol.* 174, 19-25.
- Linder, M.E. and Deschenes, R.J. (2004). Model organisms lead the way to protein palmitoyltransferases. *J. Cell Sci.* 117, 521-526.
- Linder, M.E. and Deschenes, R.J. (2007). Palmitoylation: policing protein stability and traffic. *Nat. Rev. Mol. Cell Biol.* 8, 74-84.
- Lobo, S., Greentree, W.K., Linder, M.E., and Deschenes, R.J. (2002b). Identification of a Ras palmitoyltransferase in *Saccharomyces cerevisiae*. *J. Biol. Chem.* 277, 41268-41273.
- Lobo, S., Greentree, W.K., Linder, M.E., and Deschenes, R.J. (2002a). Identification of a Ras palmitoyltransferase in *Saccharomyces cerevisiae*. *J. Biol. Chem.* 277, 41268-41273.
- Lochnit G., Geyer R., Heinz E., Rietschel E.T., Zähringer U., and Müthing J. (2001). *Glycoscience-Chemistry and Chemical Biology* (Eds.), Fraser-Reid B., Tatsuts K., and Thiun J., eds. (Berlin: Springer Verlag), pp. 2183-2249.
- Masibay, A.S., Balaji, P.V., Boeggeman, E.E., and Qasba, P.K. (1993). Mutational analysis of the Golgi retention signal of bovine beta-1,4-galactosyltransferase. *J. Biol. Chem.* 268, 9908-9916.
- McCormick, C., Duncan, G., Goutsos, K.T., and Tufaro, F. (2000). The putative tumor suppressors EXT1 and EXT2 form a stable complex that accumulates in the Golgi apparatus and catalyzes the synthesis of heparan sulfate. *Proc. Natl. Acad. Sci. U. S. A.* 97, 668-673.
- Mitchell, D.A., Vasudevan, A., Linder, M.E., and Deschenes, R.J. (2006). Protein palmitoylation by a family of DHHC protein S-acyltransferases. *J. Lipid Res.* 47, 1118-1127.
- Müller, R., Altmann, F., Zhou, D., and Hennet, T. (2002). The *Drosophila melanogaster* brainiac protein is a glycolipid-specific beta 1,3N-acetylglucosaminyltransferase. *J. Biol. Chem.* 277, 32417-32420.
- Munro, S. (1995a). A comparison of the transmembrane domains of Golgi and plasma membrane proteins. *Biochem. Soc. Trans.* 23, 527-530.
- Munro, S. (1995b). An investigation of the role of transmembrane domains in Golgi protein retention. *EMBO J.* 14, 4695-4704.
- Munster, A.K., Eckhardt, M., Potvin, B., Muhlenhoff, M., Stanley, P., and Gerardy-Schahn, R. (1998). Mammalian cytidine 5'-monophosphate N-acetylneuraminic acid synthetase: a nuclear protein with evolutionarily conserved structural motifs. *Proc. Natl. Acad. Sci. U. S. A.* 95, 9140-9145.
- Nadolski, M.J. and Linder, M.E. (2007). Protein lipidation. *FEBS J.* 274, 5202-5210.
- Nakamura, Y., Haines, N., Chen, J., Okajima, T., Furukawa, K., Urano, T., Stanley, P., Irvine, K.D., and Furukawa, K. (2002). Identification of a *Drosophila* gene encoding xylosylprotein beta4-galactosyltransferase that is essential for the synthesis of glycosaminoglycans and for morphogenesis. *J. Biol. Chem.* 277, 46280-46288.
- Nguyen, H.H., Jayasinha, V., Xia, B., Hoyte, K., and Martin, P.T. (2002). Overexpression of the cytotoxic T cell GalNAc transferase in skeletal muscle inhibits muscular dystrophy in mdx mice. *Proc. Natl. Acad. Sci. U. S. A.* 99, 5616-5621.
- Ni, M. and Lee, A.S. (2007). ER chaperones in mammalian development and human diseases. *FEBS Lett.* 581, 3641-3651.
- Nilsson, T., Lucocq, J.M., Mackay, D., and Warren, G. (1991). The membrane spanning domain of beta-1,4-galactosyltransferase specifies trans Golgi localization. *EMBO J.* 10, 3567-3575.

- North,S.J., Koles,K., Hembd,C., Morris,H.R., Dell,A., Panin,V.M., and Haslam,S.M. (2006). Glycomic studies of *Drosophila melanogaster* embryos. *Glycoconj. J.* *23*, 345-354.
- Ohno,Y., Kihara,A., Sano,T., and Igarashi,Y. (2006). Intracellular localization and tissue-specific distribution of human and yeast DHHC cysteine-rich domain-containing proteins. *Biochim. Biophys. Acta* *1761*, 474-483.
- Okajima,T., Xu,A., Lei,L., and Irvine,K.D. (2005). Chaperone activity of protein O-fucosyltransferase 1 promotes notch receptor folding. *Science* *307*, 1599-1603.
- Opat,A.S., van Vliet,C., and Gleeson,P.A. (2001). Trafficking and localisation of resident Golgi glycosylation enzymes. *Biochimie* *83*, 763-773.
- Palcic,M.M., Heerze,L.D., Pierce,M., and Hindsgaul,O. (1988). The Use of Hydrophobic Synthetic Glycosides As Acceptors in Glycosyltransferase Assays. *Glycoconjugate Journal* *5*, 49-63.
- Park,Y.I., Wood,H.A., and Lee,Y.C. (1999). Monosaccharide compositions of *Danaus plexippus* (monarch butterfly) and *Trichoplusia ni* (cabbage looper) egg glycoproteins. *Glycoconj. J.* *16*, 629-638.
- Patel,R.Y. and Balaji,P.V. (2007). Length and composition analysis of the cytoplasmic, transmembrane and stem regions of human Golgi glycosyltransferases. *Protein Pept. Lett.* *14*, 601-609.
- Paulson,J.C. and Colley,K.J. (1989). Glycosyltransferases. Structure, localization, and control of cell type-specific glycosylation. *J. Biol. Chem.* *264*, 17615-17618.
- Pedersen,L.C., Dong,J., Taniguchi,F., Kitagawa,H., Krahn,J.M., Pedersen,L.G., Sugahara,K., and Negishi,M. (2003). Crystal structure of an alpha 1,4-N-acetylhexosaminyltransferase (EXTL2), a member of the exostosin gene family involved in heparan sulfate biosynthesis. *J. Biol. Chem.* *278*, 14420-14428.
- Pinhal,M.A., Smith,B., Olson,S., Aikawa,J., Kimata,K., and Esko,J.D. (2001). Enzyme interactions in heparan sulfate biosynthesis: uronosyl 5-epimerase and 2-O-sulfotransferase interact in vivo. *Proc. Natl. Acad. Sci. U. S. A* *98*, 12984-12989.
- Politis,E.G., Roth,A.F., and Davis,N.G. (2005). Transmembrane topology of the protein palmitoyl transferase Akr1. *J. Biol. Chem.* *280*, 10156-10163.
- Putilina,T., Wong,P., and Gentleman,S. (1999). The DHHC domain: a new highly conserved cysteine-rich motif. *Mol. Cell Biochem.* *195*, 219-226.
- Qiu,X.B., Shao,Y.M., Miao,S., and Wang,L. (2006). The diversity of the DnaJ/Hsp40 family, the crucial partners for Hsp70 chaperones. *Cell Mol. Life Sci.* *63*, 2560-2570.
- Ramakrishnan,B., Boeggeman,E., and Qasba,P.K. (2002). Beta-1,4-galactosyltransferase and lactose synthase: molecular mechanical devices. *Biochem. Biophys. Res. Commun.* *291*, 1113-1118.
- Ramakrishnan,B. and Qasba,P.K. (2001). Crystal structure of lactose synthase reveals a large conformational change in its catalytic component, the beta1,4-galactosyltransferase-I. *J. Mol. Biol.* *310*, 205-218.
- Ramakrishnan,B., Shah,P.S., and Qasba,P.K. (2001). alpha-Lactalbumin (LA) stimulates milk beta-1,4-galactosyltransferase I (beta 4Gal-T1) to transfer glucose from UDP-glucose to N-acetylglucosamine. Crystal structure of beta 4Gal-T1 x LA complex with UDP-Glc. *J. Biol. Chem.* *276*, 37665-37671.
- Roth,A.F., Feng,Y., Chen,L., and Davis,N.G. (2002a). The yeast DHHC cysteine-rich domain protein Akr1p is a palmitoyl transferase. *J. Cell Biol.* *159*, 23-28.
- Roth,A.F., Feng,Y., Chen,L., and Davis,N.G. (2002b). The yeast DHHC cysteine-rich domain protein Akr1p is a palmitoyl transferase. *J. Cell Biol.* *159*, 23-28.
- Ruddock,L.W. and Molinari,M. (2006). N-glycan processing in ER quality control. *J. Cell Sci.* *119*, 4373-4380.
- Rutishauser,J. and Spiess,M. (2002). Endoplasmic reticulum storage diseases. *Swiss. Med. Wkly.* *132*, 211-222.

- Sasai,K., Ikeda,Y., Tsuda,T., Ihara,H., Korekane,H., Shiota,K., and Taniguchi,N. (2001). The critical role of the stem region as a functional domain responsible for the oligomerization and Golgi localization of N-acetylglucosaminyltransferase V. The involvement of a domain homophilic interaction. *J. Biol. Chem.* *276*, 759-765.
- Sasaki,N., Yoshida,H., Fuwa,T.J., Kinoshita-Toyoda,A., Toyoda,H., Hirabayashi,Y., Ishida,H., Ueda,R., and Nishihara,S. (2007a). Drosophila beta 1,4-N-acetylgalactosaminyltransferase-A synthesizes the LacdiNAc structures on several glycoproteins and glycosphingolipids. *Biochem. Biophys. Res. Commun.* *354*, 522-527.
- Sasaki,N., Yoshida,H., Fuwa,T.J., Kinoshita-Toyoda,A., Toyoda,H., Hirabayashi,Y., Ishida,H., Ueda,R., and Nishihara,S. (2007b). Drosophila beta 1,4-N-acetylgalactosaminyltransferase-A synthesizes the LacdiNAc structures on several glycoproteins and glycosphingolipids. *Biochem. Biophys. Res. Commun.* *354*, 522-527.
- Sato,K. and Nakano,A. (2007). Mechanisms of COPII vesicle formation and protein sorting. *FEBS Lett.* *581*, 2076-2082.
- Sato,T., Furukawa,K., Bakker,H., van den Eijnden,D.H., and van,D., I (1998). Molecular cloning of a human cDNA encoding beta-1,4-galactosyltransferase with 37% identity to mammalian UDP-Gal:GlcNAc beta-1,4-galactosyltransferase. *Proc. Natl. Acad. Sci. U. S. A* *95*, 472-477.
- Sato,T., Guo,S., and Furukawa,K. (2000). Involvement of recombinant human β 1, 4-galactosyltransferase V in lactosylceramide biosynthesis. *Res. Commun. Biochem. Cell Molec. Biol.* *4*, 3-10.
- Schietinger,A., Philip,M., Yoshida,B.A., Azadi,P., Liu,H., Meredith,S.C., and Schreiber,H. (2006). A mutant chaperone converts a wild-type protein into a tumor-specific antigen. *Science* *314*, 304-308.
- Schulz,I. (1990). Permeabilizing cells: some methods and applications for the study of intracellular processes. *Methods Enzymol.* *192*, 280-300.
- Schwientek,T., Almeida,R., Lavery,S.B., Holmes,E.H., Bennett,E., and Clausen,H. (1998). Cloning of a novel member of the UDP-galactose:beta-N-acetylglucosamine beta 1,4-galactosyltransferase family, beta4Gal-T4, involved in glycosphingolipid biosynthesis. *J. Biol. Chem* *273*, 29331-29340.
- Schwientek,T., Keck,B., Lavery,S.B., Jensen,M.A., Pedersen,J.W., Wandall,H.H., Stroud,M., Cohen,S.M., Amado,M., and Clausen,H. (2002a). The Drosophila gene brainiac encodes a glycosyltransferase putatively involved in glycosphingolipid synthesis. *J. Biol. Chem.* *277*, 32421-32429.
- Schwientek,T., Keck,B., Lavery,S.B., Jensen,M.A., Pedersen,J.W., Wandall,H.H., Stroud,M., Cohen,S.M., Amado,M., and Clausen,H. (2002b). The Drosophila gene brainiac encodes a glycosyltransferase putatively involved in glycosphingolipid synthesis. *J. Biol. Chem.* *277*, 32421-32429.
- Seeman,P. (1967). Transient holes in the erythrocyte membrane during hypotonic hemolysis and stable holes in the membrane after lysis by saponin and lysolecithin. *J. Cell Biol.* *32*, 55-70.
- Seppo,A., Moreland,M., Schweingruber,H., and Tiemeyer,M. (2000). Zwitterionic and acidic glycosphingolipids of the Drosophila melanogaster embryo. *Eur. J. Biochem.* *267*, 3549-3558.
- Smith,P.L. and Baenziger,J.U. (1988). A pituitary N-acetylgalactosamine transferase that specifically recognizes glycoprotein hormones. *Science* *242*, 930-933.
- Smotrys,J.E. and Linder,M.E. (2004). Palmitoylation of intracellular signaling proteins: regulation and function. *Annu. Rev. Biochem.* *73*, 559-587.
- Smotrys,J.E., Schoenfish,M.J., Stutz,M.A., and Linder,M.E. (2005). The vacuolar DHHC-CRD protein Pfa3p is a protein acyltransferase for Vac8p. *J. Cell Biol.* *170*, 1091-1099.
- Speel,E.J., Hopman,A.H., and Komminoth,P. (2006). Tyramide signal amplification for DNA and mRNA in situ hybridization. *Methods Mol. Biol.* *326*, 33-60.

- Spiro, R.G. (2002). Protein glycosylation: nature, distribution, enzymatic formation, and disease implications of glycopeptide bonds. *Glycobiology* *12*, 43R-56R.
- Sprong, H., Degroote, S., Nilsson, T., Kawakita, M., Ishida, N., van der, S.P., and van Meer, G. (2003). Association of the Golgi UDP-galactose transporter with UDP-galactose:ceramide galactosyltransferase allows UDP-galactose import in the endoplasmic reticulum. *Mol. Biol. Cell* *14*, 3482-3493.
- Srivatsan, J., Smith, D.F., and Cummings, R.D. (1994). Demonstration of a novel UDPGalNAc:GlcNAc beta 1-4 N-acetylgalactosaminyltransferase in extracts of *Schistosoma mansoni*. *J. Parasitol.* *80*, 884-890.
- Steffensen, R., Carlier, K., Wiels, J., Levery, S.B., Stroud, M., Cedergren, B., Nilsson, S.B., Bennett, E.P., Jersild, C., and Clausen, H. (2000). Cloning and expression of the histo-blood group Pk UDP-galactose: Gal1beta-4Glc1beta1-cer alpha1, 4-galactosyltransferase. Molecular genetic basis of the p phenotype. *J. Biol. Chem.* *275*, 16723-16729.
- Stolz, A., Haines, N., Pich, A., Irvine, K.D., Hokke, C.H., Deelder, A.M., Gerardy-Schahn, R., Wuhrer, M., and Bakker, H. (2007). Distinct contributions of beta4GalNAcTA and beta4GalNAcTB to *Drosophila* glycosphingolipid biosynthesis. *Glycoconj. J.*
- Stolz, A., Kraft, B., Wuhrer, M., Hokke, C.H., Gerardy-Schahn, R., and Bakker, H. (2006). A DHHC protein regulates activity and subcellular transport of GalNAc transferase B in *Drosophila melanogaster*. *Glycobiology* *16*, 1107.
- Sugita, M., Iwasaki, Y., and Hori, T. (1982). Studies on glycosphingolipids of larvae of the green-bottle fly, *Lucilia caesar*. II. Isolation and structural studies of three glycosphingolipids with novel sugar sequences. *J. Biochem. (Tokyo)* *92*, 881-887.
- Teasdale, R.D. and Jackson, M.R. (1996). Signal-mediated sorting of membrane proteins between the endoplasmic reticulum and the golgi apparatus. *Annu. Rev. Cell Dev. Biol.* *12*, 27-54.
- Togayachi, A., Akashima, T., Ookubo, R., Kudo, T., Nishihara, S., Iwasaki, H., Natsume, A., Mio, H., Inokuchi, J., Irimura, T., Sasaki, K., and Narimatsu, H. (2001). Molecular cloning and characterization of UDP-GlcNAc:lactosylceramide beta 1,3-N-acetylglucosaminyltransferase (beta 3Gn-T5), an essential enzyme for the expression of HNK-1 and Lewis X epitopes on glycolipids. *J. Biol. Chem* *276*, 22032-22040.
- Vadaie, N., Hulinsky, R.S., and Jarvis, D.L. (2002). Identification and characterization of a *Drosophila melanogaster* ortholog of human beta1,4-galactosyltransferase VII. *Glycobiology* *12*, 589-597.
- Vadaie, N. and Jarvis, D.L. (2004). Molecular cloning and functional characterization of a Lepidopteran insect beta4-N-acetylgalactosaminyltransferase with broad substrate specificity, a functional role in glycoprotein biosynthesis, and a potential functional role in glycolipid biosynthesis. *J. Biol. Chem* *279*, 33501-33518.
- Valdez-Taubas, J. and Pelham, H. (2005). Swf1-dependent palmitoylation of the SNARE Tlg1 prevents its ubiquitination and degradation. *EMBO J.* *24*, 2524-2532.
- van Die, I., Bakker, H., and van den Eijnden, D.H. (1997). Identification of conserved amino acid motifs in members of the beta1->4-galactosyltransferase gene family. *Glycobiology* *7*, v-viii.
- van Die, I., van Tetering, A., Bakker, H., van den Eijnden, D.H., and Joziassie, D.H. (1996). Glycosylation in Lepidopteran insect cells: Identification of a beta 1->4-N-acetylgalactosaminyltransferase involved in the synthesis of complex-type oligosaccharide chains. *Glycobiology* *6*, 157-164.
- van Meer, G. (2001). What sugar next? Dimerization of sphingolipid glycosyltransferases. *Proc. Natl. Acad. Sci. U. S. A* *98*, 1321-1323.
- van Remoortere, A., Hokke, C.H., van Dam, G.J., van Die, I., Deelder, A.M., and van den Eijnden, D.H. (2000). Various stages of schistosoma express Lewis(x), LacdiNAc, GalNAc beta1-4 (Fuc alpha1-3)GlcNAc and GalNAc beta1-4(Fuc alpha1-2Fuc alpha1-3)GlcNAc carbohydrate epitopes: detection with monoclonal antibodies that are characterized by enzymatically synthesized neoglycoproteins. *Glycobiology* *10*, 601-609.

- van, D., I., van Tetering, A., Bakker, H., van den Eijnden, D.H., and Joziase, D.H. (1996). Glycosylation in lepidopteran insect cells: identification of a beta 1-->4-N-acetylgalactosaminyltransferase involved in the synthesis of complex-type oligosaccharide chains. *Glycobiology* 6, 157-164.
- Varki, A., Cummings, R.D., Esko, J.D., Freeze, H.H., Hart, G.W., and J., M. (1999). *Essentials of glycobiology*. (Cold Spring Harbor Laboratory Press, Cold Spring Harbor).
- Wandall, H.H., Pedersen, J.W., Park, C., Levery, S.B., Pizette, S., Cohen, S.M., Schwientek, T., and Clausen, H. (2003). *Drosophila* egghead encodes a beta 1,4-mannosyltransferase predicted to form the immediate precursor glycosphingolipid substrate for brainiac. *J. Biol. Chem.* 278, 1411-1414.
- Wandall, H.H., Pizette, S., Pedersen, J.W., Eichert, H., Levery, S.B., Mandel, U., Cohen, S.M., and Clausen, H. (2005). Egghead and brainiac are essential for glycosphingolipid biosynthesis in vivo. *J. Biol. Chem.* 280, 4858-4863.
- Wiegandt, H. (1992). Insect glycolipids. *Biochim. Biophys. Acta* 1123, 117-126.
- Williams, D.B. (2006). Beyond lectins: the calnexin/calreticulin chaperone system of the endoplasmic reticulum. *J. Cell Sci.* 119, 615-623.
- Williams, M.A. and McCluer, R.H. (1980). The use of Sep-Pak C18 cartridges during the isolation of gangliosides. *J. Neurochem.* 35, 266-269.
- Wuhrer, M. and Deelder, A.M. (2005). Negative-mode MALDI-TOF/TOF-MS of oligosaccharides labeled with 2-aminobenzamide. *Anal. Chem.* 77, 6954-6959.

6 Abbreviations

AA	amino acid
AP	alkaline phosphatase
ATT	6-Aza-2-thiothymine
ATP	adenosine-5'-Triphosphat
Az	acidic glycosphingolipids with one PE residue based on the nomenclature of Wiegandt
BCA	bichionic acid
BSA	bovine serum albumine
BLAST	basic local alignment search tool
β 4GalNAcT	UDP-GalNAc:GlcNAc β -R β 1,4 N-acetylgalactosaminyltransferase
β 4GalT	UDP-GalNAc:GlcNAc β -R β 1,4 galactosyltransferase
CDG	congenital disorders of glycosylation
cDNA	complementary deoxyribonucleic Acid
<i>C.elegans</i>	<i>Caenorhabditis elegans</i>
Cer	ceramide
CHO	chinese hamster ovary
COP	coat protein
CRD	cystein-rich domain
DHB	2,5-Dihydroxybenzoic acid
DHHC	Asp-His-His-Cys
DHHS	Asp-His-His-Ser
dsRNA	double-stranded RNA
<i>D.melanogaster</i>	<i>Drosophila melanogaster</i>
EDTA	ethylenediaminetetraacetic acid
ER	endoplasmatic reticulum
ERAD	ER-associated degradation
ERGIC	ER-Golgi intermediated compartment
FCS	Fetal Calf Serum
Flag	amino acid sequence: DYKDDDDK
GABPI	β 4GalNAcTB pilot protein
Gal	D-galactose
GalNAc	2-Acetamido-2-deoxy-D-galactose (<i>N</i> -acetylgalactosamine)
GalT	galactosyltransferase
GFP	green fluorescence protein
Glc	D-glucose
GlcA	glucuronic acid
GlcNAc	2-acetamido-2-deoxy-D-glucose (<i>N</i> -acetylglucosamine)
GlcNAc-pNP	4-nitrophenyl <i>N</i> -acetyl- α -D-glucosaminide
GRP	glucose-regulated protein
GSL	glycosphingolipid
HA	amino acid sequence: YPYDVPDYA
HEK	human embryonic kidney
HPTLC	high-performance thin-layer chromatography
Hsp	heat shock protein
KDEL	Lys-Asp-Glut-Leu
lacdiNAc	<i>N,N'</i> -diacetyllysosidamine (GalNAc β 4,GlcNAc)

lacNAc	<i>N</i> '-acetylactosediamine (Gal β 4,GlcNAc)
mAB	monoclonal antibody
MALDI-TOF	matrix assisted laser desorption ionization-time of flight
Man	D-mannose
MS	mass spectroscopy
Myc	amino acid sequence: EQKLISEEDL
NP-40	nonylphenyl-polyethylene glycol
Nz	zwitterionic glycosphingolipids with one PE residue based on the nomenclatur of Wiegandt
OST	oligosaccharyltransferase
PAT	palmitate acyl transferase
PAGE	polyacrylamide gelelectrophoresis
PBS	phosphate-buffered saline
PCR	polymerase chain reaction
PE	phosphoethanolamine
RNAi	RNA interference
RP	reverse-phase
RT	room temperature
SDS	sodium dodecylsulfate
SiaT	sialyltransferaseS
TMD	trans membrane domain
TMHMM	prediction of transmembrane helices based on a hidden markov model
Tris	trihydroxymethylaminomethane
UDP	uridine diphosphate
v/v	volume/volume
w/v	weight/volume

7 Lebenslauf

PERSÖNLICHE DATEN:

Name : Anita Stolz
Adresse : Hammersteinstr. 13a
30177 Hannover
Email : stolz.anita@mh-hannover.de
Geburtstag : 17.08.1979
Geburtsort : Essen
Staatsangehörigkeit : deutsch
Familienstand : ledig

SCHULISCHE AUSBILDUNG:

1986 – 1990 : Besuch der Großenbruchsule, Essen- Altenessen
1990 – 1999 : Besuch der B. M. V. –Schule Essen
04.06.1999 : Erhalt der allgemeinen Hochschulreife

STUDIUM:

1999 – 2001 : Grundstudium Biochemie an der Universität Hannover
September 2001 : Vordiplom
Schwerpunkte: Anorganische Chemie, Biochemie, Botanik, Organische Chemie, Physik, Physikalische Chemie, Zoologie
Okt. 2001- Okt. 2004 : Hauptstudium Biochemie
April 2004 : Diplomprüfungen
Schwerpunkte: Biochemie, Biophysikalische Chemie, Immunologie
April-Oktober 2004 : Diplomarbeit im Institut für Zelluläre Chemie bei Prof. Dr. Rita Gerardy-Schahn an der Medizinischen Hochschule Hannover

PROMOTION:

Januar 2005- : Promotion am Institut für Zelluläre Chemie
März 2008 bei Prof. Dr. Rita Gerardy-Schahn
an der Medizinischen Hochschule Hannover

8 Publikationsliste

WISSENSCHAFTLICHE VERÖFFENTLICHUNGEN:

Thomas Haselhorst, Anja Münster-Kühnel, **Anita Stolz**, Melanie Oschlies, Joe Tiralongo, Rita Gerardy-Schahn and Mark von Itzstein (2005)

“Probing a CMP-Kdn synthetase by ^1H , ^{31}P , and STD NMR spectroscopy“ *Biochem Biophys Res Commun.*, **327**, 565-570

Stolz,A., Haines,N., Pich,A., Irvine,K.D., Hokke,C.H., Deelder,A.M., Gerardy-Schahn,R., Wuhrer,M., and Bakker,H. (2008). Distinct contributions of beta4GalNAcTA and beta4GalNAcTB to *Drosophila* glycosphingolipid biosynthesis. *Glycoconj. J.* 2008 Feb;25(2):167-75. Epub 2007 Sep 18

Stolz,A., Wuhrer, M., Kraft,B., Deelder,A.M., Hokke ,C.H., Gerardy-Schahn,R., and Bakker,H. Golgi Targeting and Activity of *Drosophila* β 4GalNAcTB Requires a DHHC-Protein Family Member as a Pilot. (submitted manuscript)

Stolz,A., Kraft,B., Gerardy-Schahn,R., and Bakker,H. Transmembrane topology and characterization of the β 4GalNAcTB pilot protein (GABPI). (manuscript in preparation)

KONGRESSBEITRÄGE:

Thomas Haselhorst, Anja Münster-Kühnel, **Anita Stolz**, Melanie Oschlies, Joe Tiralongo, Rita Gerardy-Schahn and Mark von Itzstein (2004)

“Investigations of rainbow trout Cytidine-5'-monophosphate (CMP-) sialic acid synthetase based on ^1H , ^{31}P and STD NMR spectroscopy” *Glycobiology*, **14**, 1103

Anita Stolz, Manfred Wuhrer, Cornelis Hokke, Rita Gerardy-Schahn, Hans Bakker

“GalNAc-transferases involved in *Drosophila* glycolipid biosynthesis.” International Symposium of the SFB 593 (April 06-08, 2005, Marburg, Germany)

Anita Stolz, Manfred Wuhrer, Ron Hokke, Rita Gerardy-Schahn, Hans Bakker

„A DHHC protein dependent GalNAc-transferase involved in *Drosophila* glycolipid biosynthesis.” XVIII International Symposium on Glycoconjugates (September 04-09, 2005, Florence, Italy)

Anita Stolz, Manfred Wuhrer, Ron Hokke, Rita Gerardy-Schahn, Hans Bakker

“*Drosophila* β 1,4GalNAc-transferase requires a DHHC-protein for activity” 16th Joint Meeting of the “Studiengruppe Glykobiologie der GBM” the “Nederlandse Vereniging voor Glycobiologie” the “Group Lillois de Glycobiologie” and the “Belgian Working Group for Glycoscience” (October, 27-29, 2005, Hannover, Germany)

Anita Stolz, Benjamin Kraft, Manfred Wuhrer, Cornelis Hokke, Rita Gerardy-Schahn, Hans Bakker

“A glycosyltransferase regulating DHHC protein with chaperone activity from *Drosophila melanogaster*”

17th Joint Meeting of the “Studiengruppe Glykobiologie der GBM” the “Nederlandse Vereniging voor Glycobiologie” the “Group Lillois de Glycobiologie” and the “Belgian Working Group for Glycoscience”(November , 5-7, 2006, Bruges, Belgium)

Anita Stolz, Benjamin Kraft, Manfred Wuhrer, Cornelis Hokke, Rita Gerardy-Schahn, Hans Bakker (2006)

“A DHHC protein regulates activity and subcellular transport of GalNAc transferase B in *Drosophila melanogaster*” *Glycobiology*, **16**, 1107

Anita Stolz, Benjamin Kraft, Manfred Wuhrer, Cornelis Hokke, Rita Gerardy-Schahn, Hans Bakker (2006)

“*Drosophila* β 1,4GalNAc transferase requires a DHHC protein for activity and subcellular transport” 58. Mosbacher Kolloquium (March, 29-31, 2007, Mosbach/Baden, Germany)

Anita Stolz, Benjamin Kraft, Manfred Wuhrer, Cornelis H. Hokke, Rita Gerardy-Schahn, Hans Bakker

“Transmembrane topology and characterisation of the β 4GalNAcTB pilot protein (GABPI).”

18th Joint Meeting of the “Studiengruppe Glykobiologie der GBM” the “Nederlandse Vereniging voor Glycobiologie” the “Group Lillois de Glycobiologie” and the “Belgian Working Group for Glycoscience” (November , 4-6, 2007, Lille-Lesquin, France)

Anita Stolz, Benjamin Kraft, Manfred Wuhrer, Cornelis H. Hokke, Rita Gerardy-Schahn, Hans Bakker

“Biological function of the β 4GalNAcTB pilot protein (GABPI) in glycosphingolipid biosynthesis of *Drosophila melanogaster*.”

GlycoDev 2007- EMBO Workshop on Glycoscience and Development (December, 9-12, 2007, Lille, France)

VORTRÄGE UND PREISE:

„A glycosyltransferase regulating DHHC protein with chaperone activity from *Drosophila melanogaster*”

17th Joint Meeting of the “Studiengruppe Glykobiologie der GBM” the “Nederlandse Vereniging voor Glycobiologie” the “Group Lillois de Glycobiologie” and the “Belgian Working Group for Glycoscience”(November , 5-7, 2006, Bruges, Belgium)

“A DHHC protein regulates activity and subcellular transport of GalNAc transferase B in *Drosophila*”

Meeting of the Society for Glycobiology (November, 15-19, 2006, Universal City, California)

“A glycosyltransferase regulating DHHC protein with chaperone activity from *Drosophila melanogaster*”

BBQ Seminar of the Medizinische Hochschule Hannover (March, 23., 2007, Hannover, Germany)

“Biological function of the β 4GalNAcTB pilot protein (GABPI) in glycosphingolipid biosynthesis of *Drosophila melanogaster*.”

GlycoDev 2007- EMBO Workshop on Glycoscience and Development (December, 9-12, 2007, Lille, France)

Poster award on the XVIII International Symposium on Glycoconjugates (September 04-09, 2005, Florence, Italy) for the poster topic “Enzymology of Glycoconjugates”

9 Erklärung zur Dissertation

Hierdurch erkläre ich, dass die Dissertation

“Characterization of the β 4GalNAc transferases and the β 4GalNAcTB Pilot Protein (GABPI)
from *Drosophila melanogaster*”

selbstständig verfasst und alle benutzten Hilfsmittel sowie evtl. zur Hilfeleistung
herangezogene Institutionen vollständig angegeben wurden.

Die Dissertation wurde nicht schon als Diplom- oder ähnliche Prüfungsarbeit verwendet.

Hannover, den 04.01.2008

Anita Stolz

10 Danksagung

An dieser Stelle möchte ich mich bei allen bedanken, die zum Gelingen dieser Arbeit beigetragen haben.

Ich bedanke mich bei Prof. Rita Gerardy-Schahn für ihre Unterstützung und Förderung dieser Arbeit und besonders für die Fähigkeit, einem immer wieder die nötige Motivation zurückgeben zu können, wenn diese verloren zu sein scheint.

Ein besonderer Dank gilt Dr. Hans Bakker für seine Betreuung und das Anvertrauen des interessanten Themas, das diese Arbeit erst möglich gemacht hat. Die Zusammenarbeit im Labor hat sehr viel Spaß gemacht und die permanente Hilfs- und Diskussionsbereitschaft und die vielen Tips und Ideen haben die Arbeit zu dem gemacht, was sie ist.

Ein ganz herzliches „bedankt!“ geht auch an Dr. Manfred Wuhrer für die tatkräftige Unterstützung und engagierte Betreuung der Massenspektrometrie dieser Arbeit. Durch die Gastfreundschaft des Laborteams in Leiden: von Manfred Wuhrer und seiner Familie, Carolien Koeleman, Ron Hokke, Arjen de Boer und Benedicta Obeng waren die Besuche dort auch immer mit Wiedersehensfreude verbunden.

Bei Dr. Andreas Pich möchte ich an dieser Stelle für die Unterstützung und die Möglichkeit bedanken, dass ich MALDI-Messungen auch in Hannover durchführen konnte.

Diplom Biochem. Benjamin Kraft gilt an dieser Stelle ein großer Dank für seine tatkräftige Unterstützung als „PRAKTIKANT!“, dann als „DIPLOMAND!“ und nun als „DOKTORAND!“, für seine kreative, ideenbringende Art und das lustige Spinnen neuer Projekte und natürlich auch für die stets offenen Ohren auch außerhalb des Labors.

Für eine tolle Zeit im Labor möchte ich Diplom Biol. Barbara Kleczka danken (Ohana!). Ihre seelische Unterstützung im Labor, die lustige Art und ihre Freundschaft fehlten in der zweiten Hälfte dieser Arbeit sehr. Allerdings waren die gebliebenen lustigen Abende mit Ictea und Karaoke immer wieder ein Genuss.

Monika Berger, Ulrike Bernard, Andrea Bethe, Hannelore Burckhardt, Bodo Dierks, Melanie Grove, Evelin Herzog, Astrid Oberbeck, Brigitte Philippens und Daniela Wittenberg danke ich für die exzellente technische und organisatorische Unterstützung im Labor, so auch für das Beantworten vieler Fragen.

An dieser Stelle sei der gesamten Arbeitsgruppe der „Zellulären Chemie“ für ein unheimlich tolles Arbeitsklima mit Kuchen, vielen netten Gesprächen im Büro, das Diskutieren von Versuchsproblemen, für die Hilfsbereitschaft bei Computerproblemen, für lustige Mensabesuche, für unvergessliche Kongresse, den Spaß mit Trockeneis, das Singen im Flur, für tolle Abende auch ausserhalb der Arbeitszeit und die stetige Hilfsbereitschaft in allen „Laborlagen“ ein herzliches Dankeschön ausgesprochen. Ich kann an dieser Stelle leider nicht alle Namen nennen (dafür reicht die Seite nicht), aber es dürfen sich alle angesprochen fühlen. Christa Zeigner danke ich für ihre Hilfe bei offiziellen Angelegenheiten und die aufmunternden Gespräche.

Weiterhin möchte ich mich bei meinen Freunden, Arne Backhaus, Almut Günzel, Britta Marohn, Christin Menneking und Alexander Wolf für eine unvergessliche Studienzeit und

auch für die viele schönen Stunden während der Promotion bedanken. Ein herzlicher Dank gilt Nilofar Nassimi mich seit der Schulzeit begleitet und auch bei größerer Entfernung immer für mich da ist.

An dieser Stelle gilt der größte Dank meinen Eltern, meinem Bruder Roland, Melanie, Fabian, Leonard und meiner Oma, die immer an mich glauben, mich unterstützen und bei besonderen Versuchstagen auch die Daumen gedrückt und an mich gedacht haben. Dieser private Rückhalt ist vom unschätzbaren Wert für mich und hat wesentlich zum Gelingen dieser Arbeit beigetragen.

Zuletzt möchte ich mich bei dem Menschen bedanken, mit dem ich auch den Rest meines Lebens teilen will. Kay, ich danke Dir einfach dafür, dass Du für mich da bist, für Deine Liebe und Deine Unterstützung.